Driving Brain Tumorigenesis: Generation and Biological Characterization of a Mutant IDH1 Mouse Model

by

Christopher James Pirozzi

Department of Pathology
Duke University

Date: _____

Approved:

_____
Hai Yan, Supervisor

_____
Oren J. Becher

_____
Salvatore V. Pizzo

_____
Debra L. Silver

_____
Anne E. West

Dissertation submitted in partial fulfillment of
the requirements for the degree of Doctor
of Philosophy in the Department of
Pathology in the Graduate School
of Duke University

2014

ABSTRACT

Driving Brain Tumorigenesis: Generation and Biological Characterization of a Mutant IDH1 Mouse Model

by

Christopher James Pirozzi

Department of Pathology
Duke University

Date: _____

Approved:

_____
Hai Yan, Supervisor

_____
Oren J. Becher

_____
Salvatore V. Pizzo

_____
Debra L. Silver

_____
Anne E. West

An abstract of a dissertation submitted in partial fulfillment of the requirements for the degree of Doctor of Philosophy in the Department of Pathology in the Graduate School of Duke University

2014

Abstract

Despite decades worth of research, glioblastoma remains one of the most lethal cancers. The identification of *IDH1* as a major cancer gene in glioblastoma provides an exceptional opportunity for improving our understanding, diagnostics, and treatment of this disease. In addition to mutations in *IDH1*, recent studies from our laboratory have characterized the genetic landscape of gliomas and have shown the cooperation between IDH1 mutations and other oncogenic alterations such at TP53 mutations. Normally, IDH1 functions in the oxidative decarboxylation of isocitrate to α-ketoglutarate, however the mutant form confers neomorphic enzymatic activity by producing D-2-hydroxyglutarate, an oncometabolite responsible for aberrant methylation in *IDH1*-mutated tumors, among other mutant IDH1-mediated phenotypes. To determine the role of mutant IDH1 *in vivo*, we generated a conditional knock-in mouse model. This genetically faithful system is both biologically and clinically relevant and will promote the understanding of mutant IDH1-mediated tumorigenesis while offering a route for therapeutic targeting.

We observed that broad expression of mutant IDH1 throughout the brain leads to hydrocephalus in 80% of animals. In assessing the earliest effects of mutant IDH1 on the brain, we determined mutant IDH1 confers a decrease in the proliferative cells of the subventricular zone of the lateral ventricle, the area which houses the neural stem cells

in embryonic and adult animals. Additionally, a perturbation to the normal neural stem cell niche was observed in these animals. Combined, this data suggests that mutant IDH1 may be affecting the signaling pathways involved in differentiation in this population of cells. *In vivo* and *in vitro* studies will further elucidate mutant IDH1's effects on the differentiation patterns of neural stem cells expressing mutant IDH1.

To express mutant IDH1 in a more restricted manner and harness spatio-temporal control, we crossed mutant animals to a Nestin-CreER^{T2} strain of mouse that permits expression of floxed alleles upon treatment with tamoxifen. Animals were sacrificed at the onset of symptoms or at 1-year of age. We observed the development of both low- and high-grade gliomas in approximately 15-percent of E18.5 tamoxifen-treated animals. All tumors were found in a *TP53*-deleted background with mutant IDH1 being detected in only those tumors with the mutant allele. Lastly, to decrease the latency and increase the penetrance of tumor formation, an orthotopic intracranial injection model was generated to allow for visualization of tumor formation and development, as well as investigation of therapeutic modalities. The models generated and the knowledge gained from these studies will offer an understanding of the biological effects of the most common mutations found in the astrocytic subset of gliomas, bringing us strides closer to determining mechanisms and therapeutic targets for *IDH1*-mutated cancers.

Dedication

This dissertation is dedicated to my family – for always being there and for the "CJ Rocks" cheers when it was needed most.

Contents

List of Tables

List of Figures

Acknowledgements

There is no short list of people who have helped me through my graduate school career. First, thanks to Hai Yan for mentorship and guidance throughout this process. To Yiping He, who has shown me the painstaking yet gratifying life of a scientist very early on in my career and whose early tough love put me on a path towards success. You have my utmost appreciation and thanks. To Paula Greer, our lab mom who really does know everything – simply put, thank you – for everything. To Cathy Wang, you brought a high-energy, upbeat vibe to my sometimes energy-lacking days…and I still don't know what the fox says. To Austin Carpenter, thank you for always keeping my head in the game and sights on the frontier, your insight into our projects has been most helpful and appreciated. To Matthew Waitkus, many thanks for insight, guidance, and critical thought towards these projects. To Cathy, Austin, and Huishan Zhu – the thousands of slides you have all sectioned were a tremendous help and contributed a great deal to the writing of this dissertation. To Patrick Killela, thank you for putting the laughs in the lab and for our collaborations that have led to several portions of this dissertation. Many thanks to all members of the Yan and He labs for the thought-provoking conversations and fun in the process: Chun-Chi Chang, Yafen Huang, Zachary Reitman, Zhaohui Wang, Ping Wang, Landon Hanson, Bill Diplas, Jinwook Shin, Lee Chen, Rui Yang, Casey Moure, and all members from the past.

Many thanks to the members of my thesis committee including Oren Becher, Sal Pizzo, Debby Silver, and Anne West – your insight and guidance through this process has ensured I got to this point and did so in a graceful manner, and I thank you for that.

Additional thanks to the Preston Robert Tisch Brain Tumor Center, specifically Roger McLendon for all help with analyzing hundreds of mouse tissue sections, and to Lisa Ehinger, Diane Satterfield, and Merrie Burnett for help with the microtome and cryosectioning. To Zuowei Su who performed many of the IHC stainings. To Cheryl Bock, for countless conversations and help with embryonic stem cells and transgenics. To Ivan Spasojevic and Ping Fan in the PK/PD facility for answering my many questions dealing with LC-MS/MS and all matters dealing with detection of 2-HG. To Ling Wang for tremendous help with antibody stainings and use of the DMD 108 imager. And to Hailan Piao for our countless conversations that always left me feeling good.

Finally, my thanks and love go out to quite possibly, the most "interesting" albeit most understanding and loving family that I could imagine, my mom Denise Pirozzi (feel free to call me Dr. Boy), my dad Ernie Pirozzi (Dr. Mosquito works for me), my sister Lauren Pirozzi (I suppose Dr. Snotface will do), and my step-mother Tracey Pirozzi. To my partner-in-crime, Jon Watkins who has been there quite literally every step of the way, ensuring that I stay as close as possible to sane.

My thanks to all for helping me make this happen.

1. Permissions and collaborative work

This dissertation contains new and novel writing and figures as well as figures and excerpts of text of published articles. The excerpts and figures from published works were reproduced with permission as described in Appendix A. Where the publisher does not require explicit permission, excerpts and figures were reproduced in accordance with the policy of the journal or publisher as described in Appendix A. The work detailed in this dissertation was performed primarily by the candidate although in some cases, the work was aided by collaborators, for instance by performing analyses or by providing biological samples as described in Acknowledgements.

1.1 Introduction: Gliomas

Gliomas are the most common primary tumor of the central nervous system accounting for approximately 30 percent of all brain tumors and 80 percent of all malignant brain tumors. It is estimated that in 2014 alone, 66,240 patients will be newly diagnosed with about 14,320 patients succumbing to the disease, making brain tumors the second leading cause of cancer-related deaths among children and males, and the fifth leading cause of cancer-related deaths among females(1,2).

Despite decades worth of research, the overall survival for patients with high-grade glioma remains dismal with a median survival of only 15 months(3). In fact, over the past four decades, the survival for this disease has remained mostly unchanged (**Figure 1**). This stagnant improvement in survival is made even more apparent when

compared to other cancers that have exhibited significant increases in survival over the past several years, including colon cancer, esophageal cancer, breast cancer, prostate cancer, and several hematopoietic cancers, among others(1,4).

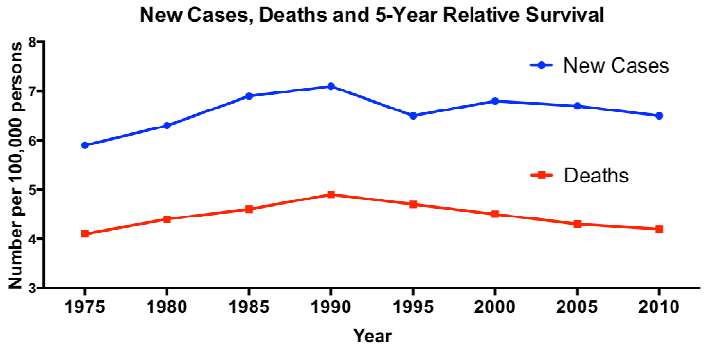

Year	1975	1980	1985	1990	1994	1998	2002	2006
5-Year Relative Survival	22.8%	22.9%	24.7%	28.5%	32.0%	30.9%	35.6%	35.4%

Figure 1: New cases, deaths and 5-year relative survival for brain and other nervous system cancer.

Brain and other nervous system cancers account for about 1.4% of newly diagnosed cancers in 2014. Though there has been a slight increase in the number of new cases in the past few decades, there has been only minimal improvement in 5-year survival. This data, adapted from the SEER Cancer Statistics Review shows all brain and nervous system cancers. The lack of improvement is even more apparent when looking at glioblastoma specifically(1).

The difficulties in treating and curing gliomas lie in several features. First, the brain is encased in a non-compromising skull; any aberrant growth within this confined area inevitably leads to compression, increased pressure, and ultimately neurological symptoms and dysfunction. Second, tumor growth in this area of confined space is

likely to interfere with the vital structures present within it. For similar reasons, resection is usually incredibly difficult and often times, incomplete. Third, gliomas tend to be highly infiltrative with microscopic spread of tumor. Even when resection appears complete, these microscopic foci promote regrowth. Lastly, due to the blood-brain-barrier as well as cell-intrinsic factors, glioma cells are largely resistant to many current therapeutics(5).

Understanding the molecular underpinnings of this most fatal disease is of the utmost importance. To this end, we sought to determine the genetic aberrations most commonly found in gliomas, recapitulate the human disease through generation of genetically faithful mouse models and to utilize these models for both understanding the development and progression of these tumors, as well as investigation of therapeutic modalities.

This chapter will present background to gliomas as a disease and encompasses their classification, etiology through looking at normal developmental programs of cells of the central nervous system (CNS), as well as a discussion of the suspected cell of origin for gliomas. Subsequent chapters will discuss our work in determining the genetic signatures of gliomas, generation of our genetically faithful mouse models that harbor those mutations we identified in our signatures, followed by a mechanistic look at how these mutations in our genetic signatures function to promote tumorigenesis.

1.1.1 World Health Organization Classification of Tumors

The World Health Organization (WHO) categorizes the over 120 different types of brain tumors based on the cells that the tumor is composed of as well as the behavior of the tumors themselves. Histologic features, genetic aberrations, and malignant behavior are all taken into account when grading these tumors on a scale of I through IV. Grade I tumors exhibit low proliferative activity and the great potential for cure following surgical resection(6). Grade II tumors are low-grade malignancies with low levels of mitotic activity. Their tendency to be diffusely infiltrative makes complete resection difficult and thus recurrence and progression to higher-grade lesions prevalent(7,8). Median survival among patients diagnosed with Grade II tumors is 5 to 7 years. Grade III tumors display histological evidence of malignancy, including nuclear atypia and mitotic activity. Patients with Grade III tumors display a median survival of 2 to 5 years(3). Similar to Grade II tumors, Grade III tumors can progress to the secondary Grade IV tumors which include the glioblastomas (GBMs). These tumors are malignant, mitotically active, and display necrosis, increased cellularity, and microvascular proliferation(8). The invasive nature, rapid proliferative capacity, and ability of recurrence gives patients diagnosed with GBM a dismal median survival of only 12 to 15 months(3). Grade IV GBMs can be further subdivided into primary and secondary GBM, with primary GBM arising *de novo* and secondary GBM arising as a progression from lower grade lesions including Grade II and Grade III tumors. Though

histologically very similar and often impossible to distinguish histologically, primary and secondary GBM are genetically distinct diseases.

1.1.2 Neural Development and Cells of the CNS

By the end of gastrulation, neural stem cells (NSCs) are poised to give rise to all cell types of the CNS of the developing organism, including but not limited to, neurons and glial cells which include the astrocytes and oligodendrocytes. Following emergence of the neural plate, two folds will form and fuse, generating the neural tube. The NSCs will form a single layer of cells lining the center of the neural tube, which will ultimately become the ventricles of the brain. The neural progenitor cells in the most rostral region of the neural tube give rise to the brain. Rapid growth ensues forming the primary brain vesicles including the prosencephalon, the mesencephalon, and the rhombencephalon, the primitive structures of the forebrain, midbrain, and hindbrain, respectively(9). Neuron production will occur through gestation, and once produced, they will migrate away from the proliferative regions of the ventricular zone to their proper location among the six-layered neocortex. During this period, neural progenitor cells divide symmetrically in order to populate the many cells that are required for the functional brain. As time progresses, asymmetric divisions commence with the progenitor cell remaining in the proliferative zone, and the differentiated cell migrating outwards to take its place in the cortex. As the brain develops and expands, radial glial cells are enlisted to form tracks on which the migrating neurons can follow. The radial glial cells

will extend basal processes that attach to the pial surface of the brain while their nucleus is anchored in the ventricular zone allowing for migrating neurons to populate their respective cortical layers in an "inside-out" fashion, with earlier migrating neurons forming the deepest layers of the brain (layer VI), and later migrating neurons forming the more superficial layers (layer I)(9).

Though neurogenesis peaks during gestation, it does occur in the adult brain, specifically in the subventricular zone (SVZ), an epithelium that lines the walls of the lateral ventricle, as well as in the subgranular layer of the dentate gyrus of the hippocampus, though not nearly as robust as during fetal development(10). The glial progenitors give rise to the major support cells of the CNS, the glial cells, which generate more than 50% of the cells in the human brain and are suspected of dividing and differentiating for an extended period after birth, and even through adult life(11). The glial cells include the astrocytes and oligodendrocytes. Astrocytes function in providing structural support, regulating water balance and ion distribution, and maintaining the blood-brain barrier. Additionally, astrocytes have roles in neuropeptide production and synaptic transmission, as well as implications in response to injury. On the other hand, oligodendrocytes ensheathe neuronal axons with myelin to provide insulation and facilitate signal conduction.

As mentioned, neurogenesis precedes gliogenesis and the transition is referred to as the gliogenic switch. This switch is believed to be induced through a variety of

factors that are usually location dependent, however recent studies have shown signals from differentiated neurons may induce astrocytic differentiation(12-14). Astrocyte precursors have the ability to undergo robust proliferation outside of the typical germinal centers of adult animals and in doing so, are able to generate both transit amplifying astrocytes as well as multipotent NSCs(15). This suggests that under certain conditions, normal astrocytes have inherent properties similar to those of NSCs.

Oligodendrocytes, another type of glial cell that arises from the expansion and differentiation of NSCs, are formed from multiple progenitor pools throughout the developing embryo. In the postnatal brain however, the major source of oligodendroglial progenitor cells (OPCs) is in the SVZ at the tips of the lateral ventricles. From here, the OPCs will migrate into the white matter where they will stop dividing and differentiate to form mature myelinating oligodendrocytes(14). Additionally, a population of OPCs can be found in the white matter itself.

Humans undergo prolonged neural development, with the prefrontal cortex being one of the last components to mature. It is not until 10 years of age that the brain reaches its adult volume. Myelination continues well into adolescence and into early adulthood. At this time, synaptic pruning correlates with a loss of prefrontal grey matter and this reorganization of the prefrontal cortex is what is believed to impart higher cognitive processes including executive function, social cognition and judgment(16). It is possible that this structural reorganization of the prefrontal cortex

and subsequent change in gene expression, migration, and metabolic utilization during adolescence may impart a susceptibility to these cells making them more prone to mutagenic hits, and thus tumorigenesis.

1.1.3 Cell of Origin for Gliomas

The identification of the cell of origin for a cancer opens up several avenues of pursuit that ultimately leads to great potential in understanding the biology behind tumor development as well as offering a more concise means of therapeutic investigation. Unfortunately, such a pursuit for gliomas has been hindered by difficulties in ascertaining the specific cell of origin for this devastating disease. Though a precise cell of origin is unknown, there are several suitable candidates including NSCs, OPCs, transit amplifying cells, or differentiated glial cells that either undergo a process of dedifferentiation or become fully transformed(17). The fact that gliomas can be composed largely of astrocytes (astrocytomas), oligodendrocytes (oligodendrogliomas), or a mixture of the two (oligoastrocytomas), contributes to the difficulties of resolving a specific cell type as a cell of origin.

NSCs are one of the leading candidates as the cell of origin for gliomas. There are many shared features between NSCs and cancer cells of the CNS; they both exhibit robust proliferation that is coupled with the potential to generate a diversity of progeny. Additionally, the behavior among NSCs and cancer cells of the CNS are similar. For example, both display high motility, an affinity for blood vessels and white matter

tracts, and perhaps most interesting, both have activation of similar developmental signaling pathways(18). Experimental data implicating NSCs as the cell of origin for gliomas is on the rise. In animal models, when areas which housed the NSCs were infected with virus for oncogene delivery, these cells underwent transformation and induced formation of GBM(19). This was not observed when the oncogenes were delivered to differentiated astrocytes, suggesting that the NSC population is more susceptible to transformation. NSCs inherently have certain expression patterns activated, including pro-mitotic genes, telomerase activity, and anti-apoptotic genes. By comparing this pattern of expression to those of other, more differentiated cell types, it becomes plausible to figure these cells are already en route to being fully transformed. Lastly, if NSCs are the cell of origin for gliomas, it would explain the observed heterogeneity. As NSCs or progenitor cells are capable of differentiating into astrocytes or oligodendrocytes, the stage at which a NSC becomes transformed could theoretically dictate whether a tumor is predominately astrocytic, oligodendrocytic, or a mixture of the two.

In an extension of the first endogenous genetic tumor suppressor mouse model, it was found that embryonic, early postnatal, and adult NSCs can give rise to malignant astrocytomas *in vivo*(20). The same was not observed when these same mutations were incorporated into mature cell types. This lends credence to the hypothesis that NSCs are the cell of origin for gliomas.

Alternatively, another candidate for the cell of origin for gliomas are the OPCs. In an elegant study utilizing mosaic analysis with double markers (MADM), a system permitting lineage tracing and subsequent analysis of individual cell lineages and their implication as cells of origin, Liu *et al*., show that gliomagenesis only occurred when mutations were incorporated in NSCs that gave rise to mutant OPCs(21). Cells that were derived from NSCs, but were not OPCs failed to generate tumors. This suggests that even if a mutation occurs in the NSC, only if they are able to generate OPCs with the mutation, will tumors develop; thus stressing the importance of a mutations cellular dependency.

The precise cell of origin for gliomas is unknown. Though there are candidates available: either NSCs, OPCs, or differentiated glial cells, the heterogeneity of the tumors themselves may suggest that these are distinct diseases each with their own respective cell of origin(17,22). It may be possible that the different subtypes of gliomas originate from different cell of origins, or it may be that they originate from the same cell of origin, but as the tumor develops, gives rise to different cell types via differentiation, mutation acquisition, or cues from the microenvironment.

Due to the convincing body of literature implicating NSCs as the cell of origin, we have centered our studies on generating genetically faithful mouse models with the cell of origin for gliomas being the NSC. These will be discussed further in subsequent chapters.

2. Introduction: Mutations in *Isocitrate Dehydrogenase 1* (*IDH1*) in Gliomas

With the culmination of the Human Genome Project on April 14th, 2003, we have thus embarked on the Post-Genome era. Having taken 13 years and approximately $2.7 billion to complete, this endeavor has set the stage for tremendous advancements in understanding the molecular underpinnings of variation within humans as well as the genetic basis for disease. With goals within reach of sequencing a genome at a cost of $1000 and the time to do so taking only a few days, efforts have been put forth to sequence and characterize the genomic aberrations present in human tumors. Initiatives including The Cancer Genome Atlas (TCGA) have begun to sequence cancers with priority going towards those cancers exhibiting poor prognosis and an overall public health impact. To date, TCGA has successfully and completely sequenced 31 cancers, with data for all but 4 ready for public availability.

Due to the dismal prognosis and the inability to improve survivability, GBM was one of the first cancers to be sequenced by the TCGA in an effort to acquire a baseline knowledge of GBM genetics(23). Similar efforts from our group in collaboration with others, focused on a brute-force genome-wide mutational analysis of GBM where 20,661 protein coding genes were sequenced in 22 GBMs(24). In addition to sequencing, focal copy number alterations including amplifications and deletions, as well as gene expression studies were performed. The ultimate goal was to determine the genetic

alterations in GBM for application towards diagnostics, prognostics, and therapeutic targeting. Several findings resulted from these studies. For one, many of the molecular features already identified to have a pathogenic role in GBM were validated. These included mutations in core components of the retinoblastoma tumor suppressor (RB), TP53 tumor suppressor, and receptor tyrosine kinase (RTK) pathways(23,24). Identification of disrupted pathways in GBM has provided guidance in determining treatment for patients, in among the first validations of personalized medicine for GBM. For example, patients with inactivating mutations in *CDKN2A* or *CDKN2C* or amplifications in *CDK4* or *CDK6* would be candidates for treatment with CDK inhibitors, however this treatment would likely be ineffective for patients with *RB1* mutations(23). By elucidating those specific alterations in a patient-specific manner, therapeutics targeting those pathways directly can be investigated as opposed to a one-size-fits-all therapeutic approach where those therapeutics could likely be instigating pathway activation, leading to ineffective treatment, or even more aggressive cancer growth.

These genetic studies have additionally identified several pathways and genes previously unknown to be altered in GBM. The most frequently mutated of these candidate genes is that of *isocitrate dehydrogenase 1* (*IDH1*) found on chromosome 2q33(24). Subsequent larger and more comprehensive studies from our own lab has sequenced 445 CNS and 494 non-CNS tumors and found that not only was *IDH1*

mutated in GBM, but it was mutated in as high as 80 percent of a particular subset of gliomas. The mutations were observed in the progressive gliomas, those tumors that arise as a progression from the Grade II, Grade III, and secondary Grade IVs(25). *IDH1* was not mutated in any Grade I tumors and only 6 out of 123 primary GBMs; suggesting IDH1 is a relatively early hit in tumorigenesis and may be a driver for malignancy as the tumors progress from low-grade (Grade II) tumors to higher-grade tumors (Grade III and secondary Grade IV). In fact, in comparing the genetics of gliomas as they progress, it was observed that mutations in *IDH1* often precede other aberrations that were once thought to be very early hits including mutation of *TP53* or chromosomal loss of 1p/19q(26).

Additionally, it was found that in those progressive gliomas that were not mutated in IDH1, the homologous gene, IDH2, was mutated. Every mutation found in IDH1 was located at the 132nd residue, and it was most commonly mutated from arginine to histidine, however a series of missense mutations were observed at this residue(25). In those tumors mutated in IDH2, it was the analogous residue that was affected, arginine-172, and it was most commonly mutated to a lysine. Determining the functional effects of this mutation required inspection of the protein's crystal structure where it was observed that Arg-132 in IDH1 (and similarly, Arg-172 in IDH2) lied in the active site of the enzyme, thereby suggesting that these mutations may have an effect on the normal enzymatic activity of IDH1(25). In fact, in structural comparisons, it was

noted that when the substrate, isocitrate, is present and complexes with the wildtype form of the protein, it forms hydrogen bonds with Arg-132 of IDH1 (and similarly, Arg-172 in IDH2). However, the lack of appropriate side chains when arginine is replaced with histidine prevents isocitrate from making those hydrogen bonds within the active site of the enzyme. The implication is that the enzyme-substrate affinity may be compromised when the mutant form is present(27).

To assess the effects mutant IDH1 is having requires knowledge of its normal activity. Normally, IDH1 acts in the tricarboxylic acid (TCA) cycle where it functions in the oxidative decarboxylation of isocitrate to α-ketoglutarate (α-KG) in a $NADP^+$-dependent manner(28). This is one of the irreversible steps of the TCA cycle that is essential for cellular respiration. To elucidate the effects mutant IDH1 has on metabolism, metabolite profiling was performed via liquid chromatography-electrospray ionization-mass spectrometry (LC-MS) on cells transfected with either wildtype or mutant IDH1(29). It was observed that in mutant cells, there was a loss of the oxidative decarboxylation function of isocitrate to form α-KG. However, subsequent analyses including targeted triple-quadrupole LC-MS-MS validated that in IDH1 mutant cells, there was a gain of enzymatic function in the NADPH-dependent reduction of α-KG to a new metabolic product, 2-hydroxyglutarate (2-HG)(29) (**Figure 2**). 2-HG was further detected in tumors at levels 100-fold higher in *IDH1* mutant tumors than in *IDH1* wildtype tumors (5μmol to 35μmol 2-HG per gram of tumor tissue.

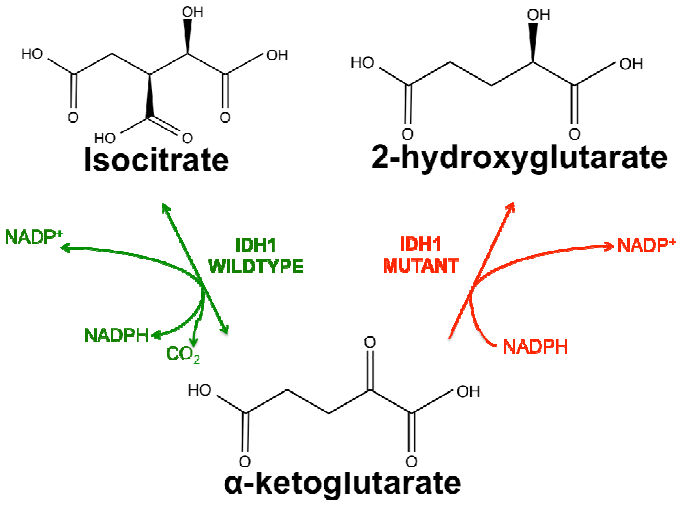

Figure 2: Function of wildtype and mutant IDH1.

Wildtype IDH1 normally functions in the oxidative decarboxylation of isocitrate to α-KG in an $NADP^+$ dependent reaction. This is an active component of the TCA cycle. Mutant IDH1 confers neomorphic enzymatic activity in its production of 2-HG.

The finding that the metabolic product of mutant IDH1 is production of 2-HG is interesting on several levels. For one thing, there are patients with a disorder called D-2-hydroxyglutaric aciduria usually caused by germline mutations in the gene *D-2-hydroxyglutarate dehydrogenase*(30). These patients generate elevated levels of 2-HG and present with many neurological phenotypes including developmental delay, epilepsy, and varying degrees of encephalopathy, as well as hypotonia, dysmorphic features, and cardiomyopathy(31). Additionally, mild ventriculomegaly was observed as an enlargement of the frontal subarachnoid spaces and subdural effusions. Several other patients also presented with delayed cerebral maturation and subependymal cysts(32).

In patients that have L-2-hydroxyglutaric aciduria, there appears to be an increased risk for developing brain tumors as well. One paper, a case series of four patients with this disease, describes the development of brain tumors ranging in diagnosis from primitive neuroectodermal tumor, oligodendroglioma, and low-grade astrocytoma(33). The broad effects of 2-HG on the brain in these 2-hydroxyglutaric aciduria patients suggests that 2-HG does in fact perturb cells of the CNS and offers good rationale for suspecting mutant IDH1's ability to produce elevated levels of 2-HG as a major component for brain tumor induction.

2.1 The genetic landscape of gliomas

Rarely are tumors formed as a result of a single hit. On the contrary, cancer is a disease of genomic alterations, requiring multiple hits to fully transform a cell and promote tumorigenesis. The average number of mutations in common solid tumors (colon, breast, brain, or pancreas) is about 33 to 66 mutations(34). Of course, depending on the tumor type, the suspected induction of the mutation, as well as the pathways that are involved, the number of mutations will vary. For example, melanoma will harbor approximately 200 mutations per tumor likely due to ultraviolet light inducing mutations, whereas pediatric tumors harbor far fewer mutations, approximately 9.6 mutations per tumor. It is thus the purpose and consequence of these large sequencing projects to identify the mutations present in these tumors, screen for those mutations that have the most effect on tumorigenesis and are likely drivers, and subsequently

elucidate the biological ramifications of them. Additionally, it will be imperative to determine how these mutations are cooperating to promote tumorigenesis.

We have recently completed several studies determining the genetic landscape of progressive glioma(35-37). Our initial study was in determining the genetic signature for the progressive astrocytomas, specifically the diffuse astrocytomas (Grade II), anaplastic astrocytomas (Grade III), and the secondary GBMs (Grade IV). This involved the exome sequencing of a large cohort of tumors. Subsequently, we sought to use the markers identified in our exomic sequencing studies, together with previously reported genetic markers to assess whether we can identify the various subtypes of gliomas via a DNA-based sequencing method that could complement the traditional histopathological means of diagnosis.

2.1.1 The genetic landscape of progressive astrocytomas

In an effort to establish the genetic landscape of progressive astrocytomas, we sequenced the exomes of a total of 57 gliomas. Included in our cohort were 7 diffuse astrocytomas (Grade II), 16 anaplastic astrocytomas (Grade III), 2 oligoastrocytomas (grade II), 4 oligoastrocytomas (Grade III), 1 secondary GBM (Grade IV), and 27 primary GBM (Grade IV).

2.1.1.1 Genetic alterations of diffuse astrocytomas (Grade II)

Exome sequencing of 7 diffuse astrocytomas (Grade II) revealed 93 somatic mutations. On average, Grade II astrocytomas contained 13 somatic mutations, with

92% of targeted regions covered by 10x high quality reads or more. Copy number gains or deletions were not observed in these samples, however mutations in *IDH1*, *ATRX*, and *TP53* were found to be co-mutated in 43% of the Grade II astrocytoma cohort.

2.1.1.2 Genetic alterations of anaplastic astrocytomas (Grade III)

Exome sequencing of 16 anaplastic astrocytomas (Grade III) revealed 576 mutations. On average, Grade III astrocytomas contained 36 somatic mutations with 92% of targeted regions covered by 10x high quality reads or more. In addition to co-occurring mutations in *IDH1*, *ATRX*, and *TP53*, mutations in the Notch signaling pathway, including *NOTCH1*, *NOTCH2*, *NOTCH4*, and *NOTCH2NL* were observed in 31% of the Grade III astrocytoma cohort.

2.1.1.3 Genetic alterations of GBMs (Grade IV)

Exome sequencing of 28 GBMs identified 1,177 somatic mutations. Primary GBMs on average contained 42 somatic mutations with 93% of targeted regions covered by 10x high quality reads or more. Copy number alterations were frequent in this cohort of tumors, averaging 32 events per tumor. Confirming previous studies, the EGFR/PTEN/PI(3)K pathway was the most frequently affected pathway. In our cohort, *EGFR* was altered in 46%, *PTEN* in 14%, *PIK3CA* in 10%, and *PIK3R1* in 13% of GBMs(23,24,38,39). Several of these above mutations were also identified in the lower grade gliomas. Interestingly, *PIK3CA* mutations were found exclusively in *IDH1* wildtype tumors, those tumors displaying the worst survival.

2.1.1.4 Summation of the genetic landscape of astrocytomas

In determining the genetic landscape of the progressive astrocytomas, we determined that there are not an overwhelming number of genetic aberrations that are present. In the earliest of the progressive astrocytomas, there are on average 13 somatic mutations per tumor. We corroborated previous data showing that there is a co-occurrence of mutations in *IDH1*, *ATRX*, and *TP53* in these tumors. This signature persists throughout the astrocytic family of gliomas, suggesting their co-occurrence is imperative for the initiation, development and/or maintenance of the progressive gliomas. Additionally, we identified that in the Grade III astrocytomas, several members in the Notch signaling pathway were mutated. Lastly, we show that the mutation spectrum among primary and secondary GBMs is quite distinct, lending credence to the belief that though histologically similar, primary and secondary GBMs are genetically distinct diseases. A thorough summation of the findings from this study can be found in **Figure 3**.

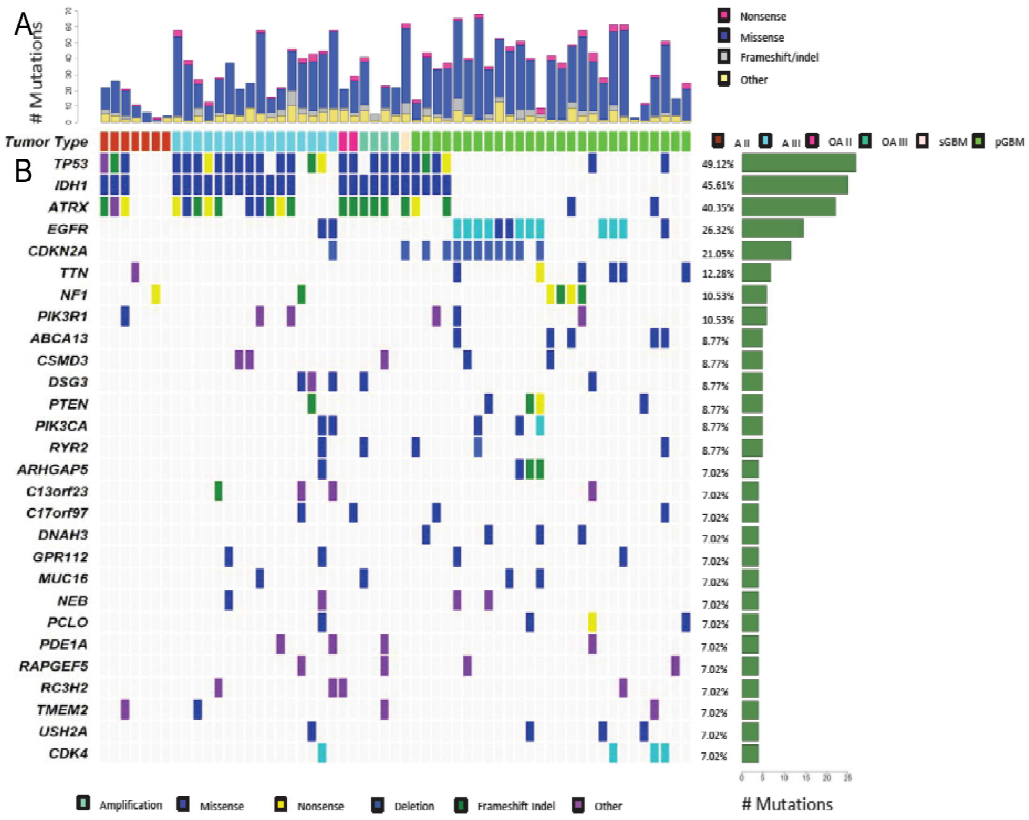

Figure 3: The genetic landscape of progressive gliomas.

Mutational analysis utilizing exome sequencing of matched tumor and normal pairs for 57 progressive astrocytomas, oligoastrocytomas, and GBMs. (A) Distribution of mutation types (Nonsense, Missense, Frameshift/Indel, Other) are reported for each tumor. (B) Depiction of mutation spectrum for each tumor is shown. Represented are genes mutated in four or more gliomas. The frequency (%) and number of gene alterations in the tumor cohort is represented on the right.

2.2 Refining the classification of malignant gliomas

Based on previous publications, it appeared there were genetic markers that tended to associate more closely with certain subsets of gliomas over others. These markers together with the mutation status of *IDH1* and *IDH2* had the potential to classify the various subtypes of gliomas. This would offer a genetic-based strategy to diagnose tumors that would complement the current histopathology-based means of diagnosis, a process that often exhibits variability based on institution and misdiagnosis. To this end, we sought to assess whether we could utilize these markers to classify the various subtypes of gliomas.

Prior exomic sequencing studies have shown the presence of mutations in *homolog of Drosophila capicua* (*CIC*) and *far-upstream binding protein 1* (*FUBP1*) in CNS samples (40). Separately, studies aimed at identifying genetic lesions of pancreatic tumors identified inactivating mutations in *Alpha thalassemia/mental retardation syndrome X-linked* (*ATRX*) in pancreatic neuroendocrine tumors(41). An expansion of this study into tumors of other origin described that these tumors displayed the alternative lengthening of telomere (ALT) phenotype and when they looked at a variety of tumors, they found that this phenotype as well as the inactivating mutations in *ATRX* were present in tumors of the CNS (42). Though there have been no mechanistic studies proving definitively that mutations in *ATRX* cause ALT, the association in our studies and many others have shown it to be incredibly tight with as many as 49 out of 50 *ATRX*

mutated tumors displaying the ALT phenotype and out of 21 gliomas with *ATRX* intact, zero exhibited the ALT phenotype(35).

We sought to define the mutation status of these genes in complement with the mutation status of *IDH1* and *IDH2* with the goal of classifying the various subtypes of gliomas. To this end, we analyzed the loci of 363 brain tumors consisting of 203 astrocytic tumors of varying grade, 50 oligodendrogliomas of varying grade, 40 oligoastrocytomas (mixed tumors displaying characteristics of both astrocytomas and oligodendrogliomas), as well as 5 Grade II ependymomas, and 65 Grade IV medulloblastomas.

We observed frequent occurrence of mutations in *ATRX* in the astrocytic subset of gliomas including Grade II astrocytomas (67%), Grade III astrocytomas (73%), secondary GBMs (Grade IV, 57%), and in the mixed oligoastrocytomas (68%). This was in contrast to those ATRX mutations observed in primary GBMs (4%) and oligodendrogliomas (14%). *ATRX* most commonly harbored frameshift mutations or nonsense mutations leading to a truncated protein, which together accounted for 91% of the mutations observed.

The association between alterations in *ATRX* and other mutations was assessed and it was found that 99% of those tumors harboring ATRX mutations also displayed mutations in *IDH1* or *IDH2*. 94% of these same tumors also contained mutations in *TP53*. This data offers the genetic landscape for astrocytomas, a signature that has been

validated several times since this publication through our own published work as well as others (**Figure 4**)(36,37,43,44).

A further correlation that was observed was in assessing those tumors that displayed the ALT phenotype. ALT is an alternative means of immortalization that relies on homologous recombination, and thus stabilization of the telomeric regions. This allows the cells to divide indefinitely without encountering the end-replication problem. ALT occurs in the minority of cancers, only about 15%, whereas the majority of cancers and immortalized cells induce expression of telomerase, an enzymatic based mechanism for telomere maintenance and circumvention of the end-replication problem(45). It has been shown that astrocytomas in particular tend to have ALT, however not oligodendrogliomas(46,47). In our studies, we show that there is an incredibly tight association between mutations in *ATRX* and the ALT phenotype, to the extent that 100% of gliomas that had the ALT phenotype also had mutations in *ATRX*. Additionally, neither the ALT phenotype nor mutations in *ATRX* were observed in the oligodendrogliomas. The link between *ATRX* mutations and ALT has been reported several times now, however there is a lack of functional data supporting a mechanism for how *ATRX* loss-of-function induces ALT.

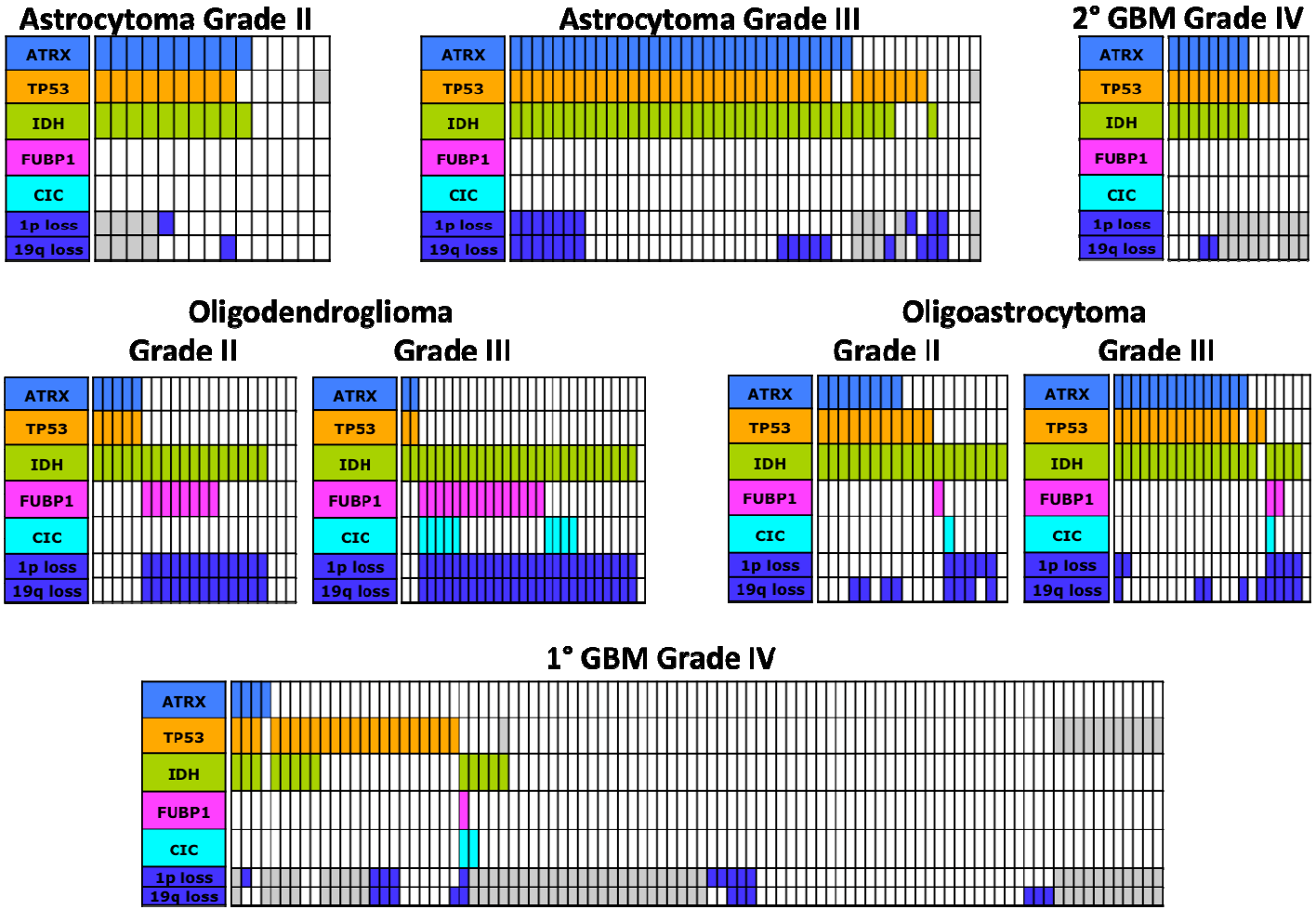
Astrocytoma Grade II
ATRX
TP53
IDH
FUBP1
CIC
1p loss
19q loss
Astrocytoma Grade III
ATRX
TP53
IDH
FUBP1
CIC
1p loss
19q loss
2° GBM Grade IV
ATRX
TP53
IDH
FUBP1
CIC
1p loss
19q loss
Oligodendroglioma
Grade II
Grade III
ATRX
TP53
IDH
FUBP1
CIC
1p loss
19q loss
ATRX
TP53
IDH
FUBP1
CIC
1p loss
19q loss
Oligoastrocytoma
Grade II
Grade III
ATRX
TP53
IDH
FUBP1
CIC
1p loss
19q loss
ATRX
TP53
IDH
FUBP1
CIC
1p loss
19q loss
1° GBM Grade IV
ATRX
TP53
IDH
FUBP1
CIC
1p loss
19q loss

Figure 4: Genetic landscape of gliomas

Distribution of mutations in *ATRX*, *TP53*, IDH (*IDH1* or *IDH2*), *CIC*, *FUBP1*, and chromosomal loss of 1p/19q among gliomas show signatures specific for each type of glioma. *ATRX*, *TP53*, and IDH display a co-mutated status among the astrocytomas of Grade II, III, and secondary Grade IV. This is in contrast to the Grade II and Grade III oligodendrogliomas that show mutations in *FUBP1* and *CIC* as well as chromosomal loss of 1p/19q. Oligoastrocytomas present with mutations in either IDH, *ATRX*, and *TP53* or in IDH, and *FUBP1* or *CIC*, or with loss of 1p/19q, suggesting that though tumors appear mixed histologically, genetically these tumors have the signature of either astrocytoma or oligodendroglioma, but not both. Also shown is the mutation spectrum of primary GBM showing it is genetically distinct disease. Note: cells shaded in gray indicate no data was available for those samples.

The presence of mutations in *CIC* and *FUBP1* were also determined and found to occur in the Grade II (38% and 14%, respectively) and Grade III (52% and 31%, respectively) oligodendrogliomas. This occurrence was in contrast to the presence of these mutations in primary GBMs, which was 1% and 2%, respectively. Interestingly, these mutations were completely absent (0%) in the Grade II and Grade III astrocytic tumors. In all cases where there were mutations in *CIC* or *FUBP1*, *IDH1* or *IDH2* was mutated, and were found to also co-occur with chromosomal loss of 1p/19q. This data offers the genetic landscape for oligodendrogliomas (**Figure 4**).

The survival data for the different glioma subtypes is consistent with what is expected based on histopathological diagnosis alone. Those patients harboring mutations in *IDH1* or *IDH2* and in *ATRX* typically have astrocytomas. These patients have a median survival of 51 months. Those patients with mutations in *IDH1* or *IDH2* and *CIC* or *FUBP1* typically have oligodendrogliomas and have a median survival of 96 months. Lastly, those patients with primary GBM, who tend to not have mutations in any of the above genes, tend to have the worst prognosis, with a median survival of 13 months. In all cases, those patients who had mutations in *IDH1* or *IDH2* had a better survival then in those patients without mutations. This has been reported several times and is a consistent finding, however little is known as to the etiology of *IDH1* mutant tumors and how they confer a survival advantage(24,25,35-37,48).

The genetic signatures we have identified are capable of distinguishing between oligodendrogliomas, astrocytomas, oligoastrocytomas, as well as primary and secondary GBMs. Primary and secondary GBMs have conferred tremendous difficulties to the neuropathologist as they are histologically very similar with few, if any distinguishing features other than secondary GBMs arising from preceding lesions. Our genetic profile for these tumors complements the traditional histology-based means of diagnosis for these diseases. Additionally, the ability to perform sequencing-based diagnosis is a cost-effective and efficient alternative that comprises an inherently unbiased approach to diagnosis. This can help resolve the issue of inter-institutional discrepancies in histological diagnosis of the same samples. Promoting consistent diagnoses will comparably aid in consistent therapeutic intervention, likely contributing to enhanced survival.

2.3 Mutant IDH1 in tumorigenesis

In addition to gliomas, mutations in *IDH1* and *IDH2* have been detected in chondrosarcoma, enchondroma, Ollier disease and Maffuci syndrome, intrahepatic cholangiocarcinoma, a small percentage of prostate cancer, angioimmunoblastic T-cell lymphoma, and acute myeloid leukemia (AML), among others(49-56). The high incidence of mutations in *IDH1* and *IDH2* in gliomas, together with them being mutated in such a variety of other cancers strongly implicates the involvement of these mutated genes in disease initiation and development. A precise and specific mechanism for how

mutant *IDH1* and *IDH2* solicits its effects are unknown, however there are no shortage of publications speculating and offering some convincing data toward particular mechanisms. Due to IDH1's promiscuous activity throughout a cell, the mechanism by which mutant IDH1 imparts its tumorigenic activity is likely a convergence of various perturbed intracellular pathways. The pathways that mutant IDH1 and 2-HG have been implicated in or suspected of having an effect on are summarized in **Figure 5**.

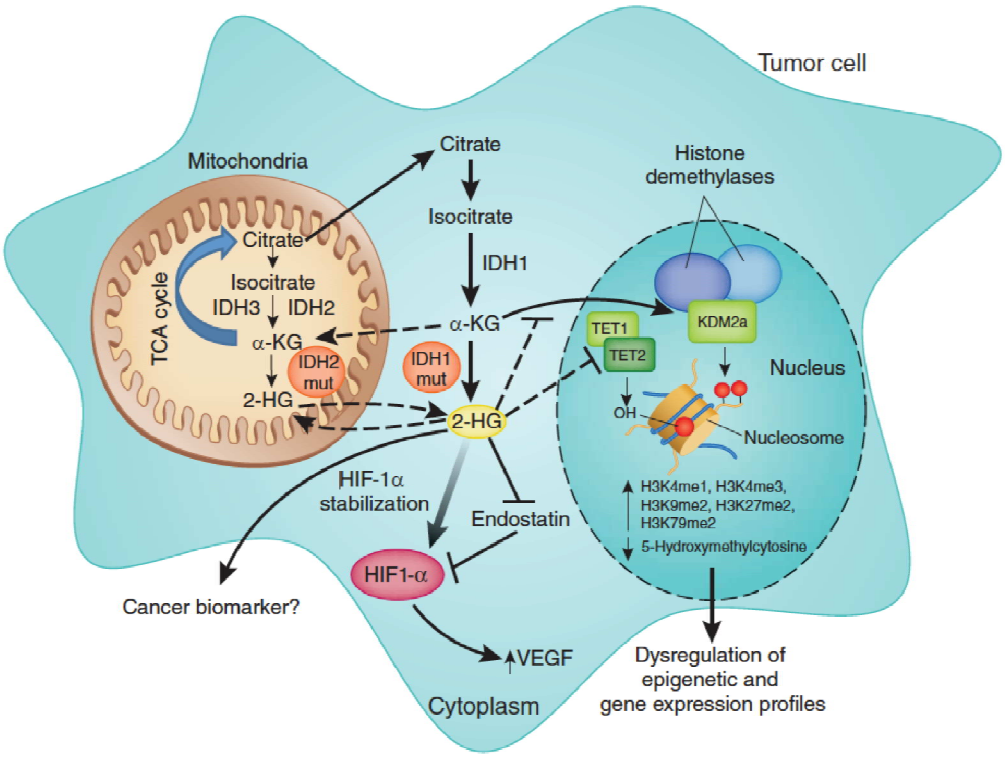

Figure 5: Mutant IDH1 and 2-HG signaling pathways.

The metabolic product of mutant IDH1 (and mutant IDH2) alters a number of downstream cellular activities that could be implicated in tumor development and progression. 2-HG competitively inhibits α-KG binding to several histone demethylases, leading to aberrant histone modification. 2-HG also inhibits TET2 hydroxymethylases, decreasing levels of 5-hmC and perturbing methylation patterns. Subsequent effects on regulation of gene expression have been observed. It can be reasoned that 2-HG also leads to increased VEGF signaling through stabilization of Hif1α, leading to increased angiogenesis though this is controversial with conflicting data. Reprinted by permission from Macmillan Publishers Ltd: Nature Publishing Group as described in Appendix A(57).

2.3.1 Biology and biochemistry of mutant IDH1

From its discovery, determining the effects of mutant IDH1 on cells has been an active pursuit of investigation. Conflicting results have arisen in terms of mutant IDH1's effects on basic cellular processes including cell proliferation and ability to form colonies in soft agar. Studies utilizing immortalized human astrocytes infected with either IDH1-R132H or IDH1-WT found that mutant cells acquired a proliferative advantage over wildtype and also acquired the ability to form colonies in soft agar(58). It was noted that this phenotype required upwards of 14 passages in order to become apparent. Another study has shown that expression of mutant IDH1 actually confers a negative impact on cell proliferation *in vitro* and *in vivo*(59). In this study, Bralten et al., utilized established glioma cell lines and overexpressed either wildtype or mutant IDH1. A marked decrease was observed in those mutant IDH1 expressing cell lines. This was corroborated when the cells were injected intracranially into mice. Tumors that developed from mutant lines displayed decreased proliferation, altered migration, as well as prolonged survival (40.3 days for mice injected with mutant IDH1 expressing cells versus 29 days for mice injected with wildtype IDH1 expressing cells)(59). There were no observable differences in apoptosis in these cells, suggesting that the cells were able to persist despite high production of 2-HG. To elucidate whether this phenotype was specifically due to the production of 2-HG, they treated wildtype cells with supernatant containing 2-HG and recapitulated their *in vitro* data, suggesting the

reduction in proliferation is at least in part due to accumulation of 2-HG. The effects of mutant IDH1 on cell proliferation can be a cell context-dependent phenomenon. However, considering the difficulties in propagating patient derived cell lines and xenografts harboring mutant IDH1, it is very plausible that mutant IDH1 alone may not display an aggressive tumorigenic phenotype that we observe in human disease without the incorporation of additional mutagenic hits(60,61).

There have been several studies investigating the biochemistry of isocitrate dehydrogenase (IDH). IDH functions as a homodimer with each homolog comprising a large domain, clasp domain, and a small domain that interact to expose the active site to substrate. IDH1 transitions between an inactive open, an inactive semi-open, and a catalytically active closed conformation(28). Mutations in humans always present in a heterozygous state which promotes the formation of wildtype:wildtype homodimers, mutant:mutant homodimers, as well as mutant:wildtype heterodimers, the latter of which were found to produce α-KG much less efficiently than their wildtype homodimer counterpart , however were able to reduce it to 2-HG(29,62). This leads to the question whether mutant IDH1 confers dominant negative activity. To address this, $NADP^+$ activity was assayed in a human oligodendroglial cell line that overexpressed wildtype or mutant IDH1 that were FLAG-MYC tagged in the presence of the isocitrate substrate. These studies showed that mutant:wildtype heterodimers had a significantly lower reaction rate than wildtype:wildtype homodimers. Wildtype IDH1

overexpression lead to an increase in $NADP^+$ in lysate, however in mutant lines, there was little effect on this activity showing that mutant IDH1 does not dominantly inhibit wildtype activity and it must be eliciting its tumorigenic effects in ways other than affecting wildtype biochemistry directly(63).

The data supplied by the TCGA has been a huge resource(23). Building from this work and expanding into gene expression analysis, Verhaak et al., generated a robust gene expression-based molecular classification system of GBM that has been an equally valuable resource to compare and assess faithfulness of cell lines and xenografts to human disease(38). In this classification, GBM is divided into Proneural, Neural, Classical, and Mesenchymal subtypes, each one corresponding to a unique gene expression profile. Briefly, the Classical subtype contained amplifications of chromosome 7 that was paired with loss of chromosome 10 in addition to amplification of *EGFR* and lack of mutations in *TP53*. The neural stem cell marker *NES* as well as Notch, and Sonic hedgehog pathways are expressed in this subtype. The Mesenchymal subtype consisted of loss of region 17q11.2, mutations in and low expression of NF1, as well as higher expression of mesenchymal markers including *CHI3L1* and *MET*. The Proneural subtype displayed alterations in *PDGFRA* and *IDH1*, and concurrent mutations in *TP53*. This group showed high expression of oligodendrocytic developmental genes including *PDGFRA*, *NKX2-2*, and *OLIG2*. Several proneural developmental genes were activated in this class such as *SOX* genes, *DCX*, *DLL3*, *ACL1*,

and *TCF4*. Lastly, the Neural subgroup exhibited expression of neuron markers including *NEFL*, *GABRA1*, *SYT1*, and *SLC12A5*.

Subsequent studies looking at DNA methylation profiles of GBMs and low-grade gliomas found that there was a distinct subgroup of gliomas that displayed a unique methylation profile enriched in the CpG islands of a subset of genomic loci(64). This profile was termed the Glioma CpG Island Methylator Phenotype (G-CIMP), a phenotype that has been observed and characterized in other cancers including colorectal cancer(65). 87.5% of those gliomas that displayed G-CIMP were found to be categorized in the Proneural subgroup. Additionally, those patients with G-CIMP tumors tended to be diagnosed at an earlier age and had a more favorable prognosis. These are all reminiscent of the features attributed to patients with mutations in *IDH1* and in fact, there was tight association between G-CIMP and mutations in *IDH1*.

Promoter CpG island hypermethylation generally results in transcriptional silencing of associated genes and in fact, several of the hypermethylated foci in these samples included markers of mesenchyme, tumor invasion, and extracellular matrix, all of which were found to be downregulated when looking at gene expression patterns in these samples(64). Interestingly, the Mesenchymal subgroup of gliomas displays a more aggressive phenotype, whereas the Proneural subgroup tend to exhibit a more favorable prognosis, suggesting that this more aggressive nature may be due to induction of a mesenchymal gene pattern due to the silencing of particular gene sets.

Several studies, including from our own lab, have sought to assess the contribution of mutant IDH1 and determine a causal effect for G-CIMP. By either expressing mutant IDH1 in human astrocytes, or generating isogenic cell lines incorporating the IDH1-R132H mutation, it was found that mutant IDH1 is responsible for remodeling the methylome and inducing G-CIMP(66,67). Additionally, it was found that the gene expression profile for mutant IDH1 expressing immortalized human astrocytes was similar to the profile found in low-grade gliomas suggesting these *in vitro* lines are faithfully recapitulating the expression patterns observed in human disease(66).

2.3.2 2-HG inhibits α-KG dependent dioxygenases

Determining a mechanism for the G-CIMP and the subsequent gene expression changes observed in IDH1-mutated gliomas required a closer examination of the biochemistry of the enzyme. As mentioned previously, mutant IDH1 confers both a loss-of-function as well as a gain-of-function. It has been reported that there is a reduction of α-KG to produce high levels of 2-HG(29). Structurally, these products are nearly identical except at the C2 location; where in α-KG there is a carbonyl group, this is replaced with a hydroxyl group in 2-HG (**Figure 2**)(68). Considering the high levels of 2-HG present, it is highly suspected that this molecule that is nearly identical to α-KG will competitively inhibit the class of enzymes that is dependent on α-KG as a substrate for their activity, that is the α-KG dependent dioxygenases. In fact, though it is shown that 2-HG is a relatively weak antagonist of α-KG, it is capable of perturbing the

function of many α-KG dependent dioxygenases especially when at high levels, such as the case is in IDH1 mutant tumors(68-73).

According to the GenBank DNA database, there are approximately 70 known and putative α-KG dependent dioxygenases that could be compromised by elevated levels of 2-HG. Their effects range in scope from epigenetic regulation and gene expression to implications in angiogenesis and tumor aggressiveness(72). Specifically, those that have received the most attention with regard to being affected in *IDH1* mutated cells are the Ten-Eleven Translocation (TET) proteins involved in DNA methylation, the Jumonji-C domain-containing histone demethylases, and the prolyl hydroxylases regulating hypoxia-inducible factor (HIF) signaling.

2.3.2.1 Ten-Eleven Translocation proteins and 5-hydroxymethylcytosine in glioma

It turns out that both DNA methylation and histone methylation, two facets of epigenetic regulation affecting gene expression, are controlled by α-KG dependent dioxygenases. The role that 2-HG plays in effecting these α-KG dependent dioxygenases is an active pursuit of research.

The TET family of proteins, including and specifically that which is produced from the *TET2* gene, is involved in normal development as well as many diseases, including glioma and myeloid leukemias. Interestingly, mutations in *TET2* are mutually exclusive with mutations in *IDH1* or *IDH2*, suggesting the two genes may have similar pathogenic roles. The normal function of the TET proteins is to catalyze the conversion

of 5-methylcytosine (5mC) to 5-hydroxymethylcytosine (5hmC)(73). It is suspected that this process is the first step in the pathway leading to the demethylation of cytosine residues, and thus is strongly implicated in processes of gene regulation throughout development. In fact, it was observed that the expression and activity of the TET proteins decrease as the cells differentiate. The subsequent effects were observed when looking at the promoter regions of embryonic stem (ES) cell specific genes where there was a reduction in 5hmC levels and an increase in the 5mC levels at ES cell specific loci(74). However, as the cell differentiates, the opposite was observed, with 5hmC levels increasing and 5mC levels decreasing. The observation that the 5hmC mark is enriched in promoters with the histone 3 lysine 27 trimethylation (H3K27me3) mark, a mark correlated with transcriptional silencing, and the histone 3 lysine 4 trimethylation (H3K4me3) mark, a mark correlated with transcriptional activity, suggests that 5hmC contributes to the poised chromatin signature found in developmentally regulated genes and may represent a major event in generating an active gene expression state of tissue-specific genes(75,76). It was additionally found that not only is 5hmC elevated in more differentiated cell types and less so in ES cells, but it was observed that these reduced levels of 5hmC also applies to cancer cells(77).

Taking into account that mutant IDH1 induces G-CIMP, the hypermethylator phenotype, together with the findings of 2-HG inhibiting the TET family of proteins and subsequently affecting 5hmC and 5mC levels, suggests that mutations in *IDH1* may

change the expression of a large subset of genes. The fact that mutations tend to occur very early on in tumorigenesis may allow these cells to persist in a stem cell like state, thereby contributing to tumorigenesis.

To this end, eloquent studies have been performed looking at the effects of mutant IDH proteins in the hematopoietic system and characterizing gene expression and methylation profiles. These studies have further lead to the conclusion that the hypermethylator phenotype promotes a gene expression profile similar to immature or stem-like cells and can be induced through the inhibition of the TET family of proteins via 2-HG production(70). Additionally, they show that these cells display a block to differentiation and an inability to differentiate through the myeloid lineage. A block to differentiation has been observed in several other cell contexts including adipocytes, hepatocytes, cells of the hematopoietic system, as well as immortalized human astrocytes, lending credence to the notion that one of the main oncogenic activities of mutant IDH1 is that it confers a block to differentiation of cells, maintaining them in an immature state capable of proliferation(56,78,79).

2.3.2.2 Mutant IDH1's effects on histone methylation in gliomas

In a series of studies looking at the ability of 2-HG to inhibit various α-KG dependent dioxygenases, it was found that one of the more potent inhibitions occurred in the family of histone demethylation proteins including Jumonji domain containing 2A (JMJD2A) and Jumonji C-domain containing histone demethylase (JmjC)(72,80). The

family of histone demethylases plays an important role in epigenetic regulation of gene expression. Histone methylation dictates the structure, conformation, and organization of chromatin with particular modifications conferring either transcriptionally active euchromatin (H3K4, H3K36, H3K79), or transcriptionally silent heterochromatin (H3K9, H3K27, H4K20)(72). The balance between these modifications is dependent on the activity of histone methyltransferases and histone demethylases. Disruption to this balance or mutations in these regulators inevitably effect gene expression and pathogenesis. Mutant IDH1's effects on histone methylation marks have been directly linked with production of 2-HG in various papers(69,78,80). In general, it appears that mutant IDH1 confers an increase in overall histone methylation by perturbing the activity of histone demethylases via competitive inhibition with 2-HG. For IDH1 mutant tumors, there appear to be an increase in the repressive H3K9me3 and H3K27me3 marks, suggesting that mutant IDH1 may preferentially affect repressive modifications(67,78).

Histone demethylases have been characterized as tumor suppressors in some contexts and oncogenes in other contexts. This suggests that their effects overall are cell-context dependent. For IDH1 mutant tumors in particular, it will be important to investigate the particular loci that are differentially methylated in IDH1 mutant tumors compared to wildtype and determine their effects on the expression of those loci. Additionally, the histone methylation profile of cells of the CNS and of the suspected

cell of origin, whether that is NSCs or OPCs or even more differentiated cell types would be imperative as mutant IDH1's effects could yield conflicting results depending on the histone methylation profile and balance of transcriptionally active versus repressive modifications that are present in the founding cell population.

2.3.2.3 Contradictory effects of 2-HG on HIF signaling

Another member of the α-KG dependent dioxygenases that could be inhibited are the prolyl hydroxylases that regulate HIF signaling. The prolyl hydroxylases normally hydroxylate the HIF1α and HIF2α proteins. These hydroxylated proteins are then recognized and ubiquitinated by Von Hippel Lindau (VHL), a ubiquitin E3 ligase. These targeted proteins will subsequently undergo proteasomal degradation. Under hypoxic conditions however, the prolyl hydroxylases are inefficient and unable to properly hydroxylate HIF1α and HIF2α. As a result, these proteins dimerize with HIF1β and function as transcription factors that coordinate a response to hypoxia, inducing expression of a range of genes including those involved in metabolism, angiogenesis, and tumorigenesis.

The data regarding 2-HGs effects on the prolyl hydroxylases and on HIF signaling has been contradictory. This may suggest that its activity and subsequent effects may be cell-context dependent, or that there are other pathways involved, diminishing or counteracting expected results. The fact that 2-HG has weak inhibition of HIF hydroxylases under experimental conditions suggests that this would likely not

lead to HIF pathway activation and induction of downstream gene expression. Additionally, it suggests this pathway may not be the predominant mechanism for pathogenesis(80). It should be noted that when *IDH1* is mutated however, 2-HG is produced at such an excessive level that this may inhibit or perturb this pathway more than what was observed in these studies.

In vitro studies utilizing the established U87 glioblastoma cell line shows that when mutant IDH1 is ectopically expressed, there is an increase in HIF1α and an induction of downstream target genes including that of *vascular endothelial growth factor* (*VEGF*)(69,81). When cells were treated with 2-HG, a comparable result was observed. Expanding these finding into an *in vivo* context, Zhao et al., quantified HIF1α via immunohistochemistry (IHC) and found that all tumors harboring mutations in *IDH1* displayed a statistically significant increase in those cells staining positive with HIF1α(81). Together, these groups concluded that mutant IDH1, by means of 2-HG did in fact induce HIF1α through an inhibition of prolyl hydroxylases(69).

As alluded to previously, that a major oncogenic contribution of mutant IDH1 lies in its induction of HIF1α and activation of downstream target genes is a controversial topic. To further assess the association between mutations in *IDH1* and stabilization of HIF1α, Williams et al., analyzed 120 archived formalin-fixed paraffin embedded (FFPE) glioma samples and looked for association between HIF1α and the IDH1 mutation(82). The observations from this study included that HIF1α was

expressed in a subset of cells that also expressed the mutant IDH1. HIF1α was also present in areas of necrosis and perinecrotic tumor cells. It was noted however, that there were areas where mutant IDH1 was strongly expressed but HIF1α was absent, therefore leading this group to conclude there is no relation between the expression of mutant IDH1 and HIF1α(82).

Another group investigating mutant IDH1's effects on HIF1α looked at the EglN prolyl 4-hydroxylase specifically, the enzyme that incorporates the hydroxyl groups on HIF1α and targets them for degradation. However, in contrast to previous studies, they showed that when mutant IDH1 was expressed in immortalized human astrocytes, HIF1α activity was diminished and this was associated with a proliferative advantage and ability to grow in soft agar(58). These studies showed that 2-HG actually promoted EglN1 activity, leading to hydroxylation and subsequent degradation of HIF1α. This was associated with lower expression of HIF targets. Additionally, these findings were validated in an isogenic cell line derived from a human colorectal cancer line(58). Moving into an *in vivo* context, this group analyzed the gene expression pattern in the TCGA's Proneural subgroup of gliomas and found that the HIF response genes were diminished. Perhaps consistent with this set of data is that characterization of mutant IDH1 gliomas show that they tend to display a lesser degree of necrosis as well as a nonsignificant trend toward less frequent occurrence of vascular abnormalities, both indicators of decreased HIF1α activity(62,83). Considering necrosis and vascularization

are usually markers for a worse prognosis, speculative but consistent thinking in this direction would imply that due to the lesser extent of necrosis and the less frequent vascular aberrations, together with the survival advantage that mutant IDH1 glioma patients display, that there may be justification for HIF1α being diminished in mutant IDH1 gliomas.

3. Introduction: Mice as a model organism

Whether it is yeast, Drosophila, zebrafish, mouse, non-human primate, or any other model system, the contribution of these organisms to biomedical research cannot be understated or undervalued as their impact on human and animal health has been extraordinary. Inevitably, due to their small size, ease of handling and housing, short generation times, ability for genetic manipulation, and perhaps most importantly, the fact that they share about 99% of their genes with humans with extensive homology, makes the mouse one of the more commonly utilized model organisms. With genetic and physiological similarities to humans, the mouse can be used to scrutinize many physiological complexities including that of the immune, endocrine, nervous, cardiovascular, and skeletal systems. Additionally, mice tend to naturally develop many diseases that affect humans such as cancer, atherosclerosis, hypertension, diabetes, osteoporosis, and glaucoma thus making the investigation of such diseases in these animals particularly relevant with most definitely many of the same causative molecular perturbations occurring. For this reason, investigation of therapeutics targeting these naturally occurring diseases would be expected and have been shown to have similar biological consequences in mouse and human. Lastly, for those diseases that arise in humans but not mouse, through manipulation of their genome or environment, many diseases can be simulated and induced including such diseases as cystic fibrosis and Alzheimer's. This together with the ability to control for such factors as environmental

contributions or variation among animals is another reason why mouse modeling is so advantageous and thus prevalent.

Animal research has been the foundation for countless successes in the medical and public health arena, and we as humans have blindly reaped the benefits. The elimination of Poliomyelitis as a public health threat, eradication of smallpox, understanding the genetic and environmental causative factors of cancer, vaccination and immunization against typhus, diphtheria, whooping cough, and tetanus are but a few of the major accomplishments that have animal research at its foundation. Perhaps one of the most profound examples for how animal research has impacted human life is in the studies lead by Professor Pier Paolo Pandolfi of Harvard Medical School. Early in his career, he discovered the genetic mutations responsible for acute promyelocytic leukemia (APL), a cancer of the bone marrow most common in younger people. Being incredibly difficult to treat, most patients succumbed to the disease. Through the generation of genetically engineered mouse models (GEMMs) and faithfully recapitulating the human disease in mouse, Pandolfi and colleagues were able to generate targeted therapies and now, the majority of patients survive. A similar progression of events was displayed for the childhood leukemia, acute lymphoblastic leukemia (ALL). The majority of the research for this disease took place at the St. Jude Children's Research Hospital and at the time of its first investigation in 1962, survival was in the realm of 4%. Now, survival is upwards of 90%. To conclude, the impact and

necessity of animal research on human health and survival is invaluable and we have much of our health, well-being, and ability to overcome disease and sickness to our fellow animal counterparts.

3.1 Mouse models of glioma

As mentioned previously, mouse models have contributed significantly to the understanding of human disease. Animal models complement other laboratory techniques to provide a resource that permits the dissection of molecular pathways, allowing for the construction of a roadmap for pathogenesis. Additionally, pending pathogenesis is comparable with that of human disease, as is the ultimate goal, these resources provide a means for investigation of the most effective and impactful therapeutic modalities.

Animal modeling is one of the few ways to fully recapitulate human tumorigenesis and to achieve a comprehensive understanding of tumor development as it encompasses many of the variables and components of human disease from physiology, microenvironment, impact of the immune system, tissue and cellular-context, genomic contribution, and environmental components. Several different techniques are employed to generate mouse models of tumorigenesis including chemical mutagen-induced tumorigenesis, xenograft transplantations, germline genetic modifications, and somatic genetic modifications. Perhaps the most common for glioma modeling in particular are xenograft transplantations, germline genetic modifications,

and somatic genetic modifications, each presenting with their own advantages and limitations. Ultimately, the system that encompasses the sequencing data from large-scale genomic studies to assess the contribution and significance of particular mutations, combined with the ability to promote tumorigenesis in an orthotopic manner as to preserve the microenvironment and signals from within, as well as depicting the heterogeneity observed in patient tumors, and to do so with high penetrance and short latency will be the most impactful of models. In doing so, the model generated will provide the most stable foundation for preclinical data acquisition.

3.1.2 Xenografts as a model for glioma

Xenograft models entail the injection of human tumor cells into a mouse, either into the flank region or intracranially, and commonly utilize immune-compromised animals. This approach is utilized when a better understanding of the contribution of different genetic aberrations is desired. For example, by incorporating different mutations and generating sub-lines of the parental line, one could determine the contribution these mutations are having on cell proliferation, migration, aggressiveness, and metastasis *in vivo*. A representative experiment comes from Martens et al., where several GBM xenografts were engrafted. Infiltration into surrounding brain parenchyma, proliferation, and response to therapy were found to be dependent on the mutation spectrum of each GBM, specifically with regard to the presence of *EGFR* amplification(84). In addition to these biologically faithful systems allowing for an in

depth analysis of tumor development and progression, much of the power for xenograft systems lies in the investigation of therapeutic modalities to assess the most effective interventions and protocols for tumor regression. In many instances, the use of xenografts faithfully recapitulates the histological appearance and subtyping of the parental tumor of which the cell line was derived as well as the gene expression profiles(85-88). These features must be validated and ensured in each instance as there are most definitely cases where biology, genetics, or histology are lost, leading to a fundamental failure of the system with regard to relevance(89). For xenografts in particular, it has been difficult to fully recapitulate the primary human lesion as once transplanted into the mouse, the cells form well-demarcated and compact lesions as opposed to the diffusely infiltrative nature of the disease that is inherent of human gliomas. Oftentimes, xenografts require injection into immune-compromised animals, and with ever increasing data suggesting the importance of the immune system in shaping tumor progression and response to therapy, this imparts a major drawback. Additionally, the ability to generate the human derived xenograft and recapitulate the human disease *in vivo* are among the hurdles to be overcome in xenograft modeling. This is especially true for the study of *IDH1* mutated gliomas which are known for being incredibly difficult to culture *in vitro* as well as for xenograft establishment(61). Interestingly, it has been reported that xenografts tend to graft and display much more of an aggressive phenotype when they are derived from a higher-grade tumor(90).

Perhaps one of the difficulties in propagating mutant IDH1 cell lines and xenografts lie in that they tend to occur in those tumors of lower grade, including the Grade II and Grade III tumors.

3.1.3 Somatic gene transfer and the study of gliomagenesis

Xenografts, being derived from human samples, often display genetic heterogeneity both as a result of therapy that the patient has endured as well as a result of the *in vitro* culturing of the cells. When injecting these cells into mice, the precise role of particular genes and how they are interacting with the products of other genetic perturbations is unknown; similarly, the relevance to initiation, development, or maintenance of the human tumor is unknown. To this end, other modeling systems including somatic gene transfer, offer advantages. One system for gene transfer that has been particularly fruitful has utilized replication-competent avian sarcoma-leukosis virus long terminal repeat with splice acceptor (RCAS) vectors that permit the transfer of genes into transgenic mice expressing *t-va*, the avian receptor for RCAS(91,92). In this way, through the injection of either virus or virus producing avian-derived cells, genes of interest can be incorporated into cells or tissues that express the viral receptor. As mammalian cells do not express *t-va*, off target infection or gene introduction into cell types other than those in which *t-va* is being expressed in is thus avoided. An ever-expanding cohort of *tv-a* mice is being generated, however the most common ones for glioma modeling include those in which *tv-a* is expressed under control of neural

specific promoters, such as Nestin expressed in the progenitor compartment, or GFAP expressed in mature astrocytes and some progenitor cells of the SVZ, among others(89).

There are several advantages in using the RCAS/*t-va* system. For one, this system can be used to interrogate the cell of origin by determining the susceptibility of particular cell types to transformation. Additionally, the same cells can be infected with multiple viruses at the same time. Therefore, the cooperation of several genetic mutations can be investigated. Likewise, you can infect sequentially with different viruses to determine the initiation or maintenance contribution of particular mutations. One drawback for this system is that these viruses can only package genes of certain size; a rough rule is to clone in genes less than 2.5-kilobases. Though many genes are smaller than this, there are some that will be unable to be replicated due to size. Another limitation is with regard to the difficulty of incorporating mutations that present as deletions, knock-downs, or tumor suppressors. To overcome this, these mice can be crossed to other transgenic animals, including those of tumor suppressor-deficient backgrounds. Crossing to conditional transgenics further adds to the utility of this system as transfer of virus encoding Cre-recombinase can selectively activate or delete genes from *t-va* expressing cells that are infected. The fact that these animals are immune-competent provides the advantage of an intact immune system in terms of modeling and providing a relevant microenvironment. However, this can complicate injections into adult animals as inflammation and an immune response can ensue,

though it has been shown that tumors, specifically GBMs can be induced in adult animals(91).

One of several landmark studies shows the utility of the RCAS/*t-va* system while also showing the importance of different locations and thus microenvironments, on the tumor initiating ability of different oncogenes(91). In this study, Hambardzumyan et al., show that *PDGFB* can drive gliomagenesis in the SVZ, cortex, and the cerebellum suggesting that there are different cell populations throughout the adult brain that are capable of tumor formation. The same system can also be used to investigate the contribution of genetic background to tumorigenesis, scrutinize the identity of the cell of origin, or even assess the response to different therapeutics in adult gliomas.

3.1.4 Genetically engineered mouse models of gliomagenesis

GEMMs are the gold standard for modeling for many reasons. Not only can GEMMs be generated to incorporate the exact mutations found in human samples, but they can be induced to express these mutations in a tissue-specific manner at a designated time, thereby achieving spatio-temporal control that can be as restricted or as broad as the promoter in which one is using. This is accomplished through the incorporation of the Cre/LoxP system whereby the Cre-recombinase recognizes 34-base pair DNA sequences artificially and intentionally incorporated into the genome. These sites will undergo recombination and excise the intervening genomic sequence. There are many possibilities for how best to use this technology, however some include

incorporation of reporters to know when a particular gene is being recombined or expressed, or expression of Cre-recombinase could induce excision of a stop cassette that was silencing an oncogene, thereby promoting its tumorigenic activity. Alternatively, the LoxP sites can be placed such that they are located at critical regions of the gene, perhaps flanking the exons required for catalytic activity, and thus upon expression of Cre-recombinase and excision of the intervening sequence, the gene will be knocked-out. To add an additional level of control, Cre-recombinase can be induced under control of different promoters, thereby expressing Cre-recombinase and inducing either the activity of an oncogene or knocking out a gene in a tissue-specific manner, depending on what tissues the promoter is expressed in. Temporal regulation can also be achieved through the use of an inducible Cre-recombinase. In this case, Cre-recombinase is fused to a mutated hormone-binding domain of the estrogen receptor, ER^{T2}. It is only when the estrogen analog is administered that the Cre-recombinase is translocated to the nucleus where it can act on the LoxP sites and induce recombination at the sites. When the $CreER^{T2}$ is fused to a particular promoter, tamoxifen administration will induce the translocation of the recombinase to the nucleus in only those cells in which the promoter is active. In this way, one can achieve spatio-temporal control of gene deletion or oncogene activation. This allows for the investigation of the induction of different mutations at different stages of development. Additionally, through crossing with other strains of GEMMs, several mutations can be incorporated and induced within the same

cell, thereby allowing for the study of cooperativity among genetic mutations found in humans.

The generation of GEMMs and the conditional expression system alleviates many issues that arise in mouse modeling. Many times certain mutations either confer adverse effects or can be embryonic lethal to the animals. Spatio-temporal control over the induction of these mutations allows for these events to be overcome, permitting study of critical genes without the animal succumbing. Additionally, as these mutations are induced in the particular cell of interest, it is unlikely that other mutations will accrue. Therefore, the genetic stability is something that can be controlled, unlike in xenograft models. In theory, there should be no loss or gain of known or unknown genetic alterations as there is no process of *in vitro* culture or previous history of therapy. GEMMs do have intact immune systems and thus offer a more realistic and faithful microenvironment. This is advantageous for tumor growth as it promotes the appropriate interaction and signaling between tumor cells and the stroma. This is an ideal situation as it recapitulates the biology of a naturally occurring tumor and promotes the study of the cooperativity and interaction of these cells on the initiation, development, and progression of the tumor over time, as well the study of the regression of the tumor following therapeutic intervention. One drawback of GEMMs is that they cost more to generate compared to other model systems. Additionally, tumor development can be a slow process that is dependent on both the potency of the

mutation as well as the promoter in which it is being expressed. Though the refinement of expression is an advantage, it can also be a daunting task to determine the precise time, location, and cell type to induce expression of the particular mutation.

One of several examples of mouse glioma models that demonstrate the physiological relevance and value of GEMMs for future preclinical studies lies in a study by Reilly et al., where animals with mutations in *NF1* and *TP53* were crossed and found to develop a range of brain lesions including diffuse cells with atypical nuclei to large, aggressive tumors bearing several histological hallmarks(93). For example, some tumors presented with elongated astrocytic nuclei with irregular contours (diffuse astrocytoma, Grade II), while others displayed increased mitotic activity (anaplastic astrocytoma, Grade III). A subset also exhibited focal tumor masses, areas of necrosis, and even multinucleated giant cells (GBM, Grade IV). The fact that these tumors were generated *in vivo*, in a context with known genetic aberrations, without incorporating exogenous means of mutagenesis proves that this controlled system permits the study of particular genetic anomalies and is able to generate histologically faithful tumors that recapitulate the biology of human disease.

Harnessing the wealth of genetic sequencing data for human tumors, together with the determination of the genetic signatures of the family of gliomas, we were poised to generate genetically faithful mouse models that encompass those mutations and perturbed core signaling pathways that are most commonly found in human

gliomas. Our goal was to generate models that accurately reflect progressive gliomas and can be used to advance our understanding of the disease while producing a platform for preclinical testing of new treatment options.

3.2 Generation of a mutant IDH1 conditional knock-in mouse model

Our goal was to generate genetically faithful mouse models that harbor those precise mutations most commonly found in human progressive glioma. These include mutations in *IDH1*, *ATRX*, and *TP53* (**Figure 4**)(35,36). As GEMMs have already been generated for conditional deletion of *ATRX* and *TP53*, we sought to generate the first mouse model permitting the conditional expression of mutant IDH1, specifically one that expresses the most common mutation found in human gliomas, the R132H mutation(25,94,95). To fully recapitulate the mutation spectrum observed in human glioma, particularly the astrocytic subset of glioma, these newly generated mice will be crossed with previously generated animals incorporating conditional deletion of *ATRX* and conditional deletion of *TP53*(94,95). These studies allowed us to answer what the effects of these mutations are on specific cell types of the brain including the neural stem cells. The generation of these animals also allows for the understanding of why these genes are so commonly found to be co-mutated in human gliomas as well as provide a means for assessing the most effective therapeutics. Additionally, because *IDH1* is found to be mutated in so many other cancers and diseases, the models generated from

these studies will exhibit broad application and will lend insight into pathogenesis of these many other cancers and diseases(49-56).

Generation of the mutant IDH1 conditional knock-in mouse model was done in collaboration with the University of North Carolina School of Medicine Animal Models Core Facility. For this process, a targeting vector was constructed based off of the genomic sequence of the 129P2/Ola strain of mouse. The targeting construct contained the following features: a 5,426-base pair 5′ homology arm encompassing exon 2 of *IDH1* followed by a LoxP site, three copies of the SV40 polyadenylation signal, a neomycin resistance gene flanked with FRT sites, another LoxP site, and a 2,416-base pair 3′ homology arm encompassing exon 3 of *IDH1* and the R132H mutation (**Figure 6A**). In humans, the arginine-132 residue of *IDH1* is encoded by a CGT codon and is most commonly mutated to histidine, CAT. The construct generated for these studies targets the endogenous mouse locus, requiring a two-base pair change from the CGA codon for arginine to the CAC codon for histidine. This targeting construct was electroporated into 129P2/Ola mouse ES cells and recombinants were selected using G418. Polymerase-chain reaction (PCR) across the 3′ homology arm was performed to distinguish homologous recombinants from non-homologous integrants. 16 clones gave a positive signal, of which 8 were chosen for Southern blot analysis to confirm the homologous targeting. Briefly, genomic DNA was digested with the SacI restriction endonuclease. When the wildtype allele is present, this would liberate a 16.1-kilobase fragment that

could be detected through one of two probes, either a 5′ or a 3′ probe. Alternatively, when the mutant allele is present, an 8.8-kilobase fragment and a 10.3-kilobase fragment will result, each being detected by the 5′ or the 3′ probe, respectively. Clones 1F4, 2E7, 2F3, 3F1, 3G3, and 4E3 all displayed the 8.8 kilobase band indicating correct targeting (**Figure 7A and B**). Two additional probes including the 3′ probe as well as an internal probe in the neomycin gene were used. Though the 3′ probe and the neomycin probe showed similar results, the neomycin probe showed an extra band in clones 1F4, 2E7, and 2F3 suggesting that though there was proper integration, there was also a random integration site. Further screening showed that clone 2E7 contained R132H and microinjection was performed into blastocysts derived from the C57Bl/6 mouse strain (**Figure 7C**). 2E7 went produced chimeras that gave germline transmission of the targeted allele. Resultant chimeras derived from 2E7 were screened for germline transmission through PCR and sequencing based assays as will be described further in the next section.

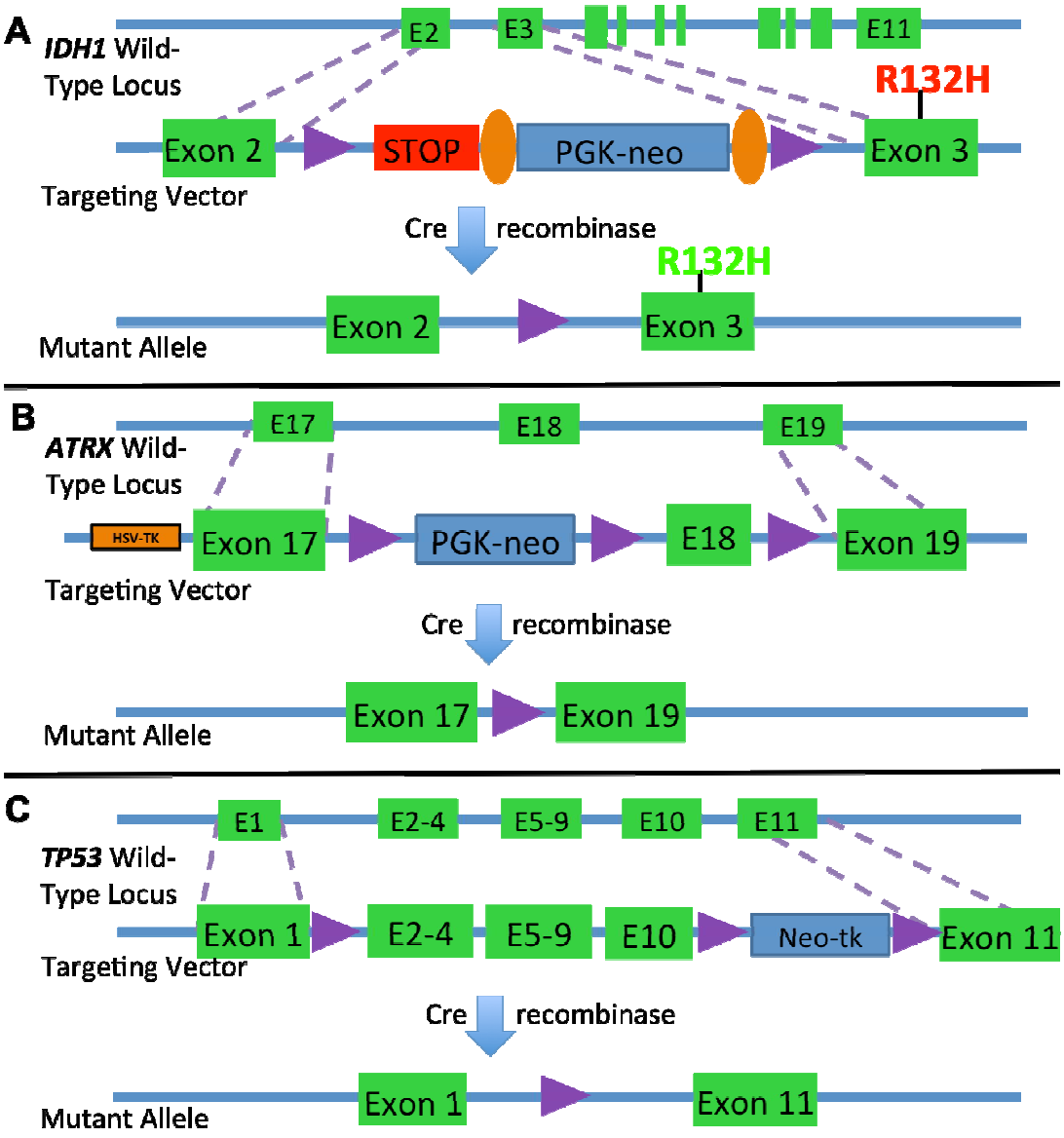

Figure 6: Generation of GEMMs.

Animals with conditional expression or deletion of those genes most commonly mutated in the astrocytic subset of gliomas were generated or gifted. (A) A floxed stop cassette upstream of the R132H mutation of *IDH1* was incorporated to generate a conditional knock-in. (B) Exon 18 of *ATRX* was floxed to generate a conditional null allele. This was described previously(94). (C) Exons 2 through 10 of *TP53* were floxed to generate a conditional deletion. This was described previously(95).

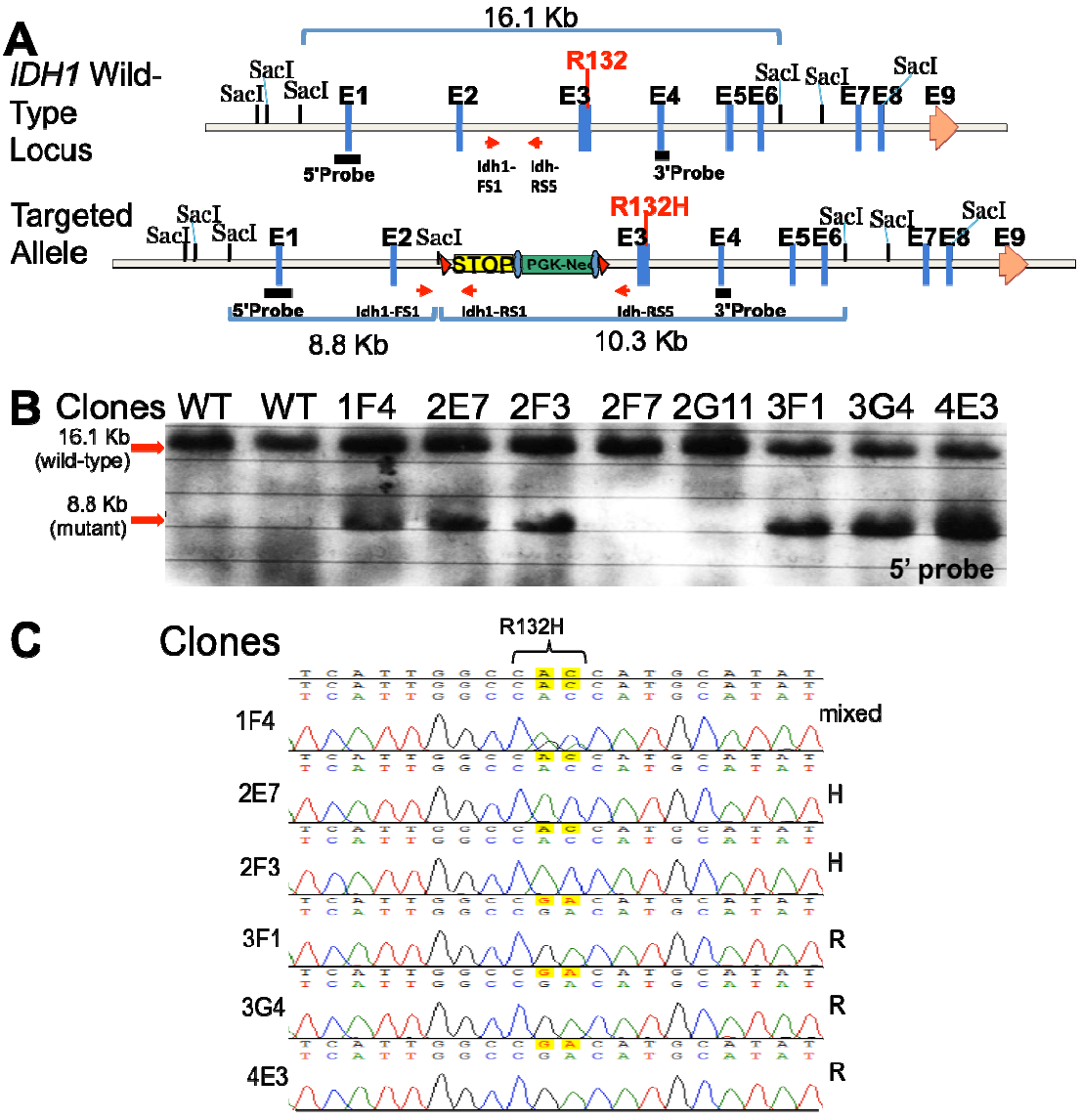

Figure 7: Validation of IDH1-R132H incorporation into the genome.

Molecular details of targeting strategy and validation for generation of IDH1-R132H conditional knock-in include (A) Presence of SacI site in mutant allele such that upon digestion, mutant allele will have an 8.8-kb and a 10.3-kb band compared to the 16.1-kb band present in the wildtype allele when visualized through Southern blot. (B) Southern blot using the 5′ probe shows 6 clones with successful integration. (C) Further screening shows of those 6 clones, 2E7 and 2F3 contain the CGA to CAC R132H mutation. 2E7 was microinjected and generated chimeras capable of germline transmission.

3.2.1 Validation of conditional knock-in IDH1-R132H mice

Chimeras were generated and bred. To ensure germline transmission and to maintain lines of conditional knock-in IDH1-R132H 129P2/Ola, PCR-based and sequencing-based assays were applied. Genomic DNA (gDNA) was obtained from either tail snips of pre-weaned animals or toe-clips from postnatal day 9 (P9) animals. In either case, the tissues underwent lysis, gDNA was extracted, and PCR and sequencing of gDNA was performed to validate the presence of the targeted allele (**Appendix D and Materials and Methods**). Two pairs of PCR primers were made to amplify either the wildtype *IDH1* allele or the targeted allele, generating a 329-base pair amplicon or a 263-base pair amplicon, respectively (**Figure 8**). Additionally, primers were generated that contained the M13(-20) forward primer to allow for efficient sequencing reactions that would amplify the mutated region allowing us to distinguish wildtype, mutant, and heterozygous animals based on the presence of the CGA or CAC codon, or a mixture of the two. PCR results of all generated animals resulted in either a wildtype band and a targeted band or only the wildtype band, suggesting that our animals were in a heterozygous state. Homozygous animals were never observed (**Table 1**). In a series of 62 crosses between IDH1-R132H/Wildtype (heterozygous) animals, 292 animals were generated with 113 Wildtype/Wildtype and 179 IDH1-R132H/Wildtype animals resulting. Zero animals were IDH1-R132H/IDH1-R132H. Performing a χ^2 analysis to test for a 1:2:1 Mendelian inheritance pattern, we determined the χ^2 value to be 102.35

with a P-value to be less than 0.0001, suggesting this was not due to chance. Additionally, failure to recover IDH1-R132H/IDH1-R132H animals (either due to embryonic or perinatal lethality) at the time of genotyping (P9) would subsequently generate a 1 to 2 ratio for Wildtype/Wildtype versus IDH1-R132H/Wildtype progeny, we derive a χ^2 value of 3.75 and a P-value of 0.0528, suggesting that this hypothesis is plausible (**Table 1**). Failure to generate IDH1-R132H/IDH1-R132H animals would not be surprising as the targeted allele is knocked-out due to the presence of the SV40 polyadenylation signal that lies upstream of the R132H mutation. Considering IDH1's active role in metabolism and the TCA cycle, it is likely that homozygous animals are not viable.

The presence of one wildtype allele and one targeted allele is ideal as once the stop cassette of the targeted allele is excised via expression of Cre-recombinase, this will generate a heterozygous state with one wildtype allele and one mutant allele, thus maintaining the genetically faithful and representative nature of our system as glioma patients present with heterozygous IDH1 mutations.

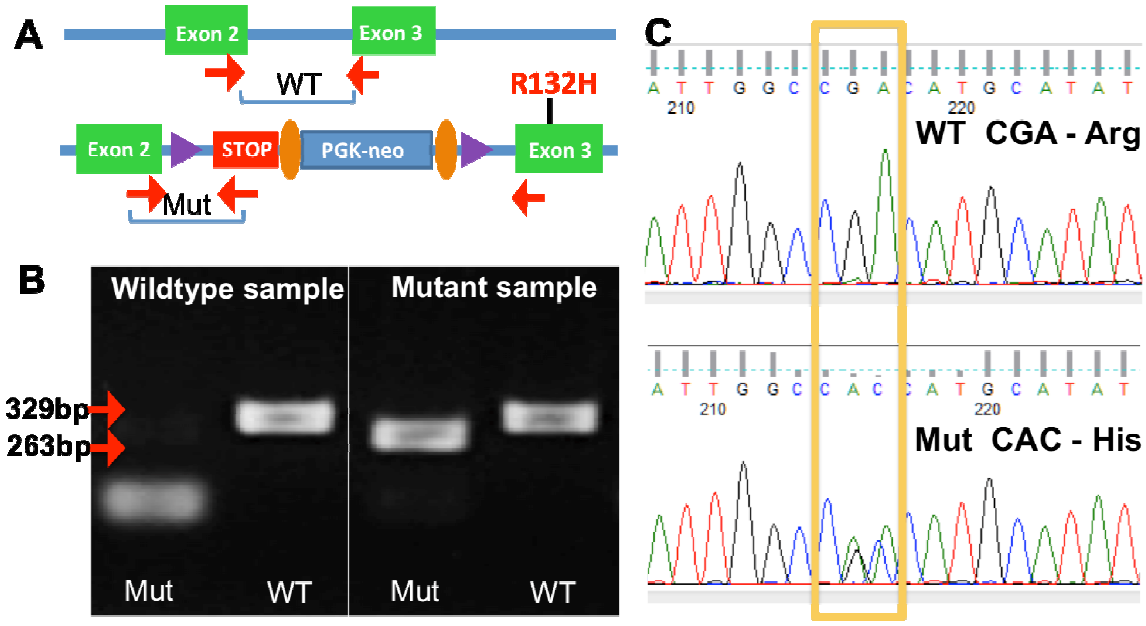

Figure 8: Genotyping validation of IDH1-R132H animals.

Genomic DNA was extracted from either tail-snips or toe-clips. Primers specific for either the wildtype allele or the mutant allele are shown in (A). (B) Wildtype allele will yield 329-basepair amplicon whereas mutant will yield 263-basepair amplicon. (C) Sequencing amplicons using primers containing the M13(-20) adaptor allow for efficient sequencing of the area spanning the mutation. Animals either display the CGA codon for arginine or a combination of CGA and CAC for histidine, implying we generate either wildtype animals or heterozygous animals. Homozygosity of R132H was not observed.

Table 1: Mendelian Genetic Assessment for Mutant IDH1 Animals.

62 crosses yielding a total of 292 progeny were assessed. Crosses were of IDH1-R132H/Wildtype with IDH1-R132H/Wildtype. Expected ratios are shown in the top panel. With a χ^2 value 102.35 and a P-value of <0.0001 it is unlikely that the lack of homozygous mutant animals was due to chance and thus the hypothesis that the progeny followed a 1:2:1 Mendelian ratio was rejected. The bottom panel shows a test for the hypothesis that there is a failure to recover animals that are homozygous mutant IDH1, and thus the expected progeny would follow a 1:2 ratio. With a χ^2 value of 3.8 and a P-value of 0.0528, the null hypothesis cannot be rejected and is thus a plausible explanation.

Mendelian Genetic Assessment for Mutant IDH1 Animals				
Hypothesis (2 degrees of freedom)	Total Number of Pups	Wildtype Animals (1/4)	Heterozygous Animals (1/2)	Homozygous Mutant Animals (1/4)
Expected number of animals (E)	292	73	146	73
Observed number of animals (O)		113	179	0
$(O_i - E_i)^2 / E_i$		21.9	7.45	73
	102.35			
P-value	<0.0001 (reject hypothesis)			

Hypothesis (1 degree of freedom)	Total Number of Pups	Wildtype Animals (1/3)	Heterozygous Animals (2/3)
Expected number of animals (E)	292	97.33	194.67
Observed number of animals (O)		113	179
$(O_i - E_i)^2 / E_i$		2.5	1.3
	3.8		
P-value	0.0528 (failure to reject hypothesis)		

3.3 Insight from genetic signatures of gliomas to generate genetically faithful mouse models

As we discovered, the genetic signature of the progressive gliomas, particularly the astrocytic subset, include mutations in *IDH1*, *ATRX*, and *TP53* (**Figure 4**)(35,36). Having generated the conditional knock-in of IDH1-R132H, we next sought to incorporate those mutations that are co-mutated with *IDH1*. Independent mouse models with conditional deletion of *ATRX* and *TP53* have been generated previously and we have obtained these animals as gifts from the respective principle investigators (**Figure 6**)(94,95).

3.3.1 Incorporation of conditional deletion of *ATRX* into genetic model

ATRX was first identified as playing a causative role in ATRX syndrome, a severe, non-progressive type of X-linked mental retardation characterized by its association with an unusual form of α-thalassemia(96). Fortunately, many functional studies of this huge gene encompassing 300-kilobases and 36 exons have been reported and the activities of the functional domains have been characterized(97-99). *ATRX* contains two functional domains. At the N-terminus is the ATRX-DNMT3-DNMT3L (ADD) domain. This ADD has been shown to impart the ability to bind DNA to the protein. In the C-terminus lies the helicase/adenosine triphosphatase (ATPase) domain, which is the enzymatic core of the protein and powers the activity of the protein(98). In patients with ATRX syndrome, mutations tend to cluster in these two regions and the

same is observed in human gliomas, with mutations clustering within these domains(35,98). These mutations are usually in the form of truncating (frameshift) or nonsense mutations (**Figure 9**).

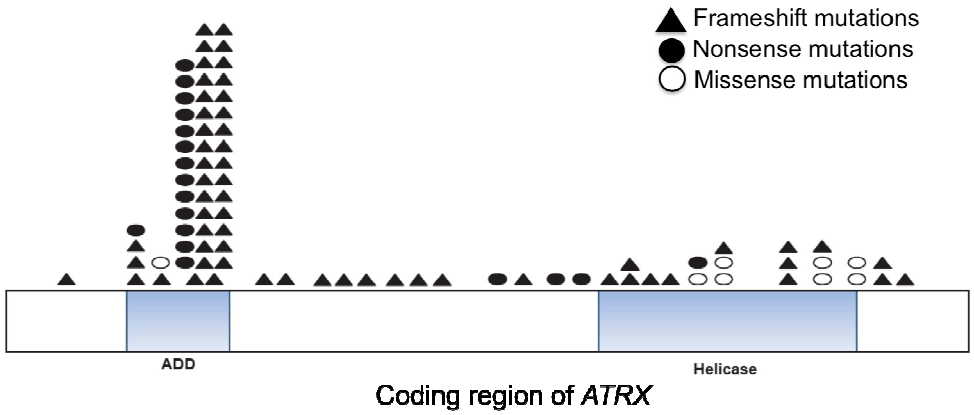

Figure 9: Distribution of ATRX mutations.

The coding sequence of *ATRX* is shown with the types mutations plotted against their location within the sequence (n=85). Shaded triangles represent frameshift mutations, and shaded circles represent nonsense mutations, suggesting the majority of ATRX mutations observed in gliomas are truncating mutations. Open circles represent missense mutations.

The conditional knock-out *ATRX* animals contained a floxed neomycin resistance cassette within intron 17 and LoxP sites flanking exon 18 of endogenous *ATRX* (**Figure 6**). Upon expression of Cre-recombinase, this yields excision of exon 18, the catalytic domain of the protein, generating the functional equivalence of a null mutation(94). These animals were crossed with our conditional knock-in IDH1-R132H animals and a

PCR-based strategy for screening progeny was used to assess the presence of the targeting construct (**Appendix D**).

3.3.2 Incorporation of conditional deletion of *TP53* into genetic model

Somatic mutations in *TP53* are among the most frequent alterations identified in human cancers and are present in almost every type of cancer(100). Normally, TP53 functions as a tumor suppressor in its regulation of the cell cycle. Though there are countless studies regarding the function of TP53 mutations in cancer, a general conclusion is that TP53 mutations are associated with changes in invasion and migration, genomic stability, angiogenesis, stem cell expansion, and apoptosis(101,102).

In generating a conditional deletion of *TP53*, LoxP sites were integrated in intron 1 and intron 10 such that upon expression of Cre-recombinase, the intervening sequence would be excised, and thus deleted (**Figure 6**)(95). PCR was performed to screen progeny and identify the compound GEMMs (**Appendix D and Materials and Methods**). In doing so, we created animals with conditional expression of mutant IDH1-R132H, as well as conditional deletion of *ATRX* and *TP53*, thereby generating the first compound genetic model harboring the most common mutations found in progressive glioma.

4. Introduction: Characterizing the effects of mutant IDH1 on the brains of GFAP-Cre; IDH1-R132H animals

The IDH1-R132H conditional knock-in model is dependent on the expression of Cre-recombinase for the stop cassette to be excised and the mutant allele to be induced. This presents many avenues to pursue as there are many strains of mouse that have Cre-recombinase expressed under control of different tissue-specific promoters. The flexibility our system provides offers a great deal of potential. With the frequency of *IDH1* mutations in several different cancers and diseases, together with the ability for tissue-specific expression utilizing the diversity of available Cre-drivers allows us to best understand mutant IDH1's role in pathogenesis in a cell-context-dependent manner. For our studies in particular, being focused on brain tumorigenesis, we were interested in expressing mutant IDH1 and its associated mutations in cells of the brain.

Initial studies involved crossing our IDH1-R132H animals to a strain of mouse that has Cre-recombinase expressed under control of the human GFAP (hGFAP) promoter. This gene encodes glial fibrillary acidic protein, an intermediate filament protein found abundantly in astrocytes. This hGFAP-Cre transgenic line consists of a 2.2-kilobase fragment derived from the 5' promoter region of the gene. This region was characterized previously and shown to be required for proper GFAP activity(103,104). hGFAP-Cre mice were shown to have Cre-recombinase expressed specifically in the brain though there was a small population of ductal cells in the liver that were

consistently positive(104). Further investigation showed that positive cells included granule cells of the cerebellum, olfactory bulb, and dentate gyrus, hippocampal pyramidal cells, gray matter of the cerebral cortex, including virtually all neuronal cells, and ependymal cells lining the ventricular system. Negative cell populations included Purkinje cells of the cerebellum, olfactory mitral cells, and spinal motoneurons, as well as choroid plexus. Expression was first visualized beginning embryonic day 13.5 (E13.5) in the dorsal and medial aspects of the telencephalon. By birth, the reporter was detected throughout the cortex and cerebellum.

When crossed to our conditional knock-in animals, the use of the hGFAP-Cre strain of mouse would promote expression of mutant IDH1 in a very broad population of cells of the CNS, initially being expressed in multipotential NSCs that give rise to most cells of the brain. This allowed us to ask what are the effects mutant IDH1 has on the CNS and what can we extrapolate from this system to learn about its function in tumorigenesis?

hGFAP-Cre animals were crossed with our conditional knock-in IDH1-R132H animals. Pups were genotyped as described in **Appendix D and Materials and Methods**. As 2-HG is the metabolic product of mutant IDH1, we sought to detect 2-HG production in the brains of our mutant animals. In collaboration with the Pharmacokinetics/Pharmacodynamics Core Facility at Duke University, and utilizing LC-MS-MS, we detected 2-HG in the brains of E15.5 animals (**Materials and Methods**).

Comparing levels of 2-HG among animals, those animals that were hGFAP-Cre; IDH1-R132H (mutant animals) displayed a level of 2-HG 200-fold higher than in those animals that were hGFAP-Cre alone (12.23μg 2-HG/mg protein versus 0.054μg 2-HG/mg protein, respectively) (**Figure 10**). This falls within range of what is observed in *IDH1* mutant tumors compared to wildtype tumors which is 54.4μg 2-HG/mg protein versus 0.1μg 2-HG/mg protein. This suggests that the system is both genetically faithful and biologically relevant as it produces 2-HG at levels comparable to those detected in human samples(63).

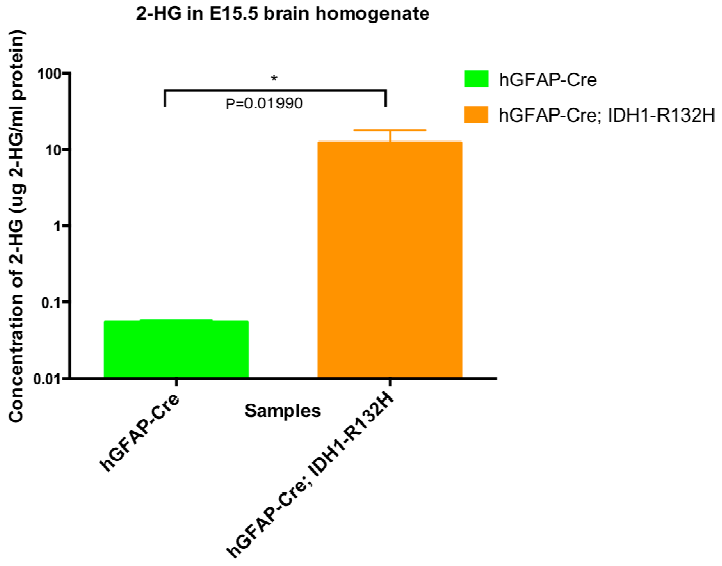

Figure 10: 2-HG in E15.5 brain homogenate.

Brains were harvested from wildtype (hGFAP-Cre) and mutant (hGFAP-Cre; IDH1-R132H) E15.5 animals. 2-HG was detected at a level 200-fold higher in mutant brains compared to wildtype (unpaired, 2-tailed t-test: P-value=0.01990). 2-HG was detected via LC-MS-MS.

4.1 Broad expression of mutant IDH1 through the CNS induces hydrocephalus

Initial experiments sought to determine the effects of mutant IDH1 on cells of the CNS. To this end, we crossed our animals to the hGFAP-Cre strain of mouse that would induce expression in a tissue-specific manner, specifically in multipotential NSCs beginning at E13.5. This leads to very broad expression throughout the cortex and cerebellum. Animals that were generated included hGFAP-Cre animals as controls and hGFAP-Cre; IDH1-R132H animals as the experimental cohort. Animals were monitored daily for any signs of neurological impairment that could be a result of tumor burden. Daily checks included observing animals for head doming, head tilts, ataxia, loss of grip capability, weight loss, dehydration, and any signs of pain including hunched posture or squinted eyes. At the earliest signs of impairment or at 1-year of age, animals would be sacrificed and their tissues harvested for analysis (**Materials and Methods**).

Physical differences among hGFAP-Cre animals and hGFAP-Cre; IDH1-R132H animals became apparent shortly after weaning age (after P21). Physical differences included gradual enlargement of the head or head doming, squinted eyes, hunched posture, and gradual immobilization (**Figure 11A,B**). This phenotype was present in 80% of those animals that had mutant IDH1 expressed under control of hGFAP. Control animals were non-phenotypic.

Median survival for those 80% of animals was approximately 25.5 days, with some living as long as 50 days, at which point they had to be sacrificed (**Figure 12**).

Animals were sacrificed via lethal dose of urethane followed by intracardiac perfusion with PBS and 10% Neutral Buffered Formalin (**Materials and Methods X**). Upon harvesting the brain, discoloration of tissue underlying the skull was observed. Dissection further showed large fluid filled cavities within an abnormal brain (**Figure 11C,D**). Formalin-fixed paraffin embedded blocks of tissue were sectioned and hematoxylin and eosin (H&E) stained (**Materials and Methods**). Histological analysis showed that the large fluid filled cavities observed grossly were representative of a severe enlargement of the lateral ventricles (**Figure 11E,F**). These features are characteristic of hydrocephalus and its induction is likely due to the broad expression of mutant IDH1 in the brain.

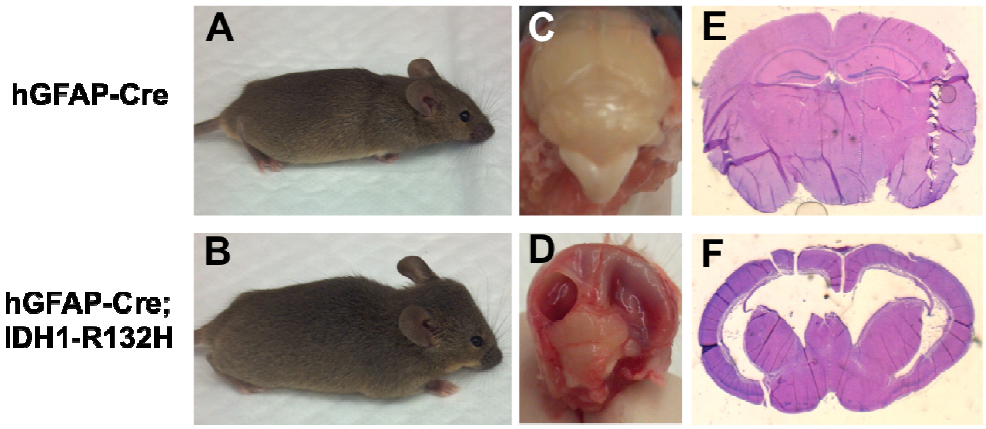

Figure 11: Broad expression of mutant IDH1 induces hydrocephalus.

By weaning age, animals expressing mutant IDH1 presented with head-doming, hunched posture, and squinted eyes (A and B). Upon dissection, mutant brains displayed large fluid-filled cavities (C and D). Histological analysis shows that these cavities were representative of a severe enlargement of the lateral ventricles indicating development of hydrocephalus (E and F). Representative images shown above obtained from P38 animals.

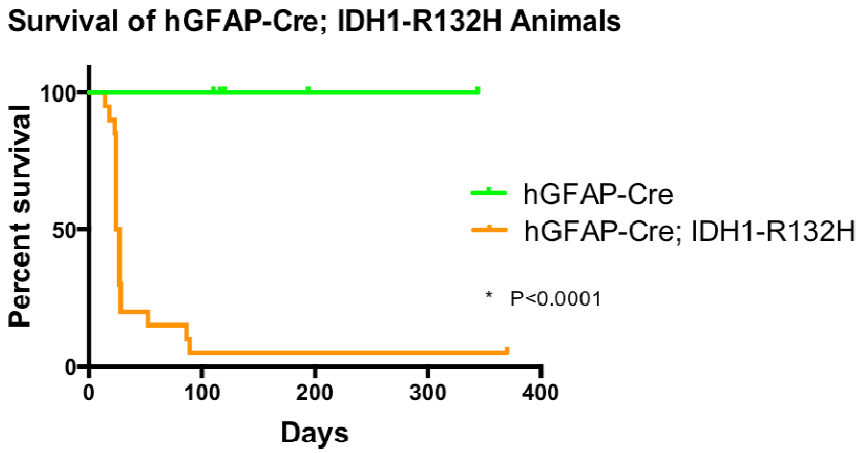

Figure 12: Survival of hGFAP-Cre; IDH1-R132H animals.

Kaplan-Meier survival curve of animals expressing mutant IDH1 broadly throughout the brain. Mutants display a significantly reduced survival (median survival 25.5 days compared to a normal-length survival for hGFAP-Cre wildtype counterparts). Log-rank (Mantel-Cox) test shows significance with P<0.0001.

According to the National Hydrocephalus Foundation, it is estimated that approximately 1 in 500 births results in hydrocephalus with another 6,000 more children developing it within the first 2 years of life. Hydrocephalus is a condition in which excessive accumulation of cerebrospinal fluid (CSF) in the brain results in a widening of the ventricular spaces. This widening creates a build up of pressure leading to harmful effects on the brain that, without treatment, will cause brain injury or even death. The accumulation of CSF can result from an overproduction of CSF by the choroid plexus or it could be due to a failure to drain CSF at the subarachnoid space(105,106). Additionally, because there is an orchestrated flow of CSF throughout the brain, a blockage of flow through the narrow Sylvian aqueduct that lies between the third and

fourth ventricles could also cause hydrocephalus and is in fact one of the primary causes of it(106). To this end, to determine whether development of hydrocephalus in mutant animals was due to an obstruction or blockage to any of these areas, coronal sections throughout the brain were made for histological analysis. Though unable to identify the etiology of hydrocephalus in these animals, we did observe some instances of aqueductal stenosis and an overall loss of cellularity in mutant brains, which may be due to elevated levels of 2-HG. We are currently working alongside a neurosurgeon at Duke University to better understand the basis for the development of hydrocephalus in these animals.

4.2 Effects of mutant IDH1 on neural development

Broad expression of mutant IDH1 throughout the brain led to a severe phenotype of hydrocephalus and deleterious effects to the brain. The early onset of this dramatic phenotype required sacrificing the animals by P40, hindering the investigation of the prolonged effects of 2-HG on the brain and making it an unlikely model for studying 2-HG's role in tumor induction. Subsequent studies analyzed brains at an earlier timepoint, prior to the deleterious effects on the brain attributed to hydrocephalus. Here, we asked what are the earliest effects mutant IDH1 is having on the brain, specifically on the neural stem cell population, a suspected cell of origin for glioma?

4.2.1 Mutant IDH1 induces foci of hemorrhagic lesions throughout cortex of developing brain

The destruction attributed to hydrocephalus on hGFAP-Cre; IDH1-R132H brains impeded downstream analysis. To assess the earliest effects of mutant IDH1 on the mouse brain and to do so on an intact brain without destructed tissue, we harvested samples from P3 animals. Harvested tissues derived from hGFAP-Cre; IDH1-R132H animals were visibly different from their hGFAP-Cre control counterparts. Dispersed throughout the cortex of the mutant animals were foci of hemorrhagic lesions (**Figure 13A and B**). These lesions were found in approximately 80% of those animals of the genotype hGFAP-Cre; IDH1-R132H. No foci were observed in the hGFAP-Cre control animals. H&E staining showed red blood cell extravasation in the mutant brains, however in the control brains, red blood cells were observed contained within vessels or capillaries (**Figure 13C and D**). Due to this phenotype, we next sought to determine what the effects were on the endothelial cells and whether there was any defect that could be causing the extravasation. IHC using the CD31 antibody was performed to detect the endothelial cells and observe any perturbations to their histology (**Figure 13E and F**). We observed vessels to be thicker and stained more intensely with CD31 in mutant brains, suggesting that these tissues may be undergoing active angiogenesis(107).

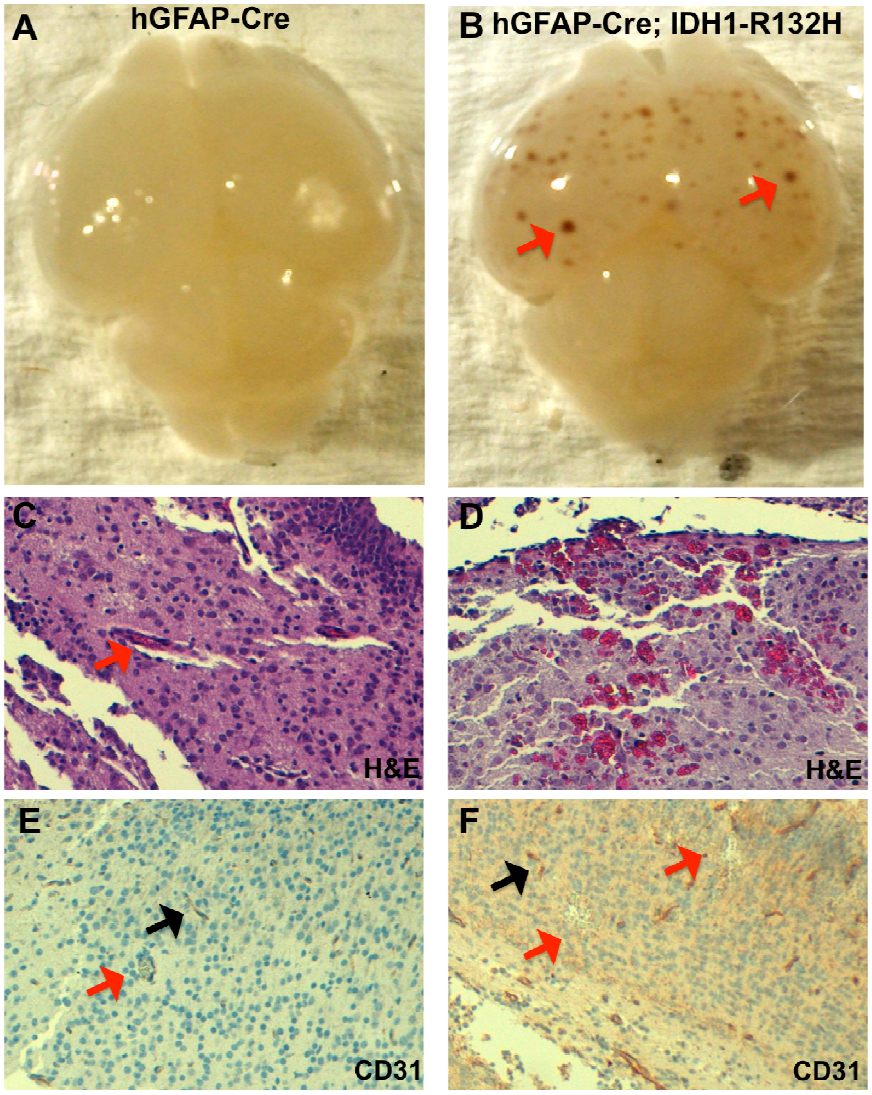

Figure 13: Mutant IDH1 induces hemorrhagic lesions.

Broad expression of mutant IDH1 throughout the brain induces foci of hemorrhagic lesions as can be seen in mutant brains compared to wildtype brains (A and B (red arrows)). H&E staining shows red blood cells within endothelial cells (red arrow) in wildtype brains (C), however, in mutant brains (D), there is mass red blood cell extravasation indicative of leaky vasculature. Tissues were stained with CD31, a marker for vasculature. In wildtype tissue (E) vasculature (black arrow) appears normal with red blood cells within the vessels (red arrow). Mutant tissue (F) shows red blood cell extravasation (red arrows) and the vessels are staining deeper, though seem mostly normal. Data collected from P3 animals.

Since generating our genetic mouse model, another mutant IDH1 mouse model has been described in the literature. Sasaki et al., generated a mouse that expressed mutant IDH1 under control of Nestin-Cre. In this case, Cre-recombinase is expressed as early as E10.5 and by E12.5, nearly all cells of the CNS express it. These animals displayed perinatal lethality coupled with massive hemorrhage throughout the cerebral hemispheres and cerebellum as well as increased numbers of apoptotic cells(108). This phenotype was observed as early as E15.5. This group also utilized a GFAP-Cre strain of mouse, one that was generated independently using a different promoter region than the one our studies relied on. Here, they observed the presence of hemorrhage, though this phenotype was variable among littermates. As mentioned previously (Section 2.3.2.3), the data describing mutant IDH1's effects on HIF1α signaling is contradictory, with one group describing 2-HG blocking prolyl hydroxylation, allowing for HIF1α stabilization, whereas another group shows 2-HG activates prolyl hydroxylases, promoting the degradation of HIF1α(58,69). Sasaki et al., attempted to resolve this issue and assess the *in vivo* effects of mutant IDH1 on HIF1α signaling and found it was stabilized, corroborating the study of Xu et al. This is a cogent argument considering HIF1α's involvement in neo-angiogenesis and induction of downstream targets including VEGF. Interestingly for our studies, this may also explain the vascular leakiness observed in hGFAP-Cre; IDH1-R132H brains as increases in HIF1α and

subsequently, VEGF have been shown to induce gaps between adjacent endothelial cells lining microvessels promoting vascular leakiness(109).

4.2.2 Mutant IDH1 perturbs the neural stem cell niche of developing animals

hGFAP-Cre; IDH1-R132H animals became symptomatic by weaning age and had to be sacrificed by P40 (**Figure 12**). Though this early termination prohibits the analysis of prolonged exposure of 2-HG on the brain, it does permit the study of the earliest effects of 2-HG on the brain, specifically on the NSC population of the developing organism. By analyzing P3 brains, we assessed the effects mutant IDH1 is having on the NSC population of the brain and determined whether there are any defects to differentiation. To date, the majority of studies dealing with mutant IDH1 and mutant IDH2 have been in the context of the hematopoietic system, adipocytes, or hepatocytes and all have shown that mutant IDH1 or mutant IDH2 confers a block to the normal differentiation patterns, leading to an accumulation of progenitor cells(56,70,78,79). Despite *IDH1* being mutated at such a high frequency in CNS tumors, it is surprising that there is a deficit of data surrounding mutant IDH1's effects on cells of the CNS in an *in vivo* context. We characterized mutant IDH1's effects on cells of the SVZ, the niche which houses the NSCs that give rise to the cells of the brain. Being the SVZ is a germinal zone, we first assessed levels of proliferative cells in this region as those stained positively for the proliferative marker, Ki67 (**Figure 14**). As expected, in hGFAP-Cre animals, there was robust proliferation in the SVZ of the lateral ventricle. The SVZ

in the same plane in hGFAP-Cre; IDH1-R132H animals displayed a reduction in the positively stained Ki67 cells, suggesting the proliferative capacity of these cells in blunted in mutant brains (**Figure 15A**).

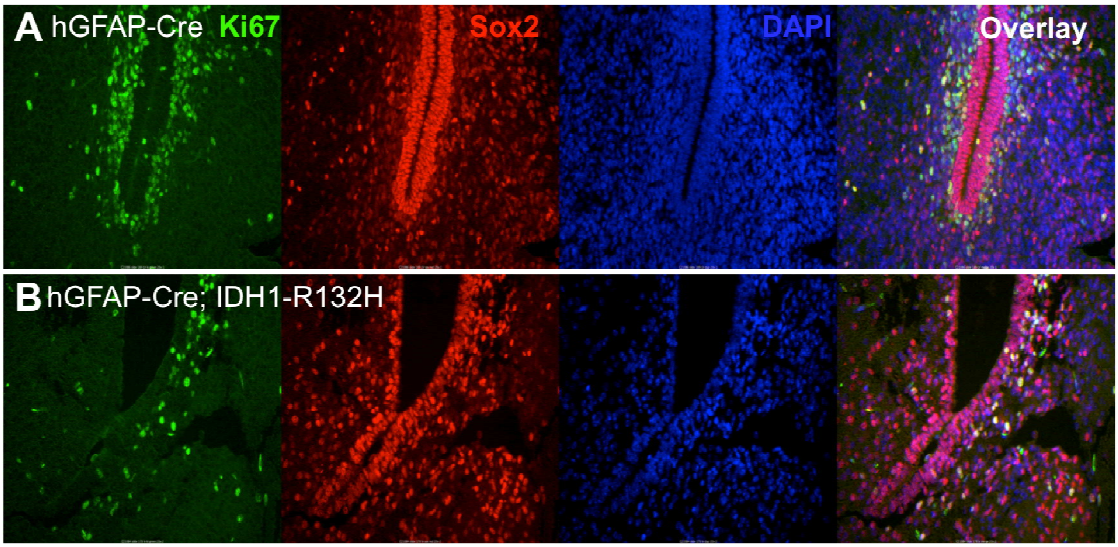

Figure 14: Mutant IDH1 confers reduced proliferative potential of the SVZ as well as perturbed NSC niche.

P3 brains from wildtype (A) and mutant (B) animals were stained with a marker for proliferation (Ki67) shown in green. Mutant animals displayed a reduced proliferative potential of the SVZ. Additionally, the NSC niche and the NSC population of the SVZ appeared perturbed in mutant brains as shown through staining with the NSC marker (Sox2), shown in red.

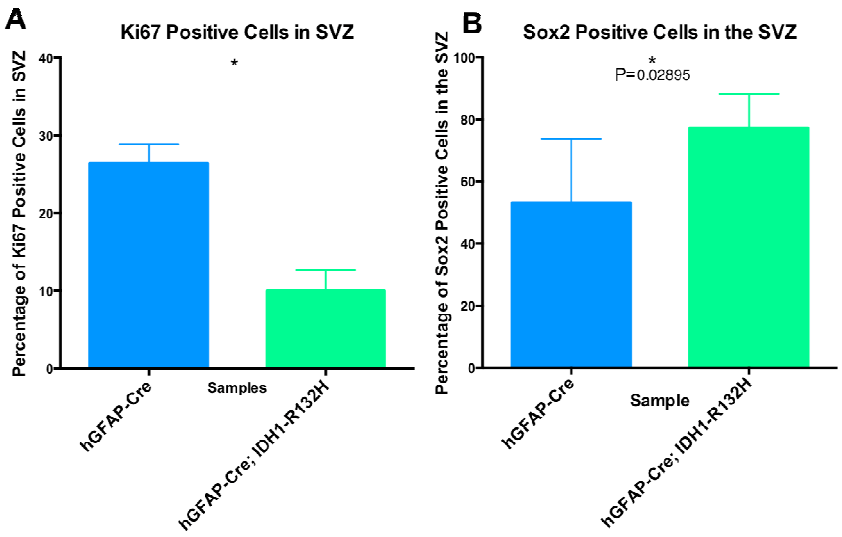

Figure 15: Effects of mutant IDH1 on the SVZ.

Quantification of Ki67 positive cells of the SVZ showed the presence of proliferative cells in the SVZ as expected in both hGFAP-Cre and hGFAP-Cre; IDH1-R132H cohorts, however in mutant brains, proliferative capacity was significantly blunted (A). Interestingly, the NSC population, as represented through Sox2 staining, shows an increase in the percentage of Sox2 positive cells in the SVZ in hGFAP-Cre; IDH1-R132H animals (B). Two hGFAP-Cre and two hGFAP-Cre; IDH1-R132H samples were used for this quantification. Two planes per sample were analyzed, all in the region of the apex of the lateral ventricle.

As explained, the NSC niche consists of the SVZ of the lateral ventricle of the brain. A variety of cell types are encompassed in this specialized niche and their proper regionalization and interaction with one another are imperative for their proper function and differentiation patterns. The SVZ niche is composed of B1-cells, considered to be the NSCs and are surrounded by multi-ciliated ependymal cells. The B1-cells give rise to C-cells, also known as transit amplifying cells that divide and generate neuroblasts, or A-cells. Those cells born in this region migrate through an extensive network to reach

the rostral migratory stream where they will further migrate to populate the olfactory bulb. Here, the cells will complete their differentiation into interneurons(110). B1-cells, those considered to be the NSCs, make contact with the lateral ventricle with a thin apical process, while also making contact with blood vessels with a long basal process. For this reason, they are divided into three different domains, with each domain interacting with critical components for signaling. For example, one domain (Domain I) of the B1-cell is in direct contact with the CSF, and thus receives soluble factors, while another domain, (Domain II) is in close contact with C-cells, permitting direct interaction with progeny. Finally, Domain III comprises a basal process making contact with blood vessels allowing for reception of paracrine and endocrine signals(111). The human brain is similarly structured as the described rodent brain, though it displays a more layered structure with Layer I consisting of an ependymal monolayer that has astrocytic processes intervening. Layer II is a gap region that is hypocellular and contains basal processes of the ependymal cells. This may function as a corridor for migrating cells. Layer III is composed of a dense ribbon of cell bodies and underlying this is the striatal brain parenchyma, Layer IV. Proliferative cells were mostly found within layers II and III(112).

As one of the suspected cells of origin for glioma are the NSCs, we sought to assess the effects mutant IDH1 was having on this population of cells. We stained with the NSC marker, Sox2, and characterized the effects on the SVZ. We observed that in

the hGFAP-Cre animals, the SVZ was very organized with a particular architectural layering consistent among wildtype animals (**Figure 14**). The Sox2 population of cells lined this area and those cells that were staining positively for this NSC marker were restricted to this region. hGFAP-Cre; IDH1-R132H animals displayed a perturbed NSC niche with Sox2 positive cells dispersed throughout the SVZ region as opposed to strictly within the region surrounding the ventricular walls. Cells were not structured in the same fashion as in control animals as is indicated through the elevated ratio of Sox2 positive cells emanating outward from the SVZ in mutant brains compared to wildtype brains (**Figure 16**). This disorganization to the niche was consistent among those animals expressing mutant IDH1 in their brain and was not observed in control animals. Interestingly, when the number of NSCs of the SVZ were calculated and normalized to the overall number of cells in the region, there was a statistically significant increase in the number of Sox2 positively stained cells in mutant brains, suggesting that mutant IDH1 may be leading to an accumulation of NSCs in the SVZ and these cells may have an enhanced migratory ability. Interestingly, a subsequent increase in proliferation has not been observed (**Figure 15**). Though the observation of mutant IDH1 yielding an accumulation of progenitor cells has been observed before in other systems including the hematopoietic system, adipocyte lineage, and hepatocyte lineage, this is the first known example describing a similar effect of mutant IDH1 on cells of the CNS in an *in vivo* context. It can be inferred that with the myriad of signaling pathways present

within the NSC niche, including SHH, Wnt, Notch, BMPs, and ephrin signaling, and many of those pathways relying on a structured cellular context, it is presumed that the perturbed architecture of this region will in fact disrupt proper neural differentiation patterns and migration of cells resulting from the NSC population.

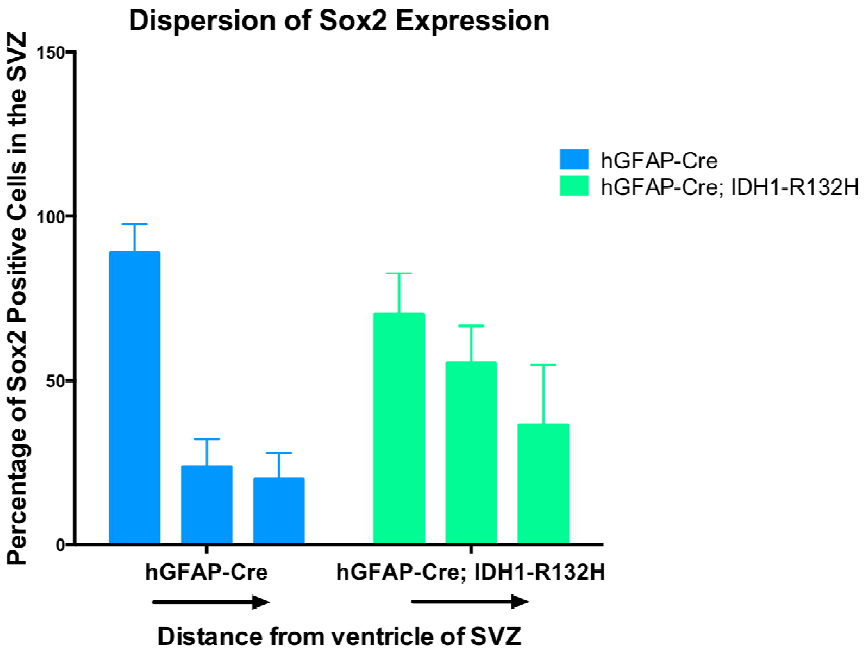

Figure 16: Mutant brains display a dispersed Sox2 population of cells.

Brains of hGFAP-Cre and hGFAP-Cre; IDH1-R132H were stained with Sox2, a marker for NSCs. Two separate planes among 2 wildtype and 2 mutant brains were analyzed. For each, a 200 X 200 pixel region placed with its left side along the ventricular wall. This is the left-most blue and green column shown above. Total nuclei and Sox2 positive cells were counted. The area immediately adjacent to this first region was then counted, followed by the region immediately adjacent to this one for a total of three regions to properly show the proportion of Sox2 positive cells throughout this region of the brain.

4.3 Discussion

We sought to determine the effects of mutant IDH1 on the mouse brain and we initiated our studies by expressing mutant IDH1 very broadly throughout the brain through the use of the hGFAP-Cre model. With this system, we were able to detect 2-HG at a level 200-fold higher than in control animals, suggesting the system was working and it was producing 2-HG at a level comparable to what is observed in human glioma samples with IDH1 mutations. 80% of these animals became symptomatic very early in development leading to a median survival of approximately 25.5 days. Upon harvesting the tissues, we determined that broad expression of mutant IDH1 in the brain induces hydrocephalus, a dramatic phenotype that made investigation of the long-term effects of 2-HG on the brain impossible. However, it is interesting to note that it has been described in a case study that those patients with 2-hydroxyglutaric aciduria do present with mild ventriculomegaly. Many believe that ventriculomegaly is early on the spectrum for development of hydrocephalus and this may be the first animal model that shows a link between 2-HG production and enlargement of the lateral ventricles. Though unlikely, it would also be interesting to know whether 2-HG can be detected in patients that do develop hydrocephalus for reasons other than 2-hydroxyglutaric aciduria.

As mentioned, though our system did not permit the study of the long-term effects of 2-HG on cells of the brain, it does permit the study of the earliest effects of

mutant IDH1 on a cell type considered to be the cell of origin for glioma, the NSCs. Observation of younger animals showed areas of hemorrhagic foci and leaky vasculature within the brain that may be due to increased levels of HIF1α as a result of elevated levels of 2-HG.

As mentioned, 20% of hGFAP-Cre; IDH1-R132H animals were asymptomatic and survived to the 1-year experimental endpoint. With no signs of any neurological impairment or hydrocephalus, it is possible that this is due to variable Cre-expression. This phenomenon has recently been characterized in a variety of Cre-driver strains and has been shown that even among littermates, there could be significant differences in the reporter readout(113). As more samples become available, it would be interesting to analyze the precise level of 2-HG being produced and determine whether there are any subtle lesions that may not have been grossly apparent. If 2-HG is being produced at detectable levels, it would be very interesting to learn what prolonged exposure would induce in these animals and whether there are any neoplastic or preneoplastic lesions present within the brain. Additionally, it would be interesting to learn whether mutant IDH1 alone or in cooperation with other mutations, such as deletions in *TP53*, would be capable of inducing tumorigenesis. Perhaps a lower level of 2-HG production over prolonged periods of time is required to promote tumorigenesis; a level that is surmounted in the 80% of symptomatic animals.

Taking into account the scope of phenotypic variation among different models, it appears that the timing of the induction of mutant IDH1 is imperative. The published Nestin-Cre system has mutant IDH1 being induced at E10.5. In our GFAP-Cre system, Cre-recombinase is induced at E12.5. In both cases, signs of hemorrhage were apparent, however in the former case, animals displayed perinatal lethality. In the latter case, animals were able to survive to post-weaning age, however they succumbed to the devastating deleterious effects of hydrocephalus. This suggests that by restricting expression to a more specific cell type, and induction of recombination at different times may circumvent issues of lethality. To this end, achieving spatio-temporal control over mutant IDH1 expression, as will be described in the following chapter utilizing our Nestin-CreER^{T2} system, may permit a model with prolonged exposure to 2-HG and thus generate a more amenable system to tumor modeling.

Despite the high frequency of *IDH1* mutations in CNS tumors, there has been a lack of data describing mutant IDH1's effects on cells of the CNS, particularly in an *in vivo* context. Most studies have relied on immortalized astrocytes or established glioma cell lines such as U87(58,59). However, our studies are among the first to characterize the effects of mutant IDH1 on the mouse brain in a genetic system. Our findings included a reduction in the proliferative cells present in the SVZ of the lateral ventricles of mutant brains. Though the reduction in proliferative cells was surprising, it is consistent with some published data suggesting that mutant IDH1 decreases rates of

proliferation(59). Together, these data offer one reason why primary cell lines that contain IDH1 mutations are so difficult to establish in culture and xenografts(61). In this same region, an increase in the Sox2 positive population was observed and these cells tended to migrate outwards from the SVZ to an extent that was not observed in wildtype brains. We can infer that considering this specialized microenvironment is critical for the regulation of proliferation and progenitor cell differentiation, it is likely that the observed disorganization perturbs the normal differentiation patterns of the resident NSCs. The signaling pathways of this region have been well characterized and include SHH, Wnt, Notch, BMPs, and ephrin signaling, therefore any disruption to the highly ordered structure that is normal for this area is likely to skew proper signaling and cues for differentiation which may have implications in tumor initiation and development(10).

5. Introduction: Achieving spatio-temporal control over expression of mutant IDH1 in the mouse brain

The previous model generated had mutant IDH1 expressed very broadly throughout the cortex and cerebellum of the brain. Though the precise etiology of the hydrocephalus that developed in these animals is as of yet, unknown, there is the possibility mutant IDH1 was expressed in critical cells too early in development leading to a developmental defect and masking any further effects that may be more relevant to tumorigenesis. In addition to the fact that mutant IDH1 induces hydrocephalus when broadly expressed throughout the brain, we also learned that early induction of mutant IDH1 can perturb the developing brain in several other ways including: 1-mutant IDH1 imparts a negative effect on the proliferative potential on cells of the SVZ; 2-mutant IDH1 promotes an accumulation of Sox2 positive NSCs in the SVZ region that tend to migrate outwards from their normal location surrounding the ventricular wall; 3-mutant IDH1 causes a structural disorganization to the SVZ; and 4-mutant IDH1 perturbs the architecture of the NSC niche, likely altering the many signaling pathways within it and subsequently effecting the normal neural differentiation patterns that are crucial to developing an intact brain. These effects of mutant IDH1 are encouraging as it suggests that by restricting expression to a more specific cell type and at a more appropriate time, that we would circumvent the lethality attributed to hydrocephalus. This would allow for the affected cells to persist longer, permitting a more thorough understanding of the

effects mutant IDH1 and 2-HG are having on these cells over a prolonged period of time. In order to restrict expression of mutant IDH1 to a more specific cell type, we crossed our mutant IDH1 conditional knock-in animals to a Nestin-CreER^{T2} strain of mouse. In contrast to the hGFAP-Cre strain of mouse used in our previous experiments, the Nestin-CreER^{T2} strain of mouse has Cre-recombinase inducibly activated under control of a tissue-specific promoter. This ligand-dependent Cre-recombinase is activated through administration of tamoxifen to the animal, at which point the Cre-recombinase is translocated to the nucleus where it imparts its excision capabilities. In the hGFAP-Cre system, Cre-recombinase was expressed beginning at E12.5 and continues to be expressed whenever and wherever GFAP is active. Though Nestin begins to be expressed at E9.5, the Cre-recombinase will only become activated once tamoxifen is administered and only in those cells expressing Nestin, thereby conferring spatio-temporal control over induction of mutant IDH1. By restricting the expression of mutant IDH1 to later stages where fewer cells would be targeted, allows us to circumvent the hydrocephalic phenotype and assess the effects of mutant IDH1 and 2-HG on the brain over prolonged periods of time. In fact, one of the many advantages of using the CreER^{T2} system is for this very reason, to bypass the untimely lethality or other undesirable effects that impede the study of the true function of a genetic alteration.

The Nestin-CreER^{T2} mouse was generated using a 1.8 kilobase fragment of rat genomic DNA containing the second intron of Nestin(114). Nestin is an intermediate

filament protein that is expressed in both neuroepithelial stem cells as well as muscle precursor cells. Prior studies have characterized enhancer regions of this gene that delineates its expression patterns; it was shown that the second intron is responsible for restricting Nestin expression to the CNS and thus the reason this region was used in the making of this transgenic animal(115). The characterization of this promoter region shows Nestin being expressed beginning at E9.5 and expressed in the ventricular and nonventricular proliferative zones of the mammalian CNS. However, it was not expressed in postmitotic neurons and glia, nor in the myotome, suggesting this enhancer region confers specificity to the NSC population. By inducing mutant IDH1 expression at specific times throughout embryonic or adult life, we would circumvent the hydrocephalic phenotype and acquire the ability to assess mutant IDH1's effects on the brain, specifically on the NSC population of the brain, a leading candidate as the cell of origin for gliomas.

5.1 Induction of mutant IDH1 in a restricted cell population in the CNS

One of the huge advantages of generating genetic mouse models is the ability to control the system. Through the variety of Cre-drivers that are available, one can achieve tissue-specific expression or knock-out of your gene of interest. Additionally, utilizing $CreER^{T2}$ drivers, you can control the timing of that tissue-specific expression or knock-out through administration of tamoxifen. Though this level of control is a huge asset and makes for a scientifically precise model, it also requires a great deal of thought

as there are often no single answers to the many questions that arise. For example, one must decide which Cre or CreER^{T2} driver to utilize. Though this is in theory straight forward, knowing the precise cell types in which Cre-recombinase is being expressed is not a trivial undertaking and is dependent on how well that tissue is characterized as well as on the markers that are available for the tissue. The extent of cellular heterogeneity within that tissue is also important as it may not be the case that every cell type within that tissue will express Cre-recombinase. To know which ones specifically are expressing will help draw conclusions when phenotypes present themselves. The CreER^{T2} system presents another set of questions including when is the proper time to treat with tamoxifen and activate Cre-recombinase. This requires accurate knowledge of the driver being used considering Cre-recombinase will not be activated unless the promoter is active. A knowledge of the gene activity itself is not always enough for this as many times the promoters are composed of different enhancer regions and may display differential expression from what the expected gene expression pattern is. Lastly, the tamoxifen treatments required to achieve an extent of recombination desired must be assessed. A single dose of tamoxifen may or may not be sufficient for particular studies. In summation, genetic models and inducible activation or knock-out of genes presents a tremendous amount of wealth and value to the studies, however they require a tremendous amount of responsible and well-informed decisions to achieve that wealth and value.

Our studies sought to induce mutant IDH1 in the SVZ of the lateral ventricle of the mouse, with the goal of targeting the NSC population. To initiate the studies, we crossed in a conditional reporter mouse that had a 1.6-kilobase fragment encoding the tdTomato protein that lied downstream of a floxed stop cassette (referred to as LSLtdTomato)(116). Upon expression of Cre-recombinase, the stop cassette would be excised inducing expression of tdTomato, a Red Fluorescent Protein (RFP) variant.

As our goal was to express mutant IDH1 in the NSC population, we additionally crossed in the Nestin-CreER^{T2} strain, described above, that has Cre-recombinase inducibly activated in the SVZ of embryonic and adult animals. Experimentally, our plan once animals were generated was to have two groups, each one treated with tamoxifen at a different time and thus inducing recombination in a restricted fashion (**Figure 17**). As our goal was to generate a faithful model of mutant IDH1-mediated gliomagenesis, and knowing that these tumors present in humans in early adulthood, we chose to treat our animals with tamoxifen at P28, a timepoint that represents early adulthood in mouse. However, in the characterization of this strain of mouse, we knew that Nestin expression significantly decreases postnatally, and that by treating at this timepoint we may not be inducing recombination in enough NSCs to promote a tumorigenic phenotype. To this end, another group of animals were treated at E18.5 via oral gavage to the pregnant dams, a timepoint that would be targeting more cells than at

P28, but not as many cells as were induced in the hGFAP-Cre system described previously (**Figure 17**).

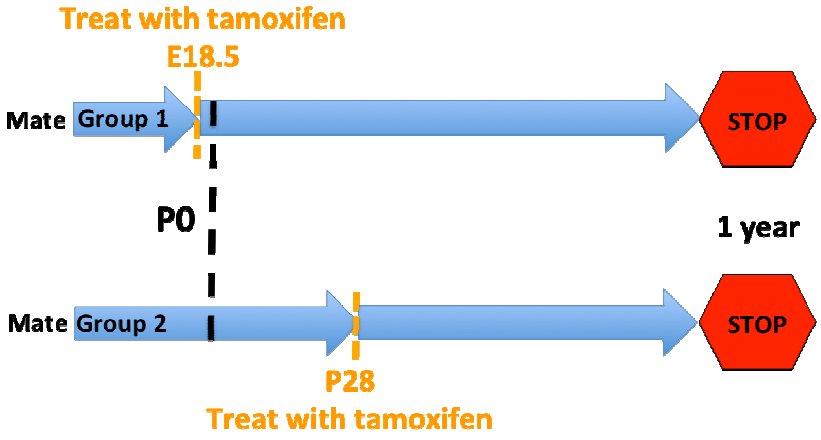

Figure 17: Experimental plan for Nestin-CreER^{T2} animals.

Mutant animals were crossed with Nestin-CreER^{T2}. Two groups were treated, one at E18.5 and another group at P28. Matings were timed based on the presence of a vaginal plug which designated E0.5dpc. At either 18.5dpc for the E18.5 timepoint or at P28, pregnant dams or experimental animals were treated with tamoxifen, respectively. At 1-year or at the earliest sign of neurological impairment, animals were sacrificed and tissues harvested for analysis.

As validation that our system was working as expected, pregnant females yielding progeny of the genotype Nestin-CreER^{T2};LSLtdTomato were treated with tamoxifen (150µl of 20mg/ml tamoxifen made up in sterile corn oil) and treated at 18.5dpc to test Cre-recombinase induction and recombination efficiency for the E18.5 timepoint (**Materials and Methods**). Pups were sacrificed at P3 to assess recombination throughout the brain. Tissues were processed as explained in **Materials and Methods** and stained with an antibody specific for RFP. As expected, those animals treated with

tamoxifen displayed robust expression of RFP in the SVZ of the lateral ventricle (**Figure 18**). It should be noted that untreated animals displayed minor random recombination events throughout the brain however, these were sporadic events and highly unlikely to impact experimental results (**Figure 18**). This could be due to leaky Cre-recombinase, a phenomenon that has been documented and is common among many characterized transgenics(117,118).

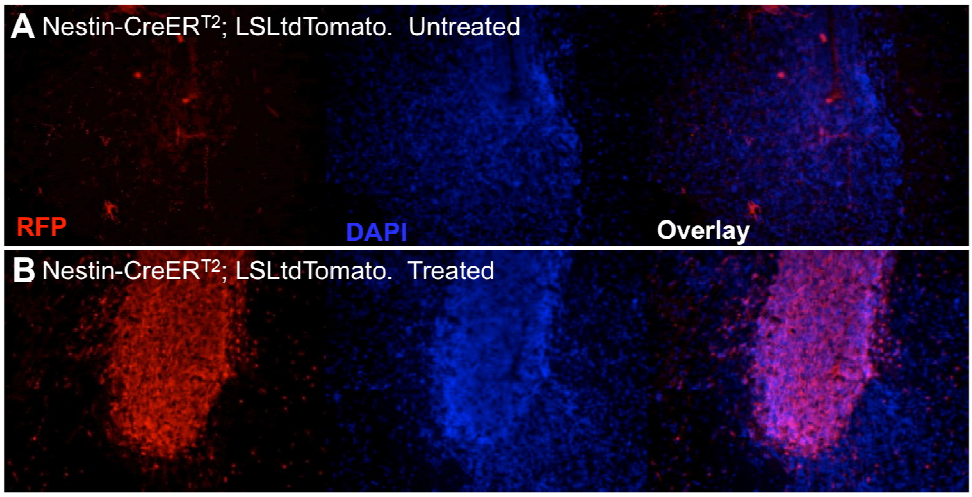

Figure 18: Treatment with tamoxifen at E18.5 induces recombination in the SVZ.

Timed matings generating Nestin-CreER^{T2}; LSLtdTomato progeny were established. At 18.5dpc, pregnant dams were either treated with tamoxifen via oral gavage or not treated. At P3, pups were sacrificed and tissues stained for RFP. (A) Untreated animals show minimal recombination and RFP induction in the SVZ suggesting a minimal level of leaky Cre-recombinase. (B) Treated animals show robust expression of RFP in the SVZ as expected, suggesting treatment with tamoxifen at E18.5 induces recombination in our cell of interest at an appropriate level.

5.2 Mutant IDH1 and TP53 deletion promote brain tumorigenesis in genetic mouse model

To achieve expression of mutant IDH1 in a cell type suspected of being the cell of origin for gliomas, while circumventing the hydrocephalic and thus, lethal phenotype that was observed when it was broadly expressed, we crossed our mutant IDH1 conditional knock-in animals to Nestin-CreER^{T2}. To fully recapitulate the mutation spectrum observed in human glioma we also incorporated conditional deletion of those other most commonly mutated genes including *ATRX* and *TP53*, as described previously. As explained, we would have two cohorts of animals with one group being treated at E18.5, and the other group being treated at P28. After several months, it became apparent that the P28 treated animals were asymptomatic under the specified conditions, that being a single dose of tamoxifen at P28. Therefore, the remainder of the studies focused on the E18.5 treated animals.

Following administration of tamoxifen to pregnant dams, animals were monitored daily for any signs of neurological impairment that could be a result of tumor burden. Daily checks included observing animals for head doming, head tilts, ataxia, loss of grip capability, weight loss, dehydration, and any signs of pain including hunched posture or squinted eyes. At the earliest signs of impairment or at 1-year of age, animals would be sacrificed and their tissues harvested for analysis (**Materials and Methods**).

These experiments were established to assess whether mutant IDH1 can induce brain tumorigenesis alone or in combination with other genetic aberrations. Once tumors formed, they would be characterized and compared to determine the role mutant IDH1 plays in tumorigenesis. Additionally, the mutations contribution to overall survival as a result of tumor aggressiveness would be assessed. The genotypes that were generated for this study include mutant IDH1 alone, *TP53* deleted alone, and mutant IDH1 with *TP53* deleted. Additionally, a cohort of animals that contained deletion of *ATRX* was incorporated.

At the culmination of this experiment, several findings were made. For one, when *IDH1* is mutated on its own, survival was indistinguishable from animals with no mutations (**Figure 19**). This corroborates previous studies and implies that mutant IDH1 requires additional mutations in order to promote a tumorigenic phenotype. To this end, tumors did form in those animals harboring mutant IDH1 and *TP53* deletion. Additionally, tumors also developed in mice with *TP53* deleted alone. It should be noted that in both cohorts, tumors were only observed when both alleles of *TP53* were deleted. Having generated essentially two groups of tumors, those tumors with mutant IDH1 and deleted *TP53*, and those with only *TP53* deleted alone, we next sought to assess the differences between these genotypically different tumors.

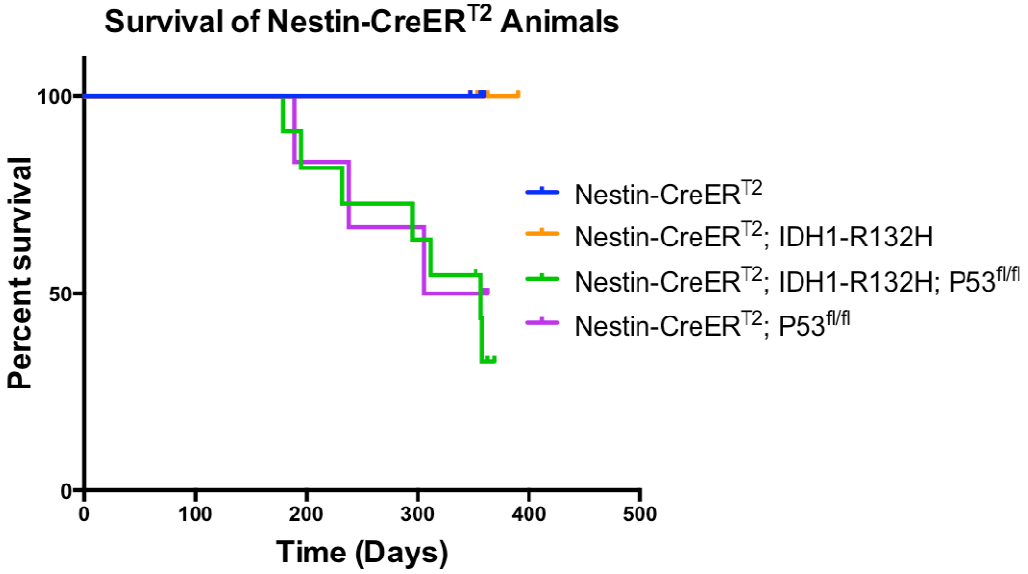

Figure 19: Survival of Nestin-CreER^{T2} animals.

Kaplan-Meier Survival Curve for animals treated at E18.5 to inducibly activate mutant IDH1, deletion *TP53*, or both. Animals were aged for 1-year. At the earliest sign of impairment or at 1-year, animals were sacrificed. Animals with mutant IDH1 activated alone exhibited no differences in survival compared to normal mice; suggesting cooperating mutations are required for tumorigenesis. When *TP53* is homozygously deleted, animals became symptomatic often displaying signs of brain tumor including head-doming and ataxia. Nestin-CreER^{T2}; IDH1-R132H; TP53$^{fl/fl}$ displayed a median survival of 357 days whereas Nestin-CreER^{T2}; TP53$^{fl/fl}$ animals displayed a median survival of 334.5 days.

To begin looking for distinguishing features between mutant IDH1; *TP53* deleted tumors, and *TP53* deleted tumors, we first sought to ensure that those tumors arising in animals containing the mutant IDH1 allele were in fact expressing the mutant IDH1 protein. To this end, we performed IHC using an antibody specific for mutant IDH1-R132H which was tested on a Nestin-CreER^{T2} brain as well as a hGFAP-Cre; IDH1-R132H brain for negative and positive control, respectively (**Figure 20**)(**Materials and**

Methods). We then tested the reactivity of the antibody on tumors derived from mutant IDH1 and *TP53* deleted tumors, and *TP53* deleted tumors alone. Only those tumors that developed in animals of the genotype Nestin-CreER^{T2}; IDH1-R132H; P53$^{fl/fl}$ showed staining with the IDH1-R132H antibody. Intense staining was observed only in the tumor area, but not in the surrounding brain parenchyma (**Figure 21**). This was in contrast to those tumors that developed in animals of the genotype Nestin- CreER^{T2}; P53$^{fl/fl}$ which showed a complete lack of staining (**Figure 21**). This suggests that mutant IDH1 is being expressed in those mutant tumors and should, in theory, be conferring a difference when compared to the IDH1 wildtype cohort of tumors.

It has been shown that gliomas with mutations in *IDH1* develop preferentially in the frontal lobe, thus we sought to determine whether tumor localization would be able to distinguish these genotypically different tumors(83). Based on location alone however, these tumors were unable to be distinguished as tumors from both genotypes presented throughout the cortex of the brain (**Figure 22**). As the brains of mice are not identical to that of humans, coupled with the structure being smaller, the fact that the tumors did not localize exclusively in the frontal area of the mouse brain is not surprising.

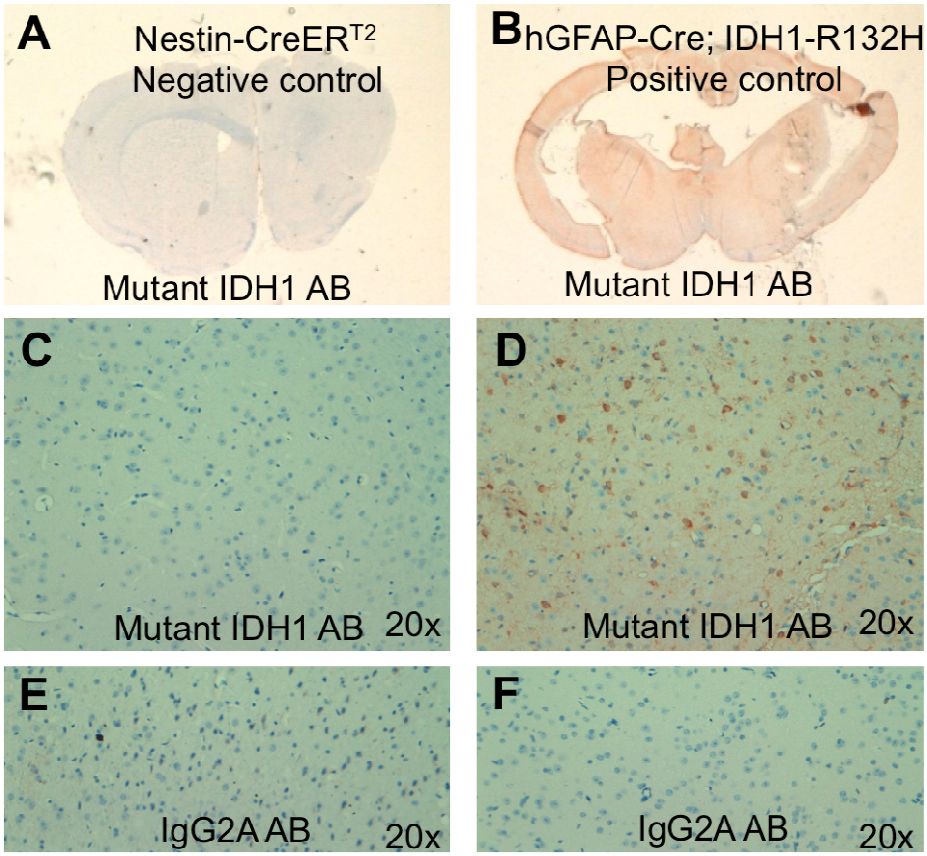

Figure 20: Optimization of the IDH1-R132H antibody.

The antibody against IDH1-R132H was tested for its reactivity against samples expressing endogenous wildtype IDH1 (A and C) (Nestin-CreER^{T2} animals-negative control) or mutant IDH1 (B and D) (hGFAP-Cre; IDH1-R132H animals-positive control). Positive staining is present only in those animals expressing mutant IDH1 (B and D). Staining with IgG2A isotype control shows no staining in either circumstance (E and F).

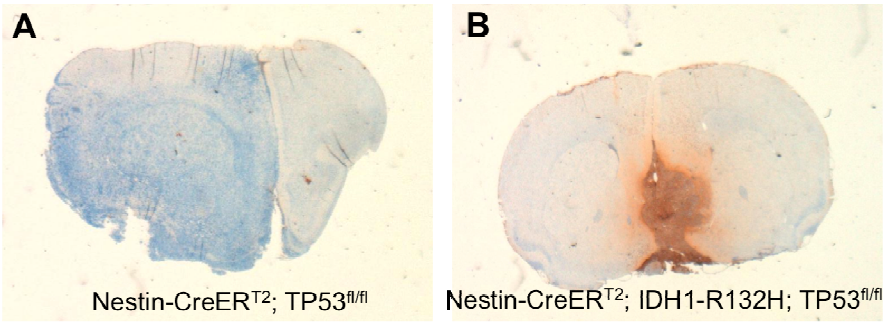

Figure 21: Detection of IDH1-R132H in tumors containing the mutant IDH1 allele.

The mutant IDH1 antibody specific for IDH1-R132H was used to detect expression of the mutant allele. *TP53* deleted tumors (A) were compared with mutant IDH1; *TP53* deleted tumors (B). Only those tumors containing the IDH1-R132H allele were positively stained with the mutant IDH1 antibody.

To better characterize the tumors that developed, they were stained with a variety of markers that neuropathologists use to aid in diagnosis. Among our antibody cohort were markers for astrocytes (GFAP), oligodendrocytes (Olig2), NSCs (Nestin), neuronal cells (NeuN or NFP), neuroendocrine cells (Synaptophysin), endothelial cells (CD31), and proliferative cells (Ki67). These markers give insight into the cell types that the tumor is composed of as well as their behavior. For example, if the tumor displays strong staining with GFAP, and has a high percentage of Ki67 positive cells, it suggests that the tumor may be an astrocytoma. These markers in combination with histology give a further understanding of the aggressiveness of these tumors. A summary of the findings derived from histology and IHC as reported by our resident neuropathologist can be found in **Table 2** and **Figure 23**. We observed that the tumors were variable in

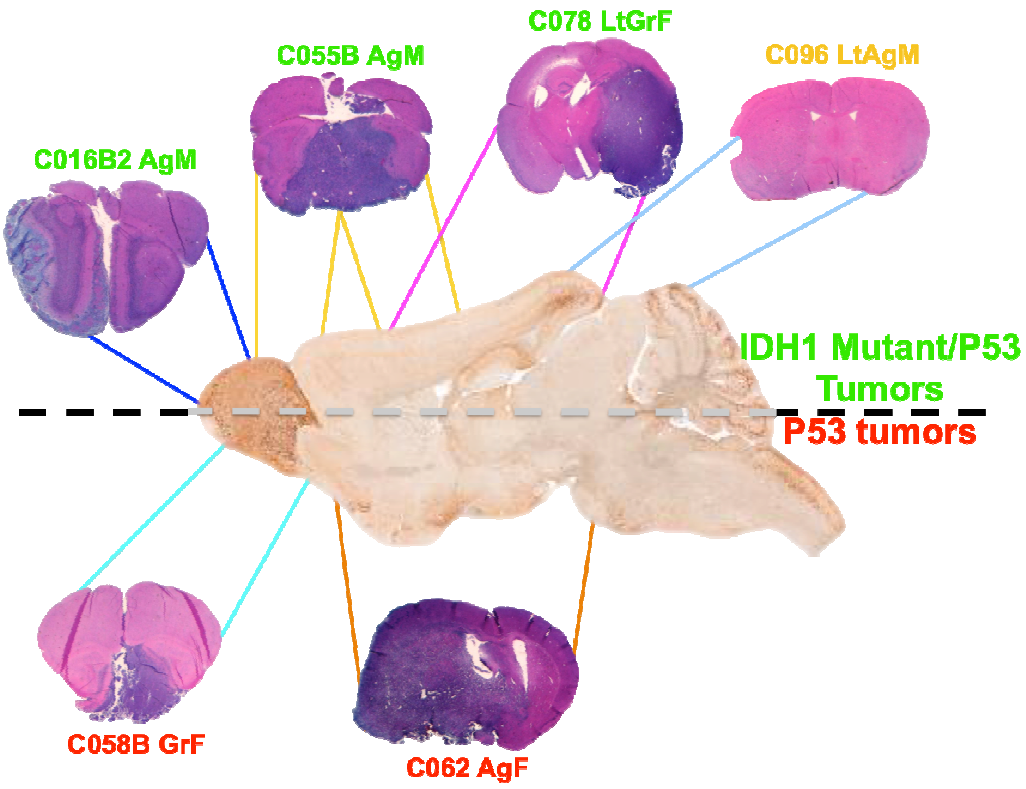

Figure 22: Tumor localization.

Mutant IDH1 tumors tend to present in the frontal lobe of human patients. To determine whether our system recapitulated this, we compared the location of the tumors that developed among Nestin-CreER^{T2}; IDH1-R132H; TP53$^{fl/fl}$ (top half) and Nestin-CreER^{T2}; TP53$^{fl/fl}$ (bottom half). Note sample C096 LtAgM shown in orange was the only low-grade glioma observed and of the genotype Nestin-CreER^{T2}; IDH1-R132H; TP53$^{fl/fl}$; ATRX$^{fl/fl}$.

their histological appearance and included diagnoses of low-grade GBM, high-grade GBM, and even an anaplastic embryonal tumor. Interestingly, the only low-grade tumor observed was of the genotype Nestin-CreER^{T2}; IDH1-R132H; P53$^{fl/fl}$; ATRX$^{fl/fl}$, the most common signature for the low-grade gliomas observed in human patients (**Figure 24**). Most other tumors were high-grade and included molecular features of GBMs including pseudopalisading necrosis and a diffuse and infiltrative nature observed through histology (**Figure 24**). The majority of the tumors stained positively for GFAP, but this was determined to be reactive astrocytosis and spanned genotypes. Additionally, giant cells were observed in several of those tumors that were IDH1 mutant (**Figure 24**). Giant cells are found in human glioma samples and there has been some thought that they are associated with a better survival(119).

Ki67, a marker for proliferative cells was also assessed. This marker is commonly used to assess the aggressiveness of a tumor and the extent of actively dividing cells. Interestingly, in our cohort, those tumors harboring the IDH1-R132H mutation and *TP53* deletion tended to have a higher proliferation index compared to those tumors with *TP53* deleted alone, with 68% compared to 38% of tumor cells staining positively for Ki67, respectively (**Figure 25**). It is to be noted that because one of the IDH1-R132H expressing tumors was very different histologically, with a chondroid-like appearance, as well as with regard to its proliferative index, this sample was removed from the comparison described above.

Lastly, we analyzed the overall survival of these animals and observed that mutant IDH1 confers a slight survival advantage of 357 days versus 334.5 days when comparing those animals of the genotype Nestin-CreER^{T2}; IDH1-R132H; P53$^{fl/fl}$ with Nestin-CreER^{T2}; P53$^{fl/fl}$ (**Figure 19**). Though not statistically significant, the trend corroborates several previous studies, including several from our own laboratory, showing those brain tumor patients with mutations in IDH1 have a prolonged survival when compared to patients with wildtype IDH1 (20 months versus 65 months for patients with anaplastic astrocytoma (Grade III) for patients with IDH1 wildtype versus mutant tumors, respectively, and 15 months versus 31 months for patients with GBM (Grade IV) for patients with wildtype versus mutant tumors, respectively)(25,37).

Table 2: IHC Characterization of Select Tumors.

Summary of findings and notes for several tumors (either Nestin-CreER^{T2}; IDH1-R132H; P53$^{fl/fl}$ or Nestin-CreER^{T2}; P53$^{fl/fl}$) that were analyzed through IHC using markers used for neuropathological diagnosis.

.

Select Tumor Characterization					
Sample Name	**C016B2**	**C055B**	**C078**	**C057A/58B**	**C062/65A-771**
Genotype	Nestin-CreER^{T2}; IDH1-R132H; P53$^{fl/fl}$	Nestin-CreER^{T2}; IDH1-R132H; P53$^{fl/fl}$	Nestin-CreER^{T2}; IDH1-R132H; P53$^{fl/fl}$	Nestin-CreER^{T2}; P53$^{fl/fl}$	Nestin-CreER^{T2}; P53$^{fl/fl}$
CD31	10% of tumor	Giant cells are +. 5% of tumor	Nice vascular pattern, no vascular proliferation	Rare perivascular +	Regions 20%, 70% hot
EMA	Negative	Giant cells are +. Rest Negative	NA	7-10% positive	Negative
GFAP	Strongly positive (reactive)	Reactive astrocytes infiltrating tumor. Tumor itself is negative	Reactive astrocytes. Rare population of positive tumor cells	Reactive astrocytes	Reactive astrocytes
Ki67	32%	65%	68%	48%	29%
Nestin	10% are 2+	1%	Negative	10%	Negative
NFP	80% are 2+	40% are 2+	90%	90% are 2+	Clusters of +
Olig2	80% are 3+	95% are +	95%	20% are 3+; 60% are 2+	80%
Synaptophysin	70% are 3+	NA	40%	90% are 2+	NA
Additional notes	Abundant intercellular mixoid matrix with mildly hypercellular proliferation of stellate cells. Has prominent chondroid appearance. Tumors infiltrate subarachnoid space. Tumor derived from external granular layer	Large carrot nuclei with prominent nucleolus. Frequent mitotic activity. Nuclear molding. Occasional giant cells. Occasional necrotic tumor cells. Tumor infiltrates perivascular region. Fairly well-circumscribed. Glioma or neuroblastoma.	Pseudopalisading necrosis. No vascular proliferation. Giant cells are present. No individual apoptotic cells or geographic necrosis. Edge is poorly circumscribed. Single cell infiltrate. Not many mitotic figures. Primary GBM.	Large carrot nuclei with significant nuclear molding. Heavy mitotic activity. Individual cell necrosis easily seen. Pigmented cells are present. Edge of tumor infiltrates perivascular region. Anaplastic medulloblastoma or ATRT.	Poorly differentiated. Nuclei are round, heterochromatic. Heavily vacuolated cytoplasm. Extensive necrosis. Starry sky appearance. Moderate pleiomorphism. Significant single cell infiltration into surrounding parenchyma. Neuroblastoma.

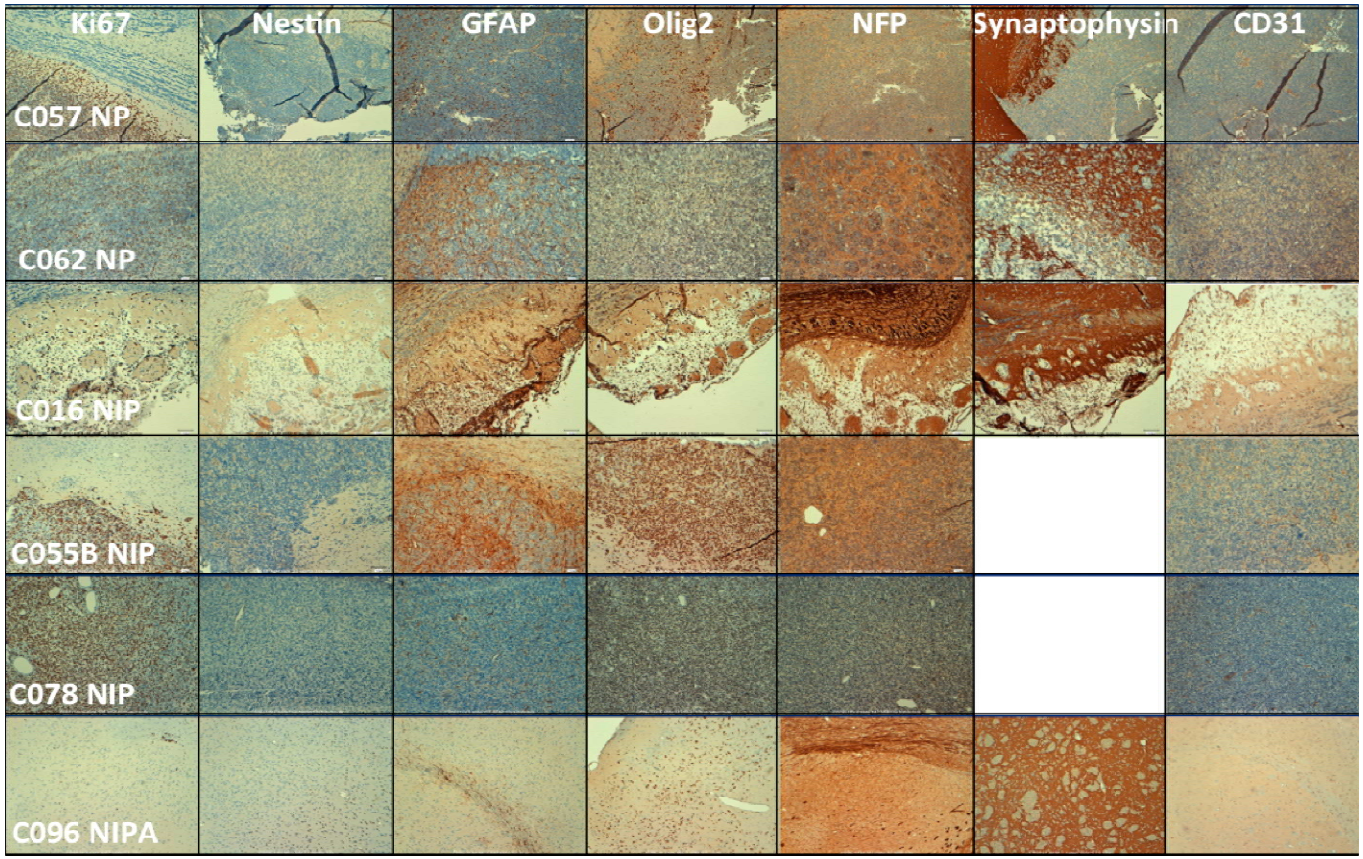

Figure 23: Tumor characterization.

To distinguish genotypically different tumors, IHC was performed with a variety of markers: Ki67 (proliferation), Nestin (NSCs), GFAP (astrocytes), Olig2 (oligodendrocytes), NFP (neurons), Synaptophysin (MBs), and CD31 (vasculature). Regions shown are either of tumor bulk or border region between tumor and normal tissue. Sample names: N-Nestin-CreER^{T2}; I-IDH1-R132H; P-P53$^{fl/fl}$; A-ATRX$^{fl/fl}$.

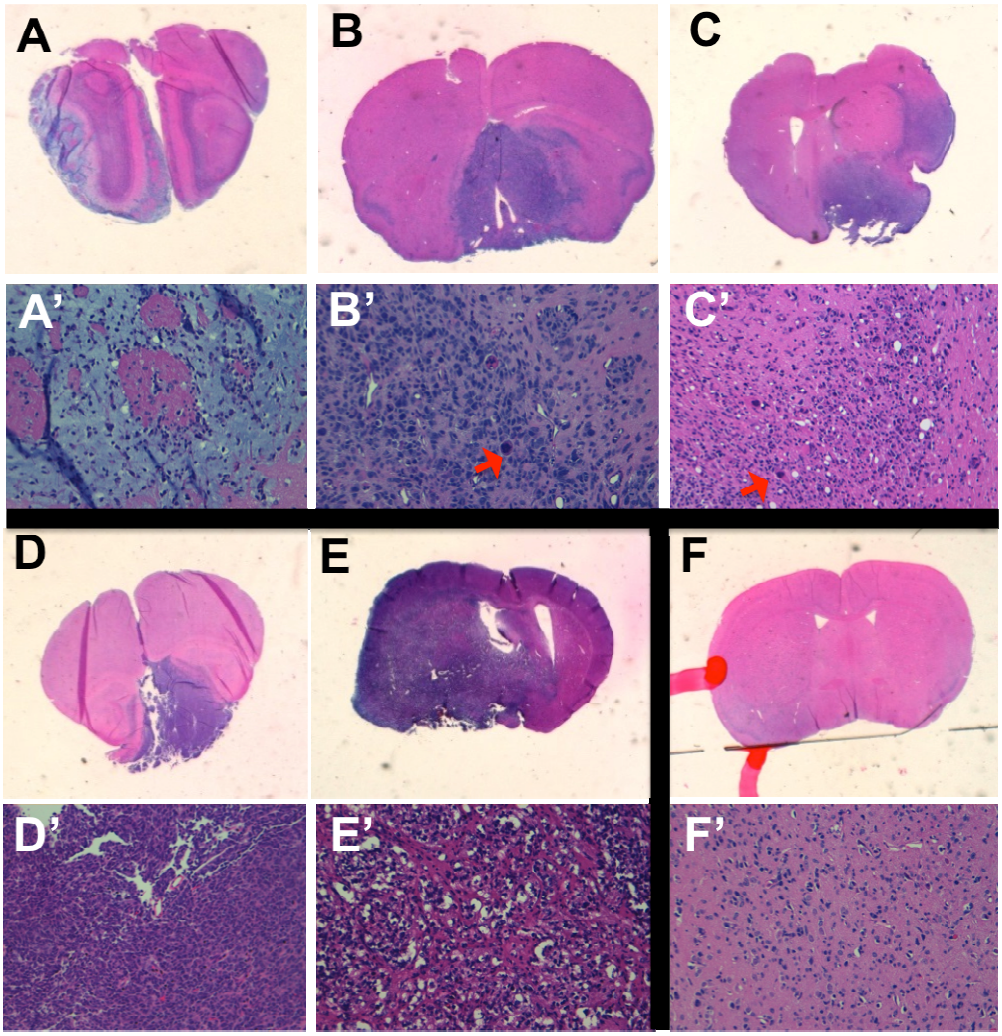

Figure 24: Histological features of brain tumors.

Representative images of tumors that developed in Nestin-CreER^{T2}; IDH1-R132H; TP53$^{fl/fl}$ animals(A-C) as well as Nestin-CreER^{T2}; TP53$^{fl/fl}$(D-E). Additionally, one low-grade tumor was observed in a Nestin-CreER^{T2}; IDH1-R132H; TP53$^{fl/fl}$; ATRX$^{fl/fl}$ animal(F). (A'-F') are 20x images of tumor region for respective samples. (A) shows a tumor of chondroid-like histology. Other tumors in this cohort were more typical with diffuse and infiltrative nature, mitotic figures, and giant cells (red arrows). (D-E) show higher levels of mitotic activity and a less-differentiated population of tumor cells. (F) shows a low-grade tumor with low levels of mitotic activity. Diffuse disease that respects borders can be seen.

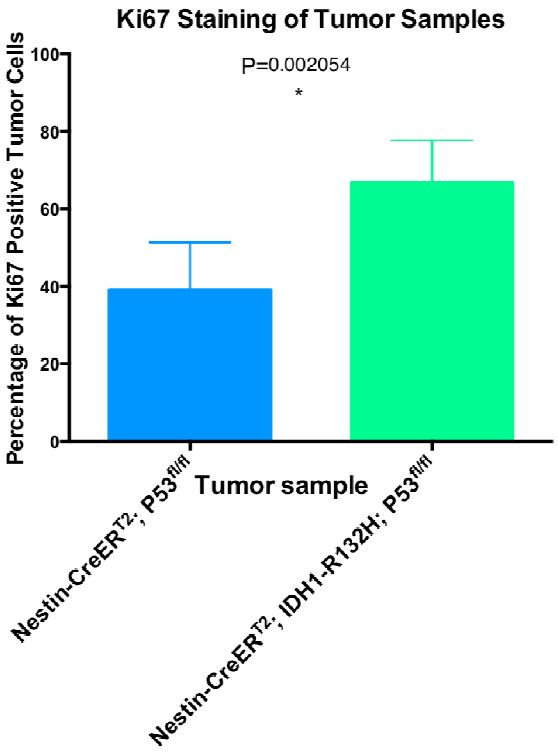

Figure 25: Mutant IDH1 tumors display heightened proliferative capacity.

Ki67 staining was compared among Nestin-CreER^{T2}; P53$^{fl/fl}$ and Nestin-CreER^{T2}; IDH1-R132H; P53$^{fl/fl}$ tumors. Tumors expressing mutant IDH1 and *TP53* deletion contained approximately 20% more proliferative cells than their *TP53* deleted alone counterpart.

5.3 Discussion

When mutant IDH1 is broadly expressed throughout the brain, as was the case when we crossed our conditional knock-in animals to hGFAP-Cre, the animals developed hydrocephalus relatively early on. This prohibited the investigation of determining mutant IDH1's effects on the brain, specifically 2-HG's effects on the brain for prolonged periods of time. To circumvent this issue and to restrict expression to one

of the leading candidates for the cell of origin for glioma, the NSCs, we crossed our animals to Nestin-CreER^{T2} which has Cre-recombinase inducibly activated in the SVZ of embryonic and adult animals. In doing so, we achieved spatio-temporal control over expression of mutant alleles. In addition to the conditional knock-in of mutant IDH1 that we generated, a conditional deletion of *TP53*, and a conditional deletion of *ATRX* were incorporated into the system. In this way, we recapitulated the genetic signature of the astrocytic subset of gliomas and were able to induce these mutations in the NSC population of the organism. Tumors developed in animals that harbored mutant IDH1 with homozygous deletion of *TP53* as well as in animals that had *TP53* deleted by itself. Mutant IDH1 was detected via IHC using an IDH1-R132 specific antibody in those tumors that contained the mutant IDH1 allele. This allows for us to assess the effects of mutant IDH1 in a genetically-based, tumor-specific context. All tumors varied histologically as well as in diagnosis making it difficult to draw distinctions among these genotypically different tumors. However, there were some features that presented only in mutant IDH1 tumors. These features included the presence of giant cells, an increased percentage of proliferative tumor cells, as indicated through Ki67 staining, as well as a trend towards a better survival when compared to the wildtype IDH1 cohort. In summary, we found that mutant IDH1 on its own is incapable of driving tumorigenesis in this system and implies that though important for tumorigenesis, as is indicated by its high frequency of mutation in glioma, it is not sufficient to induce

tumors on its own. We show that other mutations are needed in order to promote tumorigenesis, such as deletion of *TP53*, or other mutations in tumor suppressors or oncogenes that have gone uninvestigated in these sets of experiments. Though tumors developed in our system, they did so at a low penetrance with approximately 15% of treated animals becoming symptomatic. The latency was rather long for our system, with some animals showings signs of symptoms by day 179, and other animals showing no signs of symptoms or brain tumor until sacrifice and histological analysis of the brain at the 1-year timepoint. We have recently begun to utilize the data from these studies to further investigate the role of mutant IDH1 and cooperating mutations in driving tumorigenesis by implementing an orthotopic intracranial injection model based on NSCs derived from our genetic system or from serial transplanted brain tumor cells generated from our current system. This will be discussed in the following chapter discussing ongoing and future investigations stemming from these discoveries.

6. Discussion of current research and future directions

As has been discussed in previous chapters, we have utilized the power of Sanger sequencing and whole exome sequencing of both low- and high-grade gliomas to establish genetic signatures that could be used toward the stratification of human patients. We described that astrocytomas tend to harbor mutations in *IDH1* or *IDH2*, *TP53*, and *ATRX*, while oligodendrogliomas contain mutations in *IDH1* or *IDH2*, and *CIC* or *FUBP1* together with chromosomal loss of 1p/19q, all aberrations that can be relatively easily detected through PCR or hybridization reactions (**Figure 4**). Neuropathologists currently rely predominately on histological analysis of tumor tissue for patient diagnostics, however there is a great deal of inter-institutional variation and bias. This discrepancy leads to the non-uniform treatment of patients, hindering both patient outcome and analysis of effectiveness of particular drugs on specific glioma subtypes. Diagnosing glioma subtypes via molecular genetic signatures has the ability to complement histological analysis and offer a non-biased, invariable, and perhaps even binary means of diagnosis that can preclude the inter-institutional variability that plagues the field. Recently, we have discovered an additional component to the genetic signatures that makes the stratification of glioma subtypes even easier and more straightforward. That is, we identified the presence of promoter mutations in *telomerase reverse transcriptase* (*TERT*) in a large cohort of gliomas. Specifically, we found *TERT* promoter mutations in the majority of primary GBMs, *TERT* promoter mutations and

IDH1 or *IDH2* mutations in oligodendrogliomas, and mutations in *IDH1* or *IDH2* and *ATRX* but a lack of *TERT* promoter mutations in the astrocytic subset of gliomas including the secondary GBMs(37,120). Note, this paper and the findings within are explained further in **Appendix B**.

Utilizing the data obtained from our genetic studies, we sought to generate genetically faithful mouse models of glioma. We generated an IDH1-R132H conditional knock-in mouse model and crossed these animals to two different strains of mouse that have Cre-recombinase driven by either the hGFAP promoter or the Nestin promoter. When broadly expressed throughout the brain, we determined that mutant IDH1 induces a dramatic hydrocephalic phenotype. We determined that mutant IDH1 conferred a negative effect on the proliferation status of cells of the SVZ, as indicated through a reduction in the Ki67 staining in an otherwise robustly proliferative region of the brain. In the other hand, we did observe an increased percentage of Sox2 positive cells, or NSCs in this region. Upon characterizing this further, we observed that these Sox2 positive cells tended to be more dispersed, emanating from the normally tightly structured SVZ in comparison to the wildtype NSCs. With the NSC population diffuse throughout this area and an overall disorganization to this region which otherwise displays a very architectured nature, it is likely that mutant IDH1 is affecting the normal signaling pathways that are active and imperative for the proper differentiation patterns

for achieving the cellular diversity required for proper neural development of these animals.

To achieve a prolonged exposure of cells of the CNS to 2-HG such that the animals do not become symptomatic from hydrocephalus, we harnessed spatio-temporal control over expression of mutant IDH1 thereby increasing the likelihood of mutant IDH1-mediated tumor development. This was performed through inducible activation of mutant IDH1 via administration of tamoxifen in Nestin-CreER^{T2}; IDH1-R132H animals. We also incorporated additional mutations to best recapitulate the mutation spectrum observed in human glioma samples, including conditional deletion of *TP53* and conditional deletion of *ATRX*. We did observe tumor development in animals with mutant IDH1 expressed and *TP53* deleted, as well as in animals with *TP53* deleted alone. Overall, tumors were variable in nature ranging from low-grade gliomas, high-grade gliomas, and primitive neuroectodermal tumors. Most displayed an aggressive phenotype with a diffuse and infiltrative nature. Mutant IDH1 was detected in those samples harboring the mutant IDH1 allele, and mutant IDH1 was not detected in those tumors with *TP53* deleted alone suggesting there should be observable or molecular difference in those tumors expressing mutant IDH1 that should be exploited. Additionally, those tumors expressing mutant IDH1 tended to have higher levels of proliferative cells (66% compared to 38%). Despite a higher level of proliferation in these mutant animals, they did trend toward a better survival (357 days versus 334.5

days) for mutant animals versus wildtype animals. This corroborates human data in that patients presenting with mutations in *IDH1* tend to have a better survival than their wildtype counterparts.

Considering broad expression of mutant IDH1 lead to a dramatic hydrocephalic phenotype, and restricted expression of mutant IDH1 lead to development of tumors when co-mutated with *TP53*, but did so with a long latency and low penetrance, we are currently working towards improvement of the system. To this end, we have generated an orthotopic intracranial injection model utilizing NSCs derived from our genetic model. Here, we crossed in a conditional reporter mouse to our mutant IDH1 conditional knock-in animals (conditional deletion of *TP53* and conditional deletion of *ATRX* were also incorporated). NSCs were isolated from E14.5 embryos and cultured *in vitro* (**Materials and Methods**). After 1-day in culture, NSCs were infected with adenoviral Cre-recombinase. By 24-hours post-infection, expression of tdTomato was detected through fluorescence microscopy. Additionally, 2-HG was detected in only those NSCs harboring the mutant IDH1 allele following transformation with Cre-virus (**Figure 26**). These NSCs were subsequently used for orthotopic intracranial injection into recipient mice. As a pilot study, these cells were injected into NOD *scid* gamma animals (NSG), an immune-compromised strain of mouse that is commonly used for injections of cells that would otherwise promote an immune response(121). Considering these cells are capable of indefinite *in vitro* culture, this opens up a new avenue for

incorporating other mutations and drivers to best determine the cooperating nature among mutations identified in human patients.

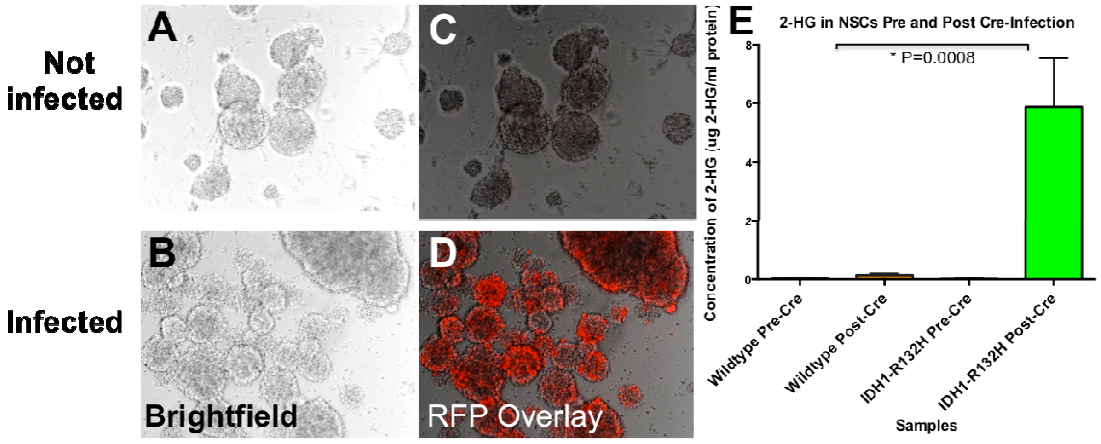

Figure 26: Derivation and induction of mutant alleles in NSCs.

NSCs were harvested from E14.5 animals and cultured *in vitro* as neurospheres (A). Cells were infected with adenoviral Cre-recombinase (B). This induced expression of the tdTomato reporter in the infected cells, but not the non-infected or wildtype cells(C and D). 2-HG was detected in only those cells that were infected with the mutant IDH1 allele(E).

mutations and drivers to best determine the cooperating nature among mutations identified in human patients.

In addition to orthotopic intracranial injections, these NSCs also permit the study of more fundamental aspects of mutant IDH1 on a biologically relevant cell line. For example, we are currently assessing the effects of mutant IDH1 on self-renewal of NSCs. Preliminary data shows that mutant IDH1 may be imparting an inhibition to the self-

renewing capabilities of NSCs, an observation that corroborates the finding of a decreased number of proliferative cells of the SVZ *in vivo*. Additionally, we are able to utilize these cells for differentiation studies and assess mutant IDH1's effects on differentiation *in vitro*. As differentiation is much easier to address in an *in vitro* system as opposed to an *in vivo* system, these NSCs will offer a tremendous advantage. Preliminary data shows that mutant IDH1 may be imparting a defect to the normal differentiation patterns of these cells, specifically into the neuronal lineage. That is, when detecting β-(III)-tubulin positive cells, a marker for mature neurons, we observe that those cells expressing mutant IDH1 have a decreased propensity for differentiating into neurons when compared to their non-infected parental cell line. This suggests that mutant IDH1 may be acting similarly in the CNS as it does in the hematopoietic system, that is, it confers a block to the differentiation.

In conclusion, we have determined the genetic signatures of gliomas and utilized those signatures to generate genetically faithful mouse models that harbor those exact mutations found most commonly in the astrocytic subset of gliomas. We have learned a great deal utilizing these models, including 1-Broad expression of mutant IDH1 induces hydrocephalus; 2-Mutant IDH1 induces hemorrhagic foci throughout the cortex of the brain when broadly expressed; a phenotype that may be due to aberrant HIF signaling as a result of elevated levels of 2-HG; 3-mutant IDH1 perturbs the NSC niche and this likely effects the many signaling pathways that are active in this area and imperative for

the differentiation patterns of these cells of the CNS; 4-the NSC population in mutant brains tend to be more dispersed, suggesting mutant IDH1 may be imparting enhanced migratory abilities to these cells; 4- mutant IDH1, when co-mutated with *TP53* is capable of inducing tumor development; 5-tumors that developed in these animals had higher levels of proliferative cells when compared to their wildtype counterparts; and 6-the survival of animals with mutant IDH1 and *TP53* deletion was slightly better than in those animals with *TP53* deleted alone.

Ultimately, the system that encompasses the sequencing data from large-scale genomic studies to assess the contribution and significance of particular mutations, combined with the ability to promote tumorigenesis in an orthotopic manner as to preserve the microenvironment and signals from within, as well as depicting the heterogeneity observed in patient tumors, and to do so with high penetrance and short latency will be the most impactful of models. In doing so, the model generated will provide the most stable foundation for preclinical data acquisition. With the exception of tumor formation with high penetrance and short latency, which will be improved in our orthotopic intracranial injection system that we established that utilizes cells derived from our genetic model, we have reached the goals of this project. With a foundation of the data presented here, together with the variety of models generated, we are poised to make great strides in understanding mutant IDH1's contribution to tumorigenesis and ultimately, making an impact on this most fatal disease.

7. Materials and Methods

7.1. Mouse husbandry

All work requiring the use of animals was done in accordance with the Duke University Institutional Animal Care and Use Committee (DUIACUC) and in accordance with the National Institutes of Health *Guide for the Care and Use of Laboratory Animals*. All work was performed under the approved animal protocol for Hai Yan: A072-13-03. Animals were maintained in a barrier facility (Duke Cancer Center Isolation Facility) and were maintained according to NIH guidelines. The animals were kept under pathogen-free conditions in sterilized plastic containers and were checked daily.

7.2 Timed matings

For experiments requiring treatment of animals with tamoxifen for an embryonic timepoint, animals were combined at a maximum of a 1:2 male:female ratio. The morning following the establishment of the mating cage, animals were checked for the presence of a vaginal plug through the use of a probe. The time the plug was identified was considered 0.5dpc.

7.3 Treatment with tamoxifen

Treatment of animals with tamoxifen was required to induce activation of Cre-recombinase in those animals of the genotype Nestin-CreER^{T2}. Tamoxifen (Sigma, T5648) was made up in pharmaceutical grade corn oil at a concentration of 20mg/ml. Solution was warmed to 37° Celsius and vortexed thoroughly until completely

dissolved. 3mgs (150ul) of tamoxifen was administered to pregnant dams at 18.5dpc via oral gavage. For P28 timepoints, adult animals were administered tamoxifen via oral gavage at a dosage of 1μg/kg.

7.4 Euthanasia and tissue collection

Every effort was made to ensure there was minimal pain and distress imparted on the animals. Mice were checked daily for any signs of impairment or abnormalities and at the earliest indication of any distress, animals were sacrificed in accordance with the IACUC Policy for Animal Euthanasia. Depending on the requirement of the tissues, adult animals were euthanized either through CO_2 asphyxiation, followed by decapitation or through administration of a lethal dose of Urethane (10μl/g of 20% Urethane made up in sterile PBS). Solution was administered through intraperitoneal injection. Animals were monitored and toe pinches were performed to ensure they were unresponsive to pain. Once unresponsive, animals underwent intracardiac perfusion with 15mls PBS followed by 15mls of 10% Neutral Buffered Formalin. All procedures were done in accordance with our OESO approved SOPs. Following perfusion, tissues were harvested and post-fixed in 10% Neutral Buffered Formalin for 24 hours at which time they were transferred to 70% Ethanol in preparation for paraffin embedding performed at the Duke University Pathology Research Histology and Immunohistochemistry Laboratory.

Animals sacrificed for the P3 timepoint were placed on ice until deeply anesthetized followed by decapitation and tissue harvesting. Brains were placed in 10% Neutral Buffered Formalin for 24 hours at which point they were transferred to either 70% Ethanol in preparation for paraffin embedding or in 20% Sucrose in PBS and placed at 4° Celsius until cryoprotected in preparation for OCT embedding.

7.5 Tissue processing

Tissues were either paraffin embedded or OCT embedded. Paraffin blocks were cut 5-6μM and placed on charged microscope slides. These slides were made for H&E staining and IHC procedures. OCT blocks were cut at 14μM and placed onto charged microscope slides and stored at -80° Celsius until ready for IF procedure.

7.6 H&E, IHC, and IF

Standard H&E procedures were performed requiring paraffin sections to undergo deparaffinization in 3 washes with Sub-X, followed by rehydration of the tissue in a graded Ethanol series, Hematoxylin staining, wash with Ammonia water, Eosin staining, dehydration in a graded Ethanol series, and a clearing in Sub-X followed by mounting with a Sub-X based mounting media.

Frozen sections were used for IF. Briefly, tissues were permeablized and blocked, stained with primary antibodies (listed in **Appendix C**) made up in blocking buffer, and incubated overnight in a humidity chamber at 4° Celsius. Slides were washed and incubated with secondary antibody made up in blocking buffer and

incubated at room temperature in the dark for 1-hour. Slides were counterstained with DAPI and mounted.

For IHC, Zuowei Su of the Duke University Pathology Research Histology and Immunohistochemistry Laboratory followed a standard protocol requiring antigen retrieval in citrate buffer (pH 6.0, 80° Celsius) and utilizing the DAKO Autostainer 3400 with antibodies listed in **Appendix C**.

7.7 Imaging

H&E and IHC samples were imaged using the Leica DMD 108. IF images were imaged on the Nikon Eclipse T2000-E.

7.8 Genotyping of animals: lysis, genomic DNA extraction, and PCR

Toe-clips were collected from P9 animals or tail-snips were collected from P21 animals. Tissue was lysed overnight at 55° Celsius in lysis buffer (100mM Tris-HCl pH 8; 5mM EDTA pH 8; 0.0% SDS; 200mM NaCl; Proteinase K, and water). Solution containing tissue were vortexed and centrifuged at 14,000G for 10 minutes. Supernatant was added to an equal volume of isopropanol and gently inverted until a precipitate formed. The precipitate was transferred to 300µl 70% Ethanol, inverted, and centrifuged at 14,000G for 10 minutes. Supernatant was removed and pellet was air dried for 10 minutes. Pellet was resuspended in 50 to 100µl of sterile H2O and further diluted 1:50 in sterile H2O. 1.5µl of diluted DNA were used for PCR reactions.

PCR master mixes contained the following: 1X Kapa Buffer A, 0.2mM dNTP, 6% DMSO, 1uM of forward primer, 1uM of reverse primer, and 0.3U Kapa2G Fast polymerase from Kapa Biosystems. Primers and expected band sizes can be found in **Appendix D**. Touchdown PCR protocol was perfomed: 1x (95°C 5 minutes); 3x (95°C 20 seconds, 64°C 20 seconds, 72°C 20 seconds), 3x (95°C 20 seconds, 61°C 20 seconds, 72°C 20 seconds), 3x (95°C 20 seconds, 57°C 20 seconds, 72°C 20 seconds), 30x (95°C 20 seconds, 55°C 20 seconds, 72°C 20 seconds), 1x (72°C 5 minutes).

7.9 NSC harvest and culture

E14.5 embryos were utilized for NSC harvest. Pregnant dams were sacrificed via CO_2 asphyxiation followed by extraction of embryos. Embryos were decapitated placed in dissection media (2% glucose on ice) and brains harvested under a dissection microscope. Cortex of brain was triturated in Complete Embryonic NeuroCult Proliferation media and spun down at 150G for 5 minutes. Cells were resuspended in Complete Embryonic NeuroCult Proliferation media and filtered through a 40μM filter. Cells were plated in Complete Embryonic NeuroCult Proliferation media at a density of $1x10^5$ cells per cm^2. For those cells harboring mutant alleles, induction with Cre-recombinase was required. 1-day post harvest, cells were infected with Cre-expressing RGD fiber modified adenovirus (Vector Biolabs, 1769) at an MOI of 10-100. 24-hours post-infection, expression of mutant alleles or conditional tdTomato was observed through immunofluorescent imaging.

7.10 2-HG detection

2-HG was detected in collaboration with the Pharmaceutical Research Pharmacokinetic/Pharmacodynamic Core Facility at Duke University. The methodology for this process has been described previously(63).

7.11 Sanger and exome sequencing

Sanger sequencing and exome sequencing was performed as described in the following publications: Jiao et al., 2012 and Killela et al., 2014 (35,36).

Appendix A

Figures 3, 4, 9 and 27 as well as content in Chapter 2 and Appendix B were generated from currently published and copyrighted material. All publications are available to reprint, modify, and copy as long as the original authors and source are cited under the Created Commons Attribution License:

Jiao, Y., Killela, P. J., Reitman, Z. J., Rasheed, A. B., Heaphy, C. M., de Wilde, R. F., Rodriguez, F. J., Rosemberg, S., Oba-Shinjo, S. M., Nagahashi Marie, S. K., Bettegowda, C., Agrawal, N., Lipp, E., Pirozzi, C., Lopez, G., He, Y., Friedman, H., Friedman, A. H., Riggins, G. J., Holdhoff, M., Burger, P., McLendon, R., Bigner, D. D., Vogelstein, B., Meeker, A. K., Kinzler, K. W., Papadopoulos, N., Diaz, L. A., and Yan, H. (2012) Frequent ATRX, CIC, FUBP1 and IDH1 mutations refine the classification of malignant gliomas. *Oncotarget* **3**, 709-722

Killela, P. J., Pirozzi, C. J., Reitman, Z. J., Jones, S., Rasheed, B. A., Lipp, E., Friedman, H., Friedman, A. H., He, Y., McLendon, R. E., Bigner, D. D., and Yan, H. (2014) The genetic landscape of anaplastic astrocytoma. *Oncotarget* **5**, 1452-1457

Killela, P. J., Pirozzi, C. J., Healy, P., Reitman, Z. J., Lipp, E., Rasheed, A. B., Yang, R., Diplas, B., Wang, Z., Greer, P. K., Zhu, H., Wang, C., Carpenter, A., Friedman, H., Friedman, A. H., He, Y., McLendon, R. E., Herndon II, J. E., Yan, H., and Bigner, D. D. (2014) Mutations in IDH1 , IDH2 , and in the TERT promoter define clinically distinct subgroups of adult malignant gliomas. *Oncotarget* **5**, 1515-1525

A License Agreement for Figure 5 was obtained from Copyright Clearance Center and was reprinted by permission from Macmillan Publishers Ltd: Nature Publishing Group

Prensner, J. R., and Chinnaiyan, A. M. (2011) Metabolism unhinged: IDH mutations in cancer. *Nature medicine* **17**, 291-293.

Appendix B

Recent studies have identified mutations in the promoter region of *TERT* in a variety of cancers including melanomas, liposarcomas, bladder cancer, urinary tract cancers, and gliomas. TERT promoter mutations were found in a particular subset of gliomas and when combined with the mutation status of *IDH1* or *IDH2*, had the ability to segregate the different glioma subtypes. In our recent publication, we identify the presence of TERT promoter mutations specifically in oligodendrogliomas and primary GBMs, however mutations were not observed in the astrocytomas or secondary GBMs (**Figure 27**)(37). Using the combined TERT promoter mutation status and IDH1/IDH2 mutation status, we were able to distinguish the histologic subtypes; GBMs were characterized as TERT mutant/IDH wildtype, Grade II and Grade III astrocytomas characterized as TERT wildtype/IDH mutant, and the majority of Grade II and Grade III oligodendrogliomas were characterized as TERT mutant/IDH mutant. Additionally, oligoastrocytomas, a subtype that presents a great deal of difficulty for neuropathological diagnosis were able to be depicted on a molecular level. We also established that these genetic signatures are reliable when compared to the overall survival of patients derived from conventional histopathological diagnosis. Mutations in the TERT promoter and in *IDH1* or *IDH2* effectively stratify patients into reproducible subgroups based on survival. The strength of these genetic signatures and their association with overall survival are illustrated by a slightly higher R^2 score than by

histology alone (0.3132 versus 0.2704). This study supports genotyping of the TERT promoter and *IDH1* and *IDH2* as a rapid economical test requiring little tumoral DNA that could help inform clinicians both with regards to diagnosis and to predicted overall survival of patients. Adapting this molecular means of diagnosis will promote consistency of diagnosis between institutions, thereby aiding in the stratification of patients and the examination of therapeutic response to treatment.

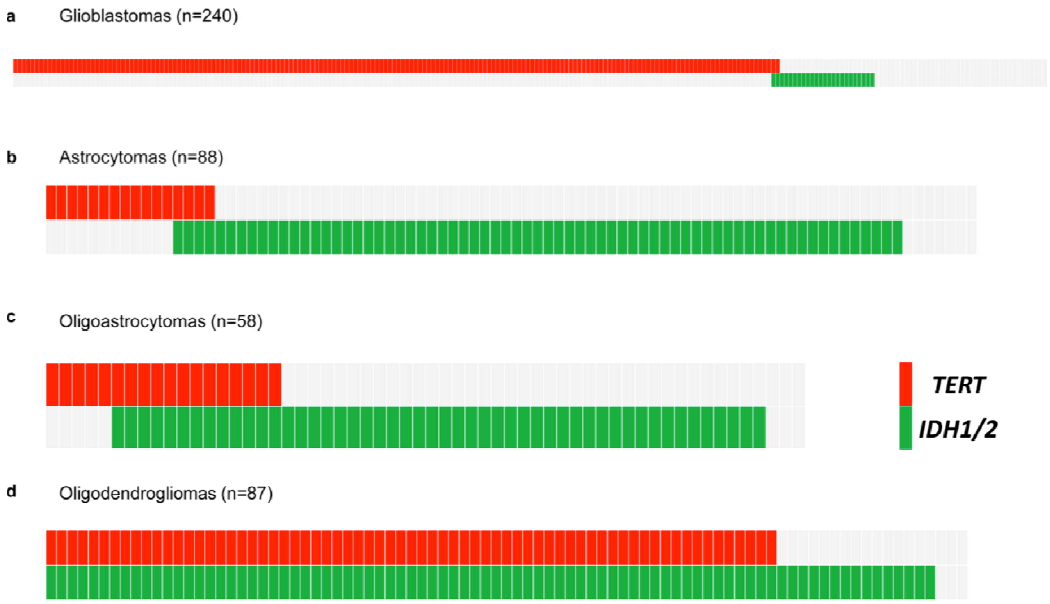

Figure 27: Distribution of TERT promoter and IDH1/2 mutations in a panel of 473 adult gliomas.

Mutational analysis of 473 adult gliomas for TERT promoter and IDH1/2 mutations. Data from 240 Grade IV GBM (A), 88 Grade II-III astrocytomas (B), 58 Grade II-III oligoastrocytomas (C), and 87 Grade II-III oligodendrogliomas (D). Mutation status is indicated by color shading, with gray coloring indicating wildtype sequence, red indicating mutations in the TERT promoter, and green indicating mutations in IDH1/2.

Appendix C

Table 3: List of Antibodies

Antibodies			
Name	Host	Dilution	Company - Catalog Number
B(III)Tubulin	Mouse	1:1000	Covance – MMS-435P
Blbp	Rabbit	1:500	Millipore – ABN14
CD31	Rabbit	1:100	Abcam - ab28364
Cleaved caspase 3	Rabbit	1:500	Cell Signaling – 9664
GFAP	Rabbit	1:1000	Novus – NB300-141
GFAP	Rabbit	1:3000	Dako – z0334
IDH1	Mouse	1:100	Dianova – H09
Ki67	Mouse	1:100	BD Pharm – 550609
Ki67	Rabbit	1:400	Thermo – RM-9106-s
Nestin	Mouse	1:100	Stem Cell Tech – 60051
Nestin	Rabbit	1:400	Sigma – N5413)
NFP	Rabbit	1:1000	Millipore – ab9568
NeuN	Mouse	1:100	Millipore – MAB377
Olig2	Rabbit	1:500	Abcam – ab136253
RFP	Rabbit	1:1000	Rockland – 600-401-379
Sox2	Rabbit	1:100	Stem Cell Tech – 60055
Synaptophysin	Rabbit	1:100	Dako – A0010

Appendix D

Table 4: Primer List

PRIMER LIST		
PRIMER NAME	SEQUENCE	BAND SIZE (in basepairs)
mATRX18 RP	TGAACCTGGGGACTTCTTTG	Mutant band=1500 Wildtype band=1000
Neo RP	CCACCATGATATTCGGCAAG	
pps1.15 FP	GGTTTTAGATGAAAATGAAGAG	
Cf	ACTGGGATCTTCGAACTCTTTGGAC	Wildtype band=420 Cre-specific band=281
Cr	GATGTTGGGGCACTGCTCATTCACC	
CreF	CCATCTGCCACCAGCCAG	
CreR	TCGCCATCTTCCAGCAGG	
IDH1 FS1 FP	GGCTGGCCTCACACTCAAGAGAT	Mutant band=263 Wildtype band=329
IDH1 RS1 RP	GCAGATCTGCAAGCTTCTGTGGAA	
IDH1 RS5 RP	GCCAGTTAGTCATAGGGTGAACCTTCC	
P53 FP	GGTTAAACCCAGCTTGACCA	Mutant band=350 Wildtype band=280
P53 RP	GGAGGCAGAGACAGTTGGAG	
Tomato/06F	AGTTCATGTACGGCTCCAAG	Wildtype band=560 Mutant band=300
Tomato/02B	TAGAGCTCTTAGACGGTCCGCTTGTACAG	
CAG/02B	GTTATGTAACGCGGAACTCC	
ROSA/02B	TAGTCTAACTCGCGACACTG	Mutant band=570
ROSA/01F	CACTTGCTCTCCCAAAGTCG	

References

1. Howlader, N., Noone, A. M., Krapcho, M., Garshell, J., Miller, D., Altekruse, S. F., Kosary, C. L., Yu, M., Ruhl, J., Tatalovich, Z., Mariotto, A., Lewis, D. R., Chen, H. S., Feuer, E. J., and Cronin, K. A. (April 2014) SEER Cancer Statistics Review, 1975-2011. *National Cancer Institute* **Bethesda, MD,** http://seer.cancer.gov/csr/1975_2011/**, based on November 2013 SEER data submission, posted to the SEER web site**

2. CBTRUS. (2012) CBTRUS Statistical Report: Primary Brain and Central Nervous System Tumors Diagnosed in the United States in 2004-2008 (March 23, 2012 Revision). *Central Brain Tumor Registry of the United States*

3. Wen, P. Y., and Kesari, S. (2008) Malignant gliomas in adults. *N Engl J Med* **359**, 492-507

4. Welch, H. G., Schwartz, L. M., and Woloshin, S. (2000) Are increasing 5-year survival rates evidence of success against cancer? *Jama* **283**, 2975-2978

5. Chow, L. M., and Baker, S. J. (2012) Capturing the molecular and biological diversity of high-grade astrocytoma in genetically engineered mouse models. *Oncotarget* **3**, 67-77

6. Louis, D. N., Ohgaki, H., Wiestler, O. D., Cavenee, W. K., Burger, P. C., Jouvet, A., Scheithauer, B. W., and Kleihues, P. (2007) The 2007 WHO classification of tumours of the central nervous system. *Acta Neuropathol* **114**, 97-109

7. Altieri, R., Agnoletti, A., Quattrucci, F., Garbossa, D., Calamo Specchia, F. M., Bozzaro, M., Fornaro, R., Mencarani, C., Lanotte, M., Spaziante, R., and Ducati, A. (2014) Molecular biology of gliomas: present and future challenges. *Translational medicine @ UniSa* **10**, 29-37

8. Collins, V. P. (2004) Brain tumours: classification and genes. *Journal of neurology, neurosurgery, and psychiatry* **75 Suppl 2**, ii2-11

9. Stiles, J., and Jernigan, T. L. (2010) The basics of brain development. *Neuropsychology review* **20**, 327-348

10. Lim, D. A., and Alvarez-Buylla, A. (2014) Adult neural stem cells stake their ground. *Trends in neurosciences* **37**, 563-571

11. Rowitch, D. H., and Kriegstein, A. R. (2010) Developmental genetics of vertebrate glial-cell specification. *Nature* **468**, 214-222

12. Barnabe-Heider, F., Wasylnka, J. A., Fernandes, K. J., Porsche, C., Sendtner, M., Kaplan, D. R., and Miller, F. D. (2005) Evidence that embryonic neurons regulate the onset of cortical gliogenesis via cardiotrophin-1. *Neuron* **48**, 253-265

13. Namihira, M., Kohyama, J., Semi, K., Sanosaka, T., Deneen, B., Taga, T., and Nakashima, K. (2009) Committed neuronal precursors confer astrocytic potential on residual neural precursor cells. *Developmental cell* **16**, 245-255

14. Gallo, V., and Deneen, B. (2014) Glial development: the crossroads of regeneration and repair in the CNS. *Neuron* **83**, 283-308

15. Kriegstein, A., and Alvarez-Buylla, A. (2009) The glial nature of embryonic and adult neural stem cells. *Annual review of neuroscience* **32**, 149-184

16. Harris, L. W., Lockstone, H. E., Khaitovich, P., Weickert, C. S., Webster, M. J., and Bahn, S. (2009) Gene expression in the prefrontal cortex during adolescence: implications for the onset of schizophrenia. *BMC medical genomics* **2**, 28

17. Visvader, J. E. (2011) Cells of origin in cancer. *Nature* **469**, 314-322

18. Sanai, N., Alvarez-Buylla, A., and Berger, M. S. (2005) Neural stem cells and the origin of gliomas. *N Engl J Med* **353**, 811-822

19. Holland, E. C., Celestino, J., Dai, C., Schaefer, L., Sawaya, R. E., and Fuller, G. N. (2000) Combined activation of Ras and Akt in neural progenitors induces glioblastoma formation in mice. *Nat Genet* **25**, 55-57

20. Alcantara Llaguno, S., Chen, J., Kwon, C. H., Jackson, E. L., Li, Y., Burns, D. K., Alvarez-Buylla, A., and Parada, L. F. (2009) Malignant astrocytomas originate from neural stem/progenitor cells in a somatic tumor suppressor mouse model. *Cancer Cell* **15**, 45-56

21. Liu, C., Sage, J. C., Miller, M. R., Verhaak, R. G., Hippenmeyer, S., Vogel, H., Foreman, O., Bronson, R. T., Nishiyama, A., Luo, L., and Zong, H. (2011) Mosaic analysis with double markers reveals tumor cell of origin in glioma. *Cell* **146**, 209-221

22. Zong, H., Verhaak, R. G., and Canoll, P. (2012) The cellular origin for malignant glioma and prospects for clinical advancements. *Expert review of molecular diagnostics* **12**, 383-394

23. (2008) Comprehensive genomic characterization defines human glioblastoma genes and core pathways. *Nature* **455**, 1061-1068

24. Parsons, D. W., Jones, S., Zhang, X., Lin, J. C., Leary, R. J., Angenendt, P., Mankoo, P., Carter, H., Siu, I. M., Gallia, G. L., Olivi, A., McLendon, R., Rasheed, B. A., Keir, S., Nikolskaya, T., Nikolsky, Y., Busam, D. A., Tekleab, H., Diaz, L. A., Jr., Hartigan, J., Smith, D. R., Strausberg, R. L., Marie, S. K., Shinjo, S. M., Yan, H., Riggins, G. J., Bigner, D. D., Karchin, R., Papadopoulos, N., Parmigiani, G., Vogelstein, B., Velculescu, V. E., and Kinzler, K. W. (2008) An integrated genomic analysis of human glioblastoma multiforme. *Science* **321**, 1807-1812

25. Yan, H., Parsons, D. W., Jin, G., McLendon, R., Rasheed, B. A., Yuan, W., Kos, I., Batinic-Haberle, I., Jones, S., Riggins, G. J., Friedman, H., Friedman, A., Reardon, D., Herndon, J., Kinzler, K. W., Velculescu, V. E., Vogelstein, B., and Bigner, D. D. (2009) IDH1 and IDH2 mutations in gliomas. *N Engl J Med* **360**, 765-773

26. Watanabe, T., Nobusawa, S., Kleihues, P., and Ohgaki, H. (2009) IDH1 mutations are early events in the development of astrocytomas and oligodendrogliomas. *Am J Pathol* **174**, 1149-1153

27. Morris, J. H., Meng, E. C., and Ferrin, T. E. (2010) Computational tools for the interactive exploration of proteomic and structural data. *Molecular & cellular proteomics : MCP* **9**, 1703-1715

28. Xu, X., Zhao, J., Xu, Z., Peng, B., Huang, Q., Arnold, E., and Ding, J. (2004) Structures of human cytosolic NADP-dependent isocitrate dehydrogenase reveal a novel self-regulatory mechanism of activity. *The Journal of biological chemistry* **279**, 33946-33957

29. Dang, L., White, D. W., Gross, S., Bennett, B. D., Bittinger, M. A., Driggers, E. M., Fantin, V. R., Jang, H. G., Jin, S., Keenan, M. C., Marks, K. M., Prins, R. M., Ward, P. S., Yen, K. E., Liau, L. M., Rabinowitz, J. D., Cantley, L. C., Thompson, C. B., Vander Heiden, M. G., and Su, S. M. (2009) Cancer-associated IDH1 mutations produce 2-hydroxyglutarate. *Nature* **462**, 739-744

30. Struys, E. A., Salomons, G. S., Achouri, Y., Van Schaftingen, E., Grosso, S., Craigen, W. J., Verhoeven, N. M., and Jakobs, C. (2005) Mutations in the D-2-hydroxyglutarate dehydrogenase gene cause D-2-hydroxyglutaric aciduria. *American journal of human genetics* **76**, 358-360

31. Chalmers, R. A., Lawson, A. M., Watts, R. W., Tavill, A. S., Kamerling, J. P., Hey, E., and Ogilvie, D. (1980) D-2-hydroxyglutaric aciduria: case report and biochemical studies. *Journal of inherited metabolic disease* **3**, 11-15

32. van der Knaap, M. S., Jakobs, C., Hoffmann, G. F., Nyhan, W. L., Renier, W. O., Smeitink, J. A., Catsman-Berrevoets, C. E., Hjalmarson, O., Vallance, H., Sugita, K., Bowe, C. M., Herrin, J. T., Craigen, W. J., Buist, N. R., Brookfield, D. S., and Chalmers, R. A. (1999) D-2-Hydroxyglutaric aciduria: biochemical marker or clinical disease entity? *Ann Neurol* **45**, 111-119

33. Moroni, I., Bugiani, M., D'Incerti, L., Maccagnano, C., Rimoldi, M., Bissola, L., Pollo, B., Finocchiaro, G., and Uziel, G. (2004) L-2-hydroxyglutaric aciduria and brain malignant tumors: a predisposing condition? *Neurology* **62**, 1882-1884

34. Vogelstein, B., Papadopoulos, N., Velculescu, V. E., Zhou, S., Diaz, L. A., Jr., and Kinzler, K. W. (2013) Cancer genome landscapes. *Science* **339**, 1546-1558

35. Jiao, Y., Killela, P. J., Reitman, Z. J., Rasheed, A. B., Heaphy, C. M., de Wilde, R. F., Rodriguez, F. J., Rosemberg, S., Oba-Shinjo, S. M., Nagahashi Marie, S. K., Bettegowda, C., Agrawal, N., Lipp, E., Pirozzi, C., Lopez, G., He, Y., Friedman, H., Friedman, A. H., Riggins, G. J., Holdhoff, M., Burger, P., McLendon, R., Bigner, D. D., Vogelstein, B., Meeker, A. K., Kinzler, K. W., Papadopoulos, N., Diaz, L. A., and Yan, H. (2012) Frequent ATRX, CIC, FUBP1 and IDH1 mutations refine the classification of malignant gliomas. *Oncotarget* **3**, 709-722

36. Killela, P. J., Pirozzi, C. J., Reitman, Z. J., Jones, S., Rasheed, B. A., Lipp, E., Friedman, H., Friedman, A. H., He, Y., McLendon, R. E., Bigner, D. D., and Yan, H. (2014) The genetic landscape of anaplastic astrocytoma. *Oncotarget* **5**, 1452-1457

37. Killela, P. J., Pirozzi, C. J., Healy, P., Reitman, Z. J., Lipp, E., Rasheed, A. B., Yang, R., Diplas, B., Wang, Z., Greer, P. K., Zhu, H., Wang, C., Carpenter, A., Friedman, H., Friedman, A. H., He, Y., McLendon, R. E., Herndon II, J. E., Yan, H., and Bigner, D. D. (2014) Mutations in IDH1 , IDH2 , and in the TERT promoter define clinically distinct subgroups of adult malignant gliomas. *Oncotarget* **5**, 1515-1525

38. Verhaak, R. G., Hoadley, K. A., Purdom, E., Wang, V., Qi, Y., Wilkerson, M. D., Miller, C. R., Ding, L., Golub, T., Mesirov, J. P., Alexe, G., Lawrence, M., O'Kelly, M., Tamayo, P., Weir, B. A., Gabriel, S., Winckler, W., Gupta, S., Jakkula, L., Feiler, H. S., Hodgson, J. G., James, C. D., Sarkaria, J. N., Brennan, C., Kahn, A., Spellman, P. T., Wilson, R. K., Speed, T. P., Gray, J. W., Meyerson, M., Getz, G., Perou, C. M., and Hayes, D. N. (2010) Integrated genomic analysis identifies clinically relevant subtypes of glioblastoma characterized by abnormalities in PDGFRA, IDH1, EGFR, and NF1. *Cancer cell* **17**, 98-110

39. Brennan, C. W., Verhaak, R. G., McKenna, A., Campos, B., Noushmehr, H., Salama, S. R., Zheng, S., Chakravarty, D., Sanborn, J. Z., Berman, S. H., Beroukhim, R., Bernard, B., Wu, C. J., Genovese, G., Shmulevich, I., Barnholtz-Sloan, J., Zou, L., Vegesna, R., Shukla, S. A., Ciriello, G., Yung, W. K., Zhang, W., Sougnez, C., Mikkelsen, T., Aldape, K., Bigner, D. D., Van Meir, E. G., Prados, M., Sloan, A., Black, K. L., Eschbacher, J., Finocchiaro, G., Friedman, W., Andrews, D. W., Guha, A., Iacocca, M., O'Neill, B. P., Foltz, G., Myers, J., Weisenberger, D. J., Penny, R., Kucherlapati, R., Perou, C. M., Hayes, D. N., Gibbs, R., Marra, M., Mills, G. B., Lander, E., Spellman, P., Wilson, R., Sander, C., Weinstein, J., Meyerson, M., Gabriel, S., Laird, P. W., Haussler, D., Getz, G., and Chin, L. (2013) The somatic genomic landscape of glioblastoma. *Cell* **155**, 462-477

40. Bettegowda, C., Agrawal, N., Jiao, Y., Sausen, M., Wood, L. D., Hruban, R. H., Rodriguez, F. J., Cahill, D. P., McLendon, R., Riggins, G., Velculescu, V. E., Oba-Shinjo, S. M., Marie, S. K., Vogelstein, B., Bigner, D., Yan, H., Papadopoulos, N., and Kinzler, K. W. (2011) Mutations in CIC and FUBP1 contribute to human oligodendroglioma. *Science* **333**, 1453-1455

41. Jiao, Y., Shi, C., Edil, B. H., de Wilde, R. F., Klimstra, D. S., Maitra, A., Schulick, R. D., Tang, L. H., Wolfgang, C. L., Choti, M. A., Velculescu, V. E., Diaz, L. A., Jr., Vogelstein, B., Kinzler, K. W., Hruban, R. H., and Papadopoulos, N. (2011) DAXX/ATRX, MEN1, and mTOR pathway genes are frequently altered in pancreatic neuroendocrine tumors. *Science* **331**, 1199-1203

42. Heaphy, C. M., de Wilde, R. F., Jiao, Y., Klein, A. P., Edil, B. H., Shi, C., Bettegowda, C., Rodriguez, F. J., Eberhart, C. G., Hebbar, S., Offerhaus, G. J., McLendon, R., Rasheed, B. A., He, Y., Yan, H., Bigner, D. D., Oba-Shinjo, S. M., Marie, S. K., Riggins, G. J., Kinzler, K. W., Vogelstein, B., Hruban, R. H., Maitra, A., Papadopoulos, N., and Meeker, A. K. (2011) Altered telomeres in tumors with ATRX and DAXX mutations. *Science* **333**, 425

43. Kannan, K., Inagaki, A., Silber, J., Gorovets, D., Zhang, J., Wolf, F., Kastenhuber, E. R., Heguy, A., Petrini, J. H., Chan, T. A., and Huse, J. T. (2012) Whole-exome sequencing identifies ATRX mutation as a key molecular determinant in lower-grade glioma. *Oncotarget*

44. Liu, X. Y., Gerges, N., Korshunov, A., Sabha, N., Khuong-Quang, D. A., Fontebasso, A. M., Fleming, A., Hadjadj, D., Schwartzentruber, J., Majewski, J., Dong, Z., Siegel, P., Albrecht, S., Croul, S., Jones, D. T., Kool, M., Tonjes, M., Reifenberger, G., Faury, D., Zadeh, G., Pfister, S., and Jabado, N. (2012) Frequent ATRX mutations and loss of expression in adult diffuse astrocytic tumors carrying IDH1/IDH2 and TP53 mutations. *Acta Neuropathol* **124**, 615-625

45. Nabetani, A., and Ishikawa, F. (2009) Unusual telomeric DNAs in human telomerase-negative immortalized cells. *Molecular and cellular biology* **29**, 703-713

46. Langford, L. A., Piatyszek, M. A., Xu, R., Schold, S. C., Jr., and Shay, J. W. (1995) Telomerase activity in human brain tumours. *Lancet* **346**, 1267-1268

47. Hiraga, S., Ohnishi, T., Izumoto, S., Miyahara, E., Kanemura, Y., Matsumura, H., and Arita, N. (1998) Telomerase activity and alterations in telomere length in human brain tumors. *Cancer research* **58**, 2117-2125

48. Hartmann, C., Hentschel, B., Wick, W., Capper, D., Felsberg, J., Simon, M., Westphal, M., Schackert, G., Meyermann, R., Pietsch, T., Reifenberger, G., Weller, M., Loeffler, M., and von Deimling, A. (2010) Patients with IDH1 wild type anaplastic astrocytomas exhibit worse prognosis than IDH1-mutated glioblastomas, and IDH1 mutation status accounts for the unfavorable prognostic effect of higher age: implications for classification of gliomas. *Acta Neuropathol* **120**, 707-718

49. Mardis, E. R., Ding, L., Dooling, D. J., Larson, D. E., McLellan, M. D., Chen, K., Koboldt, D. C., Fulton, R. S., Delehaunty, K. D., McGrath, S. D., Fulton, L. A., Locke, D. P., Magrini, V. J., Abbott, R. M., Vickery, T. L., Reed, J. S., Robinson, J. S., Wylie, T., Smith, S. M., Carmichael, L., Eldred, J. M., Harris, C. C., Walker, J., Peck, J. B., Du, F., Dukes, A. F., Sanderson, G. E., Brummett, A. M., Clark, E., McMichael, J. F., Meyer, R. J., Schindler, J. K., Pohl, C. S., Wallis, J. W., Shi, X., Lin, L., Schmidt, H., Tang, Y., Haipek, C., Wiechert, M. E., Ivy, J. V., Kalicki, J., Elliott, G., Ries, R. E., Payton, J. E., Westervelt, P., Tomasson, M. H., Watson, M. A., Baty, J., Heath, S., Shannon, W. D., Nagarajan, R., Link, D. C., Walter, M. J.,

Graubert, T. A., DiPersio, J. F., Wilson, R. K., and Ley, T. J. (2009) Recurring mutations found by sequencing an acute myeloid leukemia genome. *N Engl J Med* **361**, 1058-1066

50. Amary, M. F., Bacsi, K., Maggiani, F., Damato, S., Halai, D., Berisha, F., Pollock, R., O'Donnell, P., Grigoriadis, A., Diss, T., Eskandarpour, M., Presneau, N., Hogendoorn, P. C., Futreal, A., Tirabosco, R., and Flanagan, A. M. (2011) IDH1 and IDH2 mutations are frequent events in central chondrosarcoma and central and periosteal chondromas but not in other mesenchymal tumours. *The Journal of pathology* **224**, 334-343

51. Amary, M. F., Damato, S., Halai, D., Eskandarpour, M., Berisha, F., Bonar, F., McCarthy, S., Fantin, V. R., Straley, K. S., Lobo, S., Aston, W., Green, C. L., Gale, R. E., Tirabosco, R., Futreal, A., Campbell, P., Presneau, N., and Flanagan, A. M. (2011) Ollier disease and Maffucci syndrome are caused by somatic mosaic mutations of IDH1 and IDH2. *Nat Genet* **43**, 1262-1265

52. Pansuriya, T. C., van Eijk, R., d'Adamo, P., van Ruler, M. A., Kuijjer, M. L., Oosting, J., Cleton-Jansen, A. M., van Oosterwijk, J. G., Verbeke, S. L., Meijer, D., van Wezel, T., Nord, K. H., Sangiorgi, L., Toker, B., Liegl-Atzwanger, B., San-Julian, M., Sciot, R., Limaye, N., Kindblom, L. G., Daugaard, S., Godfraind, C., Boon, L. M., Vikkula, M., Kurek, K. C., Szuhai, K., French, P. J., and Bovee, J. V. (2011) Somatic mosaic IDH1 and IDH2 mutations are associated with enchondroma and spindle cell hemangioma in Ollier disease and Maffucci syndrome. *Nat Genet* **43**, 1256-1261

53. Wang, P., Dong, Q., Zhang, C., Kuan, P. F., Liu, Y., Jeck, W. R., Andersen, J. B., Jiang, W., Savich, G. L., Tan, T. X., Auman, J. T., Hoskins, J. M., Misher, A. D., Moser, C. D., Yourstone, S. M., Kim, J. W., Cibulskis, K., Getz, G., Hunt, H. V., Thorgeirsson, S. S., Roberts, L. R., Ye, D., Guan, K. L., Xiong, Y., Qin, L. X., and Chiang, D. Y. (2013) Mutations in isocitrate dehydrogenase 1 and 2 occur frequently in intrahepatic cholangiocarcinomas and share hypermethylation targets with glioblastomas. *Oncogene* **32**, 3091-3100

54. Ghiam, A. F., Cairns, R. A., Thoms, J., Dal Pra, A., Ahmed, O., Meng, A., Mak, T. W., and Bristow, R. G. (2012) IDH mutation status in prostate cancer. *Oncogene* **31**, 3826

55. Cairns, R. A., Iqbal, J., Lemonnier, F., Kucuk, C., de Leval, L., Jais, J. P., Parrens, M., Martin, A., Xerri, L., Brousset, P., Chan, L. C., Chan, W. C., Gaulard, P., and

Mak, T. W. (2012) IDH2 mutations are frequent in angioimmunoblastic T-cell lymphoma. *Blood* **119**, 1901-1903

56. Saha, S. K., Parachoniak, C. A., Ghanta, K. S., Fitamant, J., Ross, K. N., Najem, M. S., Gurumurthy, S., Akbay, E. A., Sia, D., Cornella, H., Miltiadous, O., Walesky, C., Deshpande, V., Zhu, A. X., Hezel, A. F., Yen, K. E., Straley, K. S., Travins, J., Popovici-Muller, J., Gliser, C., Ferrone, C. R., Apte, U., Llovet, J. M., Wong, K. K., Ramaswamy, S., and Bardeesy, N. (2014) Mutant IDH inhibits HNF-4alpha to block hepatocyte differentiation and promote biliary cancer. *Nature* **513**, 110-114

57. Prensner, J. R., and Chinnaiyan, A. M. (2011) Metabolism unhinged: IDH mutations in cancer. *Nature medicine* **17**, 291-293

58. Koivunen, P., Lee, S., Duncan, C. G., Lopez, G., Lu, G., Ramkissoon, S., Losman, J. A., Joensuu, P., Bergmann, U., Gross, S., Travins, J., Weiss, S., Looper, R., Ligon, K. L., Verhaak, R. G., Yan, H., and Kaelin, W. G., Jr. (2012) Transformation by the (R)-enantiomer of 2-hydroxyglutarate linked to EGLN activation. *Nature* **483**, 484-488

59. Bralten, L. B., Kloosterhof, N. K., Balvers, R., Sacchetti, A., Lapre, L., Lamfers, M., Leenstra, S., de Jonge, H., Kros, J. M., Jansen, E. E., Struys, E. A., Jakobs, C., Salomons, G. S., Diks, S. H., Peppelenbosch, M., Kremer, A., Hoogenraad, C. C., Smitt, P. A., and French, P. J. (2011) IDH1 R132H decreases proliferation of glioma cell lines in vitro and in vivo. *Ann Neurol* **69**, 455-463

60. Navis, A. C., Niclou, S. P., Fack, F., Stieber, D., van Lith, S., Verrijp, K., Wright, A., Stauber, J., Tops, B., Otte-Holler, I., Wevers, R. A., van Rooij, A., Pusch, S., von Deimling, A., Tigchelaar, W., van Noorden, C. J., Wesseling, P., and Leenders, W. P. (2013) Increased mitochondrial activity in a novel IDH1-R132H mutant human oligodendroglioma xenograft model: in situ detection of 2-HG and alpha-KG. *Acta neuropathologica communications* **1**, 18

61. Piaskowski, S., Bienkowski, M., Stoczynska-Fidelus, E., Stawski, R., Sieruta, M., Szybka, M., Papierz, W., Wolanczyk, M., Jaskolski, D. J., Liberski, P. P., and Rieske, P. (2011) Glioma cells showing IDH1 mutation cannot be propagated in standard cell culture conditions. *Br J Cancer* **104**, 968-970

62. Reitman, Z. J., and Yan, H. (2010) Isocitrate dehydrogenase 1 and 2 mutations in cancer: alterations at a crossroads of cellular metabolism. *J Natl Cancer Inst* **102**, 932-941

63. Jin, G., Reitman, Z. J., Spasojevic, I., Batinic-Haberle, I., Yang, J., Schmidt-Kittler, O., Bigner, D. D., and Yan, H. (2011) 2-hydroxyglutarate production, but not dominant negative function, is conferred by glioma-derived NADP-dependent isocitrate dehydrogenase mutations. *PLoS One* **6**, e16812

64. Noushmehr, H., Weisenberger, D. J., Diefes, K., Phillips, H. S., Pujara, K., Berman, B. P., Pan, F., Pelloski, C. E., Sulman, E. P., Bhat, K. P., Verhaak, R. G., Hoadley, K. A., Hayes, D. N., Perou, C. M., Schmidt, H. K., Ding, L., Wilson, R. K., Van Den Berg, D., Shen, H., Bengtsson, H., Neuvial, P., Cope, L. M., Buckley, J., Herman, J. G., Baylin, S. B., Laird, P. W., and Aldape, K. (2010) Identification of a CpG island methylator phenotype that defines a distinct subgroup of glioma. *Cancer cell* **17**, 510-522

65. Toyota, M., Ahuja, N., Ohe-Toyota, M., Herman, J. G., Baylin, S. B., and Issa, J. P. (1999) CpG island methylator phenotype in colorectal cancer. *Proc Natl Acad Sci U S A* **96**, 8681-8686

66. Turcan, S., Rohle, D., Goenka, A., Walsh, L. A., Fang, F., Yilmaz, E., Campos, C., Fabius, A. W., Lu, C., Ward, P. S., Thompson, C. B., Kaufman, A., Guryanova, O., Levine, R., Heguy, A., Viale, A., Morris, L. G., Huse, J. T., Mellinghoff, I. K., and Chan, T. A. (2012) IDH1 mutation is sufficient to establish the glioma hypermethylator phenotype. *Nature* **483**, 479-483

67. Duncan, C. G., Barwick, B. G., Jin, G., Rago, C., Kapoor-Vazirani, P., Powell, D. R., Chi, J. T., Bigner, D. D., Vertino, P. M., and Yan, H. (2012) A heterozygous IDH1R132H/WT mutation induces genome-wide alterations in DNA methylation. *Genome Res* **22**, 2339-2355

68. Cairns, R. A., and Mak, T. W. (2013) Oncogenic isocitrate dehydrogenase mutations: mechanisms, models, and clinical opportunities. *Cancer discovery* **3**, 730-741

69. Xu, W., Yang, H., Liu, Y., Yang, Y., Wang, P., Kim, S. H., Ito, S., Yang, C., Xiao, M. T., Liu, L. X., Jiang, W. Q., Liu, J., Zhang, J. Y., Wang, B., Frye, S., Zhang, Y., Xu, Y. H., Lei, Q. Y., Guan, K. L., Zhao, S. M., and Xiong, Y. (2011) Oncometabolite 2-hydroxyglutarate is a competitive inhibitor of alpha-ketoglutarate-dependent dioxygenases. *Cancer cell* **19**, 17-30

70. Figueroa, M. E., Abdel-Wahab, O., Lu, C., Ward, P. S., Patel, J., Shih, A., Li, Y., Bhagwat, N., Vasanthakumar, A., Fernandez, H. F., Tallman, M. S., Sun, Z., Wolniak, K., Peeters, J. K., Liu, W., Choe, S. E., Fantin, V. R., Paietta, E., Lowenberg, B., Licht, J. D., Godley, L. A., Delwel, R., Valk, P. J., Thompson, C. B., Levine, R. L., and Melnick, A. (2010) Leukemic IDH1 and IDH2 Mutations Result in a Hypermethylation Phenotype, Disrupt TET2 Function, and Impair Hematopoietic Differentiation. *Cancer Cell* **18**, 553-567

71. Cimmino, L., Abdel-Wahab, O., Levine, R. L., and Aifantis, I. (2011) TET family proteins and their role in stem cell differentiation and transformation. *Cell Stem Cell* **9**, 193-204

72. Losman, J. A., and Kaelin, W. G., Jr. (2013) What a difference a hydroxyl makes: mutant IDH, (R)-2-hydroxyglutarate, and cancer. *Genes & development* **27**, 836-852

73. Tahiliani, M., Koh, K. P., Shen, Y., Pastor, W. A., Bandukwala, H., Brudno, Y., Agarwal, S., Iyer, L. M., Liu, D. R., Aravind, L., and Rao, A. (2009) Conversion of 5-methylcytosine to 5-hydroxymethylcytosine in mammalian DNA by MLL partner TET1. *Science* **324**, 930-935

74. Ficz, G., Branco, M. R., Seisenberger, S., Santos, F., Krueger, F., Hore, T. A., Marques, C. J., Andrews, S., and Reik, W. (2011) Dynamic regulation of 5-hydroxymethylcytosine in mouse ES cells and during differentiation. *Nature* **473**, 398-402

75. Pastor, W. A., Pape, U. J., Huang, Y., Henderson, H. R., Lister, R., Ko, M., McLoughlin, E. M., Brudno, Y., Mahapatra, S., Kapranov, P., Tahiliani, M., Daley, G. Q., Liu, X. S., Ecker, J. R., Milos, P. M., Agarwal, S., and Rao, A. (2011) Genome-wide mapping of 5-hydroxymethylcytosine in embryonic stem cells. *Nature* **473**, 394-397

76. Serandour, A. A., Avner, S., Oger, F., Bizot, M., Percevault, F., Lucchetti-Miganeh, C., Palierne, G., Gheeraert, C., Barloy-Hubler, F., Peron, C. L., Madigou, T., Durand, E., Froguel, P., Staels, B., Lefebvre, P., Metivier, R., Eeckhoute, J., and Salbert, G. (2012) Dynamic hydroxymethylation of deoxyribonucleic acid marks differentiation-associated enhancers. *Nucleic Acids Res* **40**, 8255-8265

77. Haffner, M. C., Chaux, A., Meeker, A. K., Esopi, D. M., Gerber, J., Pellakuru, L. G., Toubaji, A., Argani, P., Iacobuzio-Donahue, C., Nelson, W. G., Netto, G. J., De

Marzo, A. M., and Yegnasubramanian, S. (2011) Global 5-hydroxymethylcytosine content is significantly reduced in tissue stem/progenitor cell compartments and in human cancers. *Oncotarget* **2**, 627-637

78. Lu, C., Ward, P. S., Kapoor, G. S., Rohle, D., Turcan, S., Abdel-Wahab, O., Edwards, C. R., Khanin, R., Figueroa, M. E., Melnick, A., Wellen, K. E., O'Rourke, D. M., Berger, S. L., Chan, T. A., Levine, R. L., Mellinghoff, I. K., and Thompson, C. B. (2012) IDH mutation impairs histone demethylation and results in a block to cell differentiation. *Nature* **483**, 474-478

79. Sasaki, M., Knobbe, C. B., Munger, J. C., Lind, E. F., Brenner, D., Brustle, A., Harris, I. S., Holmes, R., Wakeham, A., Haight, J., You-Ten, A., Li, W. Y., Schalm, S., Su, S. M., Virtanen, C., Reifenberger, G., Ohashi, P. S., Barber, D. L., Figueroa, M. E., Melnick, A., Zuniga-Pflucker, J. C., and Mak, T. W. (2012) IDH1(R132H) mutation increases murine haematopoietic progenitors and alters epigenetics. *Nature* **488**, 656-659

80. Chowdhury, R., Yeoh, K. K., Tian, Y. M., Hillringhaus, L., Bagg, E. A., Rose, N. R., Leung, I. K., Li, X. S., Woon, E. C., Yang, M., McDonough, M. A., King, O. N., Clifton, I. J., Klose, R. J., Claridge, T. D., Ratcliffe, P. J., Schofield, C. J., and Kawamura, A. (2011) The oncometabolite 2-hydroxyglutarate inhibits histone lysine demethylases. *EMBO Rep* **12**, 463-469

81. Zhao, S., Lin, Y., Xu, W., Jiang, W., Zha, Z., Wang, P., Yu, W., Li, Z., Gong, L., Peng, Y., Ding, J., Lei, Q., Guan, K. L., and Xiong, Y. (2009) Glioma-derived mutations in IDH1 dominantly inhibit IDH1 catalytic activity and induce HIF-1alpha. *Science* **324**, 261-265

82. Williams, S. C., Karajannis, M. A., Chiriboga, L., Golfinos, J. G., von Deimling, A., and Zagzag, D. (2011) R132H-mutation of isocitrate dehydrogenase-1 is not sufficient for HIF-1alpha upregulation in adult glioma. *Acta Neuropathol* **121**, 279-281

83. Lai, A., Kharbanda, S., Pope, W. B., Tran, A., Solis, O. E., Peale, F., Forrest, W. F., Pujara, K., Carrillo, J. A., Pandita, A., Ellingson, B. M., Bowers, C. W., Soriano, R. H., Schmidt, N. O., Mohan, S., Yong, W. H., Seshagiri, S., Modrusan, Z., Jiang, Z., Aldape, K. D., Mischel, P. S., Liau, L. M., Escovedo, C. J., Chen, W., Nghiemphu, P. L., James, C. D., Prados, M. D., Westphal, M., Lamszus, K., Cloughesy, T., and Phillips, H. S. (2011) Evidence for sequenced molecular evolution of IDH1

mutant glioblastoma from a distinct cell of origin. *Journal of clinical oncology : official journal of the American Society of Clinical Oncology* **29**, 4482-4490

84. Martens, T., Laabs, Y., Gunther, H. S., Kemming, D., Zhu, Z., Witte, L., Hagel, C., Westphal, M., and Lamszus, K. (2008) Inhibition of glioblastoma growth in a highly invasive nude mouse model can be achieved by targeting epidermal growth factor receptor but not vascular endothelial growth factor receptor-2. *Clinical cancer research : an official journal of the American Association for Cancer Research* **14**, 5447-5458

85. Candolfi, M., Curtin, J. F., Nichols, W. S., Muhammad, A. G., King, G. D., Pluhar, G. E., McNiel, E. A., Ohlfest, J. R., Freese, A. B., Moore, P. F., Lerner, J., Lowenstein, P. R., and Castro, M. G. (2007) Intracranial glioblastoma models in preclinical neuro-oncology: neuropathological characterization and tumor progression. *J Neurooncol* **85**, 133-148

86. Joo, K. M., Kim, J., Jin, J., Kim, M., Seol, H. J., Muradov, J., Yang, H., Choi, Y. L., Park, W. Y., Kong, D. S., Lee, J. I., Ko, Y. H., Woo, H. G., Lee, J., Kim, S., and Nam, D. H. (2013) Patient-specific orthotopic glioblastoma xenograft models recapitulate the histopathology and biology of human glioblastomas in situ. *Cell reports* **3**, 260-273

87. Chow, L. M., Endersby, R., Zhu, X., Rankin, S., Qu, C., Zhang, J., Broniscer, A., Ellison, D. W., and Baker, S. J. (2011) Cooperativity within and among Pten, p53, and Rb pathways induces high-grade astrocytoma in adult brain. *Cancer Cell* **19**, 305-316

88. Galli, R., Binda, E., Orfanelli, U., Cipelletti, B., Gritti, A., De Vitis, S., Fiocco, R., Foroni, C., Dimeco, F., and Vescovi, A. (2004) Isolation and characterization of tumorigenic, stem-like neural precursors from human glioblastoma. *Cancer research* **64**, 7011-7021

89. Rankin, S. L., Zhu, G., and Baker, S. J. (2012) Review: insights gained from modelling high-grade glioma in the mouse. *Neuropathology and applied neurobiology* **38**, 254-270

90. Laks, D. R., Masterman-Smith, M., Visnyei, K., Angenieux, B., Orozco, N. M., Foran, I., Yong, W. H., Vinters, H. V., Liau, L. M., Lazareff, J. A., Mischel, P. S., Cloughesy, T. F., Horvath, S., and Kornblum, H. I. (2009) Neurosphere formation

is an independent predictor of clinical outcome in malignant glioma. *Stem cells (Dayton, Ohio)* **27**, 980-987

91. Hambardzumyan, D., Amankulor, N. M., Helmy, K. Y., Becher, O. J., and Holland, E. C. (2009) Modeling Adult Gliomas Using RCAS/t-va Technology. *Translational oncology* **2**, 89-95

92. Uhrbom, L., and Holland, E. C. (2001) Modeling gliomagenesis with somatic cell gene transfer using retroviral vectors. *J Neurooncol* **53**, 297-305

93. Reilly, K. M., Loisel, D. A., Bronson, R. T., McLaughlin, M. E., and Jacks, T. (2000) Nf1;Trp53 mutant mice develop glioblastoma with evidence of strain-specific effects. *Nat Genet* **26**, 109-113

94. Berube, N. G., Mangelsdorf, M., Jagla, M., Vanderluit, J., Garrick, D., Gibbons, R. J., Higgs, D. R., Slack, R. S., and Picketts, D. J. (2005) The chromatin-remodeling protein ATRX is critical for neuronal survival during corticogenesis. *J Clin Invest* **115**, 258-267

95. Jonkers, J., Meuwissen, R., van der Gulden, H., Peterse, H., van der Valk, M., and Berns, A. (2001) Synergistic tumor suppressor activity of BRCA2 and p53 in a conditional mouse model for breast cancer. *Nat Genet* **29**, 418-425

96. Gibbons, R. J., Picketts, D. J., Villard, L., and Higgs, D. R. (1995) Mutations in a putative global transcriptional regulator cause X-linked mental retardation with alpha-thalassemia (ATR-X syndrome). *Cell* **80**, 837-845

97. Berube, N. G., Healy, J., Medina, C. F., Wu, S., Hodgson, T., Jagla, M., and Picketts, D. J. (2008) Patient mutations alter ATRX targeting to PML nuclear bodies. *European journal of human genetics : EJHG* **16**, 192-201

98. Gibbons, R. J., Wada, T., Fisher, C. A., Malik, N., Mitson, M. J., Steensma, D. P., Fryer, A., Goudie, D. R., Krantz, I. D., and Traeger-Synodinos, J. (2008) Mutations in the chromatin-associated protein ATRX. *Human mutation* **29**, 796-802

99. Argentaro, A., Yang, J. C., Chapman, L., Kowalczyk, M. S., Gibbons, R. J., Higgs, D. R., Neuhaus, D., and Rhodes, D. (2007) Structural consequences of disease-causing mutations in the ATRX-DNMT3-DNMT3L (ADD) domain of the chromatin-associated protein ATRX. *Proc Natl Acad Sci U S A* **104**, 11939-11944

100. Olivier, M., Hollstein, M., and Hainaut, P. (2010) TP53 mutations in human cancers: origins, consequences, and clinical use. *Cold Spring Harbor perspectives in biology* **2**, a001008

101. Muller, P. A., and Vousden, K. H. (2013) p53 mutations in cancer. *Nature cell biology* **15**, 2-8

102. Hollstein, M., Sidransky, D., Vogelstein, B., and Harris, C. C. (1991) p53 mutations in human cancers. *Science* **253**, 49-53

103. Besnard, F., Brenner, M., Nakatani, Y., Chao, R., Purohit, H. J., and Freese, E. (1991) Multiple interacting sites regulate astrocyte-specific transcription of the human gene for glial fibrillary acidic protein. *The Journal of biological chemistry* **266**, 18877-18883

104. Zhuo, L., Theis, M., Alvarez-Maya, I., Brenner, M., Willecke, K., and Messing, A. (2001) hGFAP-cre transgenic mice for manipulation of glial and neuronal function in vivo. *Genesis* **31**, 85-94

105. Perez-Figares, J. M., Jimenez, A. J., and Rodriguez, E. M. (2001) Subcommissural organ, cerebrospinal fluid circulation, and hydrocephalus. *Microscopy research and technique* **52**, 591-607

106. Huh, M. S., Todd, M. A., and Picketts, D. J. (2009) SCO-ping out the mechanisms underlying the etiology of hydrocephalus. *Physiology (Bethesda, Md.)* **24**, 117-126

107. Travasso, R. D., Corvera Poire, E., Castro, M., Rodriguez-Manzaneque, J. C., and Hernandez-Machado, A. (2011) Tumor angiogenesis and vascular patterning: a mathematical model. *PLoS One* **6**, e19989

108. Sasaki, M., Knobbe, C. B., Itsumi, M., Elia, A. J., Harris, I. S., Chio, II, Cairns, R. A., McCracken, S., Wakeham, A., Haight, J., Ten, A. Y., Snow, B., Ueda, T., Inoue, S., Yamamoto, K., Ko, M., Rao, A., Yen, K. E., Su, S. M., and Mak, T. W. (2012) D-2-hydroxyglutarate produced by mutant IDH1 perturbs collagen maturation and basement membrane function. *Genes & development* **26**, 2038-2049

109. Weis, S. M., and Cheresh, D. A. (2005) Pathophysiological consequences of VEGF-induced vascular permeability. *Nature* **437**, 497-504

110. Quinones-Hinojosa, A., Sanai, N., Soriano-Navarro, M., Gonzalez-Perez, O., Mirzadeh, Z., Gil-Perotin, S., Romero-Rodriguez, R., Berger, M. S., Garcia-Verdugo, J. M., and Alvarez-Buylla, A. (2006) Cellular composition and cytoarchitecture of the adult human subventricular zone: a niche of neural stem cells. *The Journal of comparative neurology* **494**, 415-434

111. Fuentealba, L. C., Obernier, K., and Alvarez-Buylla, A. (2012) Adult neural stem cells bridge their niche. *Cell Stem Cell* **10**, 698-708

112. Conover, J. C., and Shook, B. A. (2011) AGING OF THE SUBVENTRICULAR ZONE NEURAL STEM CELL NICHE. *Aging and disease* **2**, 149-163

113. Heffner, C. S., Herbert Pratt, C., Babiuk, R. P., Sharma, Y., Rockwood, S. F., Donahue, L. R., Eppig, J. T., and Murray, S. A. (2012) Supporting conditional mouse mutagenesis with a comprehensive cre characterization resource. *Nature communications* **3**, 1218

114. Balordi, F., and Fishell, G. (2007) Mosaic removal of hedgehog signaling in the adult SVZ reveals that the residual wild-type stem cells have a limited capacity for self-renewal. *The Journal of neuroscience : the official journal of the Society for Neuroscience* **27**, 14248-14259

115. Zimmerman, L., Parr, B., Lendahl, U., Cunningham, M., McKay, R., Gavin, B., Mann, J., Vassileva, G., and McMahon, A. (1994) Independent regulatory elements in the nestin gene direct transgene expression to neural stem cells or muscle precursors. *Neuron* **12**, 11-24

116. Arenkiel, B. R., Hasegawa, H., Yi, J. J., Larsen, R. S., Wallace, M. L., Philpot, B. D., Wang, F., and Ehlers, M. D. (2011) Activity-induced remodeling of olfactory bulb microcircuits revealed by monosynaptic tracing. *PLoS One* **6**, e29423

117. Sauer, B. (1998) Inducible gene targeting in mice using the Cre/lox system. *Methods (San Diego, Calif.)* **14**, 381-392

118. Feil, S., Valtcheva, N., and Feil, R. (2009) Inducible Cre mice. *Methods in molecular biology (Clifton, N.J.)* **530**, 343-363

119. Deb, P., Sharma, M. C., Mahapatra, A. K., Agarwal, D., and Sarkar, C. (2005) Glioblastoma multiforme with long term survival. *Neurology India* **53**, 329-332

120. Killela, P. J., Reitman, Z. J., Jiao, Y., Bettegowda, C., Agrawal, N., Diaz, L. A., Jr., Friedman, A. H., Friedman, H., Gallia, G. L., Giovanella, B. C., Grollman, A. P., He, T. C., He, Y., Hruban, R. H., Jallo, G. I., Mandahl, N., Meeker, A. K., Mertens, F., Netto, G. J., Rasheed, B. A., Riggins, G. J., Rosenquist, T. A., Schiffman, M., Shih Ie, M., Theodorescu, D., Torbenson, M. S., Velculescu, V. E., Wang, T. L., Wentzensen, N., Wood, L. D., Zhang, M., McLendon, R. E., Bigner, D. D., Kinzler, K. W., Vogelstein, B., Papadopoulos, N., and Yan, H. (2013) TERT promoter mutations occur frequently in gliomas and a subset of tumors derived from cells with low rates of self-renewal. *Proc Natl Acad Sci U S A* **110**, 6021-6026

121. Shultz, L. D., Lyons, B. L., Burzenski, L. M., Gott, B., Chen, X., Chaleff, S., Kotb, M., Gillies, S. D., King, M., Mangada, J., Greiner, D. L., and Handgretinger, R. (2005) Human lymphoid and myeloid cell development in NOD/LtSz-scid IL2R gamma null mice engrafted with mobilized human hemopoietic stem cells. *Journal of immunology (Baltimore, Md. : 1950)* **174**, 6477-6489

Biography

Christopher James Pirozzi was born on March 4th, 1985 in Brooklyn, New York to Denise A. Pirozzi and Ernie L. Pirozzi. He attended Rutgers University in New Brunswick, New Jersey where he obtained a B.A. in Genetics and a B.A. in Philosophy. Christopher was interested in biomedical research and took advantage of the undergraduate research opportunities that Rutgers University offered. During his undergraduate career, he was able to explore his interests by joining the laboratory of Dr. Nancy A. Woychik at the Robert Wood Johnson Medical School, Rutgers University (2005-2006) followed by the laboratory of Dr. Jay A. Tischfield under the guidance of Dr. Lourdes Serrano(2006-2007). His interests were further explored during an internship at the Monash Immunology and Stem Cell Laboratories in Melbourne, Australia where he decided he would pursue a graduate education in the sciences. After graduating from Rutgers, Christopher became a Research Technician at the Sloan Kettering Institute Stem Cell Research Facility at Memorial Sloan Kettering Cancer Center in New York led by Dr. Mark Tomishima (2007-2009). In 2009, Christopher entered the Developmental and Stem Cell Biology umbrella program at Duke University in Durham, North Carolina and joined the laboratory of Dr. Hai Yan in the Department of Pathology. From 2010 to 2014, Christopher focused on generating genetically faithful mouse models of glioma that he used to understand the role of mutant IDH1 in driving tumorigenesis alone and in combination with other commonly found mutations. Christopher has presented his

work at the American Association for Cancer Research (AACR) Annual Meeting (2014) and also at the National Graduate Student Symposium at St. Jude Children's Research Hospital (2014). Christopher has been an Associate Member of AACR from 2013. Christopher's work and contributions to various research is described in the following publications:

Killela PJ*, **Pirozzi CJ***, Healy P, Reitman ZJ, Lipp E, Rasheed AB, Yang R, Diplas B, Wang Z, Greer PK, Zhu H, Wang C, Carpenter A, Friedman H, Friedman AH, He Y, McLendon RE, Herndon II JE, Yan H, Bigner DD (2014) Mutations in IDH1 , IDH2 , and in the TERT promoter define clinically distinct subgroups of adult malignant gliomas. Oncotarget 5 (6):1515-1525.
***Denotes equal contribution**

Guo C, Chen LH, Huang Y, Chang CC, Wang P, **Pirozzi CJ**, Qin X, Bao X, Greer PK, McLendon RE, Yan H, Keir ST, Bigner DD, He Y (2013) KMT2D maintains neoplastic cell proliferation and global histone H3 lysine 4 monomethylation. Oncotarget 4 (11):2144-2153.

Reitman ZJ, **Pirozzi CJ**, Yan H (2013) Promoting a new brain tumor mutation: TERT promoter mutations in CNS tumors. Acta Neuropathol 126 (6):789-792.

Killela PJ*, **Pirozzi CJ***, Reitman ZJ*, Jones S, Rasheed BA, Lipp E, Friedman H, Friedman AH, He Y, McLendon RE, Bigner DD, Yan H (2013) The genetic landscape of anaplastic astrocytoma. Oncotarget 5 (6):1452-1457.
***Denotes equal contribution**

Pirozzi CJ, Reitman ZJ, Yan H (2013) Releasing the block: setting differentiation free with mutant IDH inhibitors. Cancer Cell 23 (5):570-572.

Jin G, **Pirozzi CJ**, Chen LH, Lopez GY, Duncan CG, Feng J, Spasojevic I, Bigner DD, He Y, Yan H (2012) Mutant IDH1 is required for IDH1 mutated tumor cell growth. Oncotarget 3 (8):774-782.

Jiao Y, Killela PJ, Reitman ZJ, Rasheed AB, Heaphy CM, de Wilde RF, Rodriguez FJ, Rosemberg S, Oba-Shinjo SM, Nagahashi Marie SK, Bettegowda C, Agrawal N,

Lipp E, **Pirozzi C**, Lopez G, He Y, Friedman H, Friedman AH, Riggins GJ, Holdhoff M, Burger P, McLendon R, Bigner DD, Vogelstein B, Meeker AK, Kinzler KW, Papadopoulos N, Diaz LA, Yan H (2012) Frequent ATRX, CIC, FUBP1 and IDH1 mutations refine the classification of malignant gliomas. Oncotarget 3 (7):709-722.

Guo C, **Pirozzi CJ**, Lopez GY, Yan H (2011) Isocitrate dehydrogenase mutations in gliomas: mechanisms, biomarkers and therapeutic target. Current opinion in neurology 24 (6):648-652.